Non-invasive Method to Measure Energy Flow Rate in a Pipe

Mohammed A. Alanazi

Thesis submitted to the faculty of the Virginia Polytechnic Institute and State University in partial fulfillment of the requirements for the degree of

Master of Science

In

Mechanical Engineering

Thomas E. Diller, Chair

Brian Vick

Scott T. Huxtable

12th of October 2018

Blacksburg, Virginia

Keywords: Non-invasive flow meter, Heat Flux sensor (PHFS), Parallel thermocouples, Welded thermocouple, Thermal contact resistance, Heat transfer coefficient, Flow rate, Water temperature, Parameter estimation, Correlation, Time constant

Non-invasive Method to Measure Energy Flow Rate in a Pipe

Mohammed A. Alanazi

Abstract

Current methods for measuring energy flow rate in a pipe use a variety of invasive sensors, including temperature sensors, turbine flow meters, and vortex shedding devices. These systems are costly to buy and install. A new approach that uses non-invasive sensors that are easy to install and less expensive has been developed. A thermal interrogation method using heat flux and temperature measurements is used. A transient thermal model, lumped capacitance method LCM, before and during activation of an external heater provides estimates of the fluid heat transfer coefficient h and fluid temperature. The major components of the system are a thin-foil thermocouple, a heat flux sensor (PHFS), and a heater. To minimize the thermal contact resistance $R"$ between the thermocouple thickness and the pipe surface, two thermocouples, welded and parallel, were tested together in the same set-up. Values of heat transfer coefficient h, thermal contact resistance $R"$, time constant τ, and the water temperature ℃, were determined by using a parameter estimation code which depends on the minimum root mean square RMS error between the analytical and experimental sensor temperature values. The time for processing data to get the parameter estimation values is from three to four minutes. The experiments were done over a range of flow rates (1.5 gallon/minute to 14.5 gallon/minute). A correlation between the heat transfer coefficient h and the flow rate Q was done for both the parallel and the welded thermocouples. Overall, the parallel thermocouple is better than the welded thermocouple. The parallel thermocouple gives small average thermal contact resistance $average\ R" = 0.00001\ (m2.℃/W)$, and consistence values of water temperature and heat transfer coefficient h, with good repeatability and sensitivity. Consequently, a non-invasive energy flow rate meter or (BTU) meter can be used to estimate the flow rate and the fluid temperature in real life.

Non-invasive Method to Measure Energy Flow Rate in a Pipe

Mohammed A. Alanazi

General Audience Abstract

Today, the measuring energy flow rate, measuring flow rate and the fluid temperature, in a pipe is crucial in many engineering fields. In addition, there has been increased use of energy flow rate meters in the renewable energy system and other applications such as solar thermal and geothermal to estimate the useful thermal energy. Some of the commercial energy flow rate meters are using an invasive sensor, has to be inside the pipe, including turbine flow meter and vortex shedding device. These systems are expensive and difficult to install. A new approach that uses non-invasive sensors, attached on the outside of the pipe, that are easy to install and less expensive has been developed by using the heat flux and temperature measurements. A parameter estimation routine was used to analyze the data which depends on the minimum root mean square RMS error between the calculated and experimental temperature values. A correlation between the unknown parameter, heat transfer coefficient (h), and the measured flow rate Q was done to estimate the flow rate. The results show that the new non-invasive system has good repeatability, 15.45%, high sensitivity, and it is easy to install. Consequently, a non-invasive energy flow rate meter or (BTU) meter can be used to estimate the flow rate and the fluid temperature in real life.

This work received support from King Saud University (KSU) and Saudi Culture Mission (SACM) Scholarship.

would like to express my respects and acknowledgments to

- My research advisor Dr. Tom Diller for his support and patience.
- My dissertation committee member: Dr. Brian Vick and Dr. Scott T. Huxtable.
- Support of King Saud University (KSU), and Saudi Arabian Culture Mission (SACM) Scholarship.
- All Faculty and staff members of the ME Department at Virginia Tech.
- To graduate school at Virginia Tech.
- To my family in Saudi Arabia.
- To my wife and daughters in United State of America.
- To Flux Teq, LCC, for their partneship.

Table of contents

List of Figures

List of Tables

Nomenclature

Q	Flow Rate	$(Gallon/Minute)$
h	Heat Transfer Coefficient	$(W/m2.℃)$
U	Overall Heat Transfer Coefficient	$(W/m2.℃)$
Re	Reynolds Number	$(-)$
Nu	Nusselt Number	$(-)$
$q"$	Heat Flux	$(W/m2)$
$R"$	Thermal Contact Resistance	$(m2.℃/W)$
RMS	Root Mean Square Error	$(-)$
T_w	Water Temperature	$(℃)$
T	Wall pipe Temperature	$(℃)$
τ	Time Constant	$(second)$
ρ	Pipe Density	$(Kg/m3)$
δ	Pipe Thickness	(mm)
C	Heat capacity of Pipe	$(KJ/Kg.℃)$
Qc	Calculated Flow Rate	$(Gallon/Minute)$
Qm	Measured Flow Rate	$(Gallon/Minute)$
t	Time	$(Second)$
ΔT_{wall}	Difference Wall Pipe Temperature	$(℃)$
q_s''	Sensor Heat Flux	$(W/m2)$
T_s	Measured Sensor Temperature	$(℃)$
T_{SC}	Calculated Sensor Temperature	$(℃)$
S	Sensor Sensitivity	$\mu V/(W/m2)$
E	Voltage	$(Volte)$
ε	Seebeck coefficient	$(-)$
R	Heater Resistance	(Ω)
V	Water Velocity	(m/s)

A	Heater Area	$(mm2)$
D	Pipe Diameter	(mm)
$H(t-t_j)$	Step Unit	$(-)$
Un	Uncertainty	$(\%)$
$Un, \Delta T$	Uncertainty of Thermocouple	$(\%\ of\ ℃)$
$Un, q"$	Uncertainty of Heat Flux Sensor	$(\%\ of\ W/m2)$
A	Cross Section Pipe Area	$(mm2)$
k	Water Thermal Conductivity	$(\frac{W}{m}.℃)$
υ	Kinematic Viscosity	$(m2/s)$

Chapter 1-Introduction

An energy flowmeter is a meter that measures both flow rate and temperature to determine the energy carried by a fluid. As the demand for energy is increasing, the importance of energy flowmeter devices is increasing. Because cost and quality are important to the customer and supplier[1], the energy supply companies care about the accuracy and precision of energy flowmeters to measure energy consumption. Some of the commercial and industrial sectors applications that using energy flowmeters are chiller water sub-metering, boiler feed water, thermal storage, geothermal, renewable, solar-hot water, chemical feed, power plants, energy consulting, biomass metering, waste heat recovery, HVAC, and supplying water [11]. In 2012, there are more than 54,000 new commercial buildings that are using chilled water in the USA [12]. In 2010, the USA had approximately 33,462 solar water heating installation systems [13]. As energy costs are increasing, measurements with flow rate devices are essential in many engineering applications [1]. The high cost of energy flowmeter devices has been a significant barrier to be implemented in many applications for central district cooling or heating systems, hydronic HVAC systems, and renewable systems [10]. The current market size of flowmeter devices has been estimated at $700 million per year globally [2].

The most famous devices used in many energy markets are vortex, Coriolis, orifice plate, venturi tube, axial turbine, electromagnetic, and ultrasonic [1]. The vortex shedding device has been used for the past from 25 to 30 years [8]. It operates under the vortex shedding principle which is an invasive sensor with a shedder bar [5]. It has an accuracy of approximately 1% or better [8]. It is well regarded to be reliable and flexible. However, its cost is over $ 1000 and must be mounted inside the pipe [2]. It is used for both gas and liquid flows and a wider range of flow rates [7]. In the 1980s, the Coriolis flowmeter was developed to fill the gap for mass flow rate measurements [8]. It operates by using two invasive vibrating tubes from the inlet to the outlet [3]. It can be used for multiphase flow and is common in the petroleum industry. It is not directly sensitive to density, viscosity, and temperature [7]. The repeatability and

accuracy of Coriolis flow meter, FMC-5500 series, for the liquid phase are 0.25% and 0.5 respectively [6]. However, its cost is more than $10000 [6]. The simplest and cheapest type of differential pressure meter is the orifice plate [8]. It operates under two invasive orifice plates in the top and bottom of a pipe [8]. It has pressure tapings to measure pressure drop [8]. It can be measured the flow rate from the pressure drop and the fluid density in this device. The oldest type of differential pressure meter is the venturi meter [8]. In 1887, the first venturi meter was used in an industrial application [8]. It is more expensive and more difficult to manufacture this device [8]. The axial turbine meter operates by an invasive turbine rotor in a pipe [7]. It has an uncertainty of 0.5% for liquids and 1.5% for gases [7]. It can be used for any pipe size diameter from ¼ inch to 30 inches [8]. It has a lower initial cost, but it requires more maintenance, testing, and recalibration [8]. The electromagnetic flow meter has been used for many years [8]. It depends on Faraday's law of induction [8]. It measures the flow rate by generating a magnetic field passing through the flow tube from magnetic coils [8]. It is non-invasive and easy to install [8]. In most many applications, the accuracy is from 0.5% to 2%, but in some problematic applications its accuracy is 5% [7]. The ultrasonic flowmeter development began as a joint project between government and private industries in the 1950's [4]. In the late 1960's and 1970's, it was brought into commercial applications [4]. It operates by two opposite ultrasonic transducers across the pipe [4]. It has a relationship between the speed of sound and the flow [4]. It has an accuracy of approximately 1% [4]. According to the most of ultrasonic flowmeter private industries, the ultrasonic flowmeter has cost between $1500 to $3000, but it is hard to calibrate. Further development these systems need to be developed to make them non-invasive and to optimize the cost and ease of installation.

A new approach, non-invasive thermal interrogation using heat flux and temperature measurements, has been developed in this paper to estimate the water temperature and flow rate in a pipe. The system is non-invasive, less expensive, and easy to install. The heater, heat flux sensor, and thermocouples are mounted on the top of a pipe respectively. A one-dimensional transient thermal

model, using lumped capacitance method (LCM), is developed to simplify the data processing. A parameter estimation routine was used to estimate the optimal values of heat transfer coefficient (h), time constant (τ), thermal contact resistance (R"), and water temperature (T_w). The sole aim of this paper is providing a correlation between the flow rate and heat transfer coefficient (h) to estimate the flow rate in real life. It is anticipated that the type of device will be used as part of intelligent control for energy systems.

Chapter 2- System Design and Analysis

2.1- Experimental Method

A non-invasive method to estimate the unknown parameters of a flowing fluid in a pipe was developed based on the temperature response to a measured heat flux event on the outside surface of the pipe. A heat flux sensor (PHFS) was developed at our lab to measure the heat flux coming from the heat source (electric heater) to the heat sink (water in the pipe) (fig.1). A T-type thin-foil thermocouple was used to measure the sensor temperature. It can be made in our lab by using thermocouple wires and constantan and copper foil. The temperature measurement of the pipe is a crucial measurement in non-invasive system. It is a challenge to minimize the thermal contact resistance between the thermocouple and the pipe surface. To test how to minimize the thermal contact resistance $R"$ between the thermocouple thickness and the pipe surface, two thermocouples, welded and parallel, were tested together in the same set-up (fig.2). An electric heater was purchased to provide the heat source to the pipe.

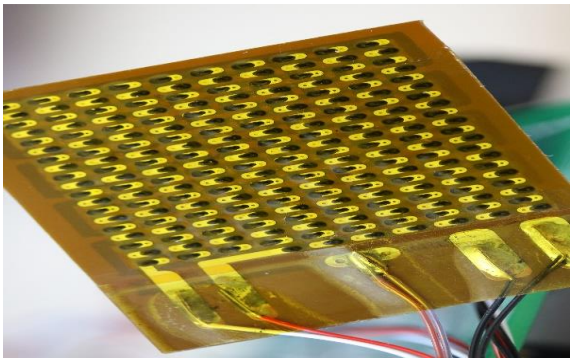

Fig. 1 Heat Flux Sensor (PHFS).

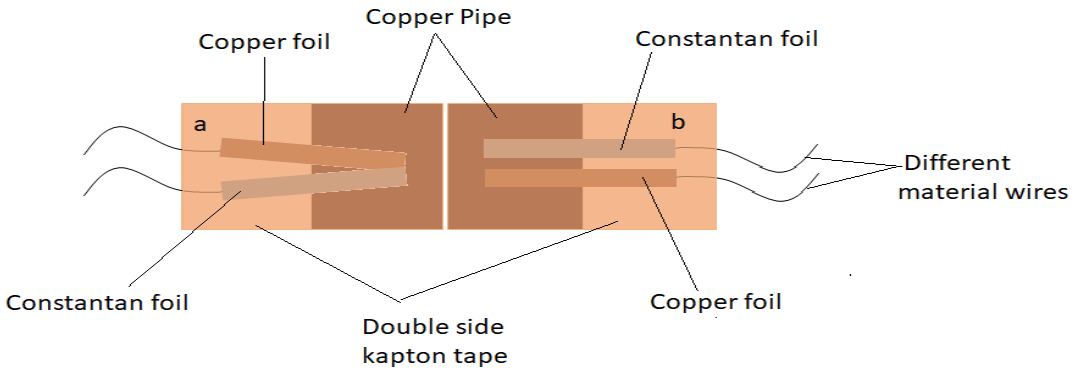

Fig. 2 (a) T-type thin-foil welded thermocouple. (b) T-type thin-foil parallel thermocouple.

According to figure 3, a lumped capacitance method (LCM) was used to analyze the system as a transient conduction problem. LCM is the simplest and most convenient method that can be used to solve transient heating and cooling problems. It is valid for a high thermal conductivity material with a small thickness, in this case, 1.27 mm. The non-invasive system is mounted on the top of a polished copper pipe by using a compression wrap. The system is covered by an insulation material to minimize heat lost to the outside environment. The electric heater is larger than the heat flux sensor (PHFS) and thermocouple to ensure one-dimensional heat transfer through the sensor. The PHFS is located on the top of the thermocouples to measure the heat flux at the same point as the temperature is measured. A single Kapton tape is located between the thermocouples and the PHFS. In fact, there is a contact resistance between the thermocouples and PHFS, but it was neglected because it is not needed in the model. The two thermocouples are located at the top of the pipe surface with the thermal contact resistance, $R"$, between the pipe and the thermocouples. The internal thermal resistance in the pipe was neglected because of the small pipe thickness. The water is flowing inside the pipe acting as the heat sink for the system. It has a heat transfer coefficient, h, and water temperature, T_w, as unknown parameters. There are two types of heat transfer coming and leaving the pipe thickness. The heat flux conduction through the PHFS is coming to the pipe thickness which increases the thermocouple temperature. The heat flux

convection to the water is leaving the pipe thickness which creates the heat transfer coefficient (h). The sensor heat flux measurements,q_s'', and the sensor temperature response are known from the experiment. From them, the wall pipe temperature governing equation is determined.

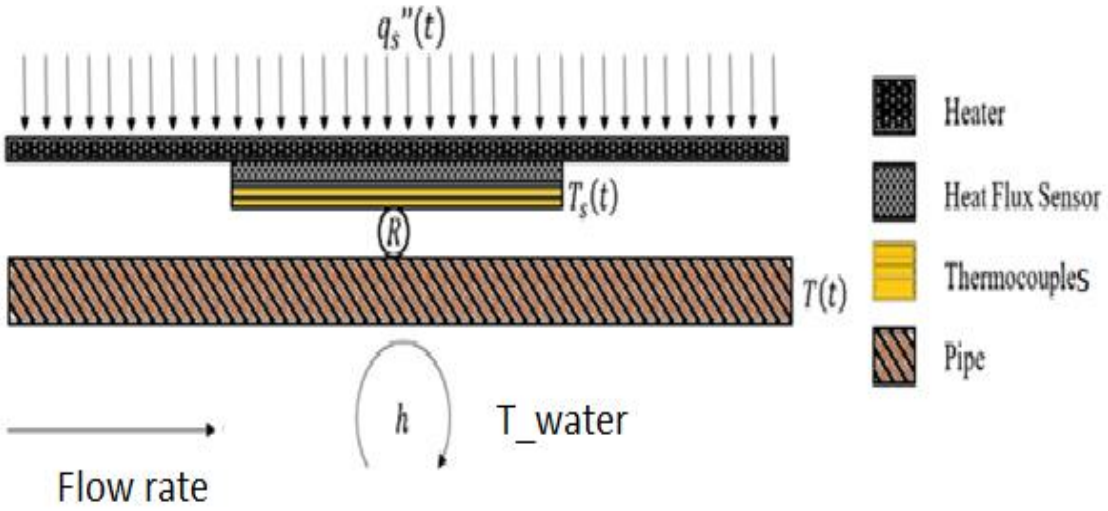

Fig. 3 System Design.

2.2- Assumptions

There are three important assumptions used in order to develop the analytical model. The first assumption, the water temperature is constant during the experimental measurement and was calculated at steady state $t = 0$. This assumption is valid because the difference in water temperature at $t = 0$ and $t = \infty$ is very small approximately $\Delta T = 0.10$ ℃. The second assumption, the internal heat conduction through the pipe thickness was assumed to be negligible. This assumption is valid because the difference in temperature between the inner and outer pipe surface calculation is very small approximately $\Delta T_{wall} = 0.02$ ℃. The last assumption, one -dimensional thermal conduction along the radial direction of

the pipe was assumed for the model. It is valid because the axial thermal conduction along the pipe under the sensor was negligible.

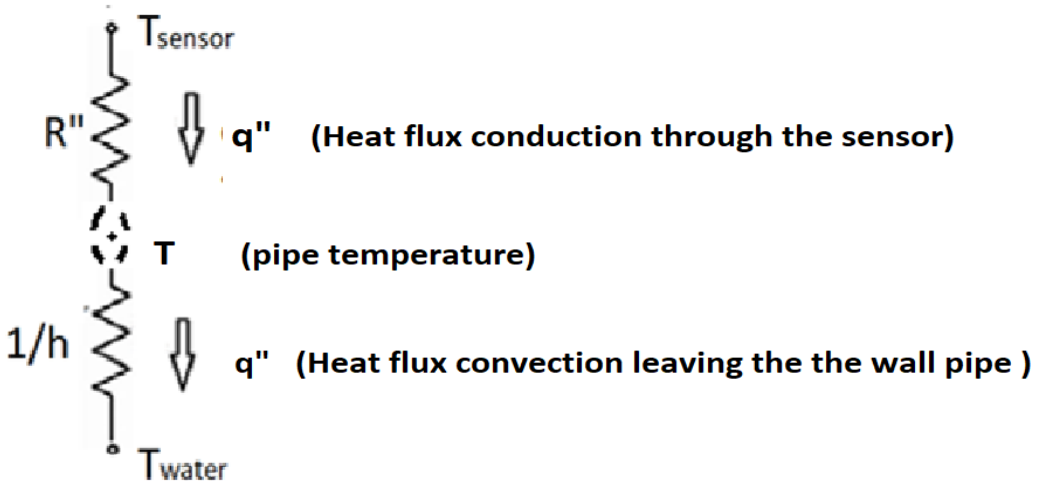

Fig.4 Equivalent thermal circuit for a series model.

2.3- Mathematical Solution

In this system, the heat flux is used as input in the model rather than the temperature. According to previous research, it hard to use the temperature measurements as input values in a model because the output calculation heat flux has more noise and is not as accurate [9]. According to figure 4&5, the mathematical model has been investigated from the energy balance on the control volume around the thickness of the pipe. Based on the Lumped capacitance method, the governing equation is

$$\rho C\delta \frac{dT}{dt} = q''_{conduction\ through\ the\ sensor\ to\ the\ pipe} - q''_{convection\ from\ the\ pipe\ to\ the\ water} \quad (1)$$

Where $\rho C\delta$ is the thermal storage of the wall pipe, $\rho(Kg/m3)$ is the density of copper pipe, C (KJ/Kg.℃) is the heat capacity of the copper pipe, δ(m) is the pipe thickness, $q''_{convection\ from\ the\ pipe\ to\ the\ water}$ (W/m2) is $h(T - T_w)$, $q''_{conduction\ through\ the\ sensor\ to\ the\ pipe}$(W/m2) is q''_s ,h $(W/m2.℃)$ is the heat

transfer coefficient, T (℃) is the pipe wall temperature, and T_w (℃) is the water temperature. In terms of the variables the governing equation is

$$\rho C\delta \frac{dT}{dt} = q_s'' - h(T - T_w) \quad (2)$$

To solve the differential equation, assume that $\theta = (T - T_w)$ and the time constant

$\tau = \frac{\rho \delta C}{h}$ (second), so the final governing equation is

$$\tau \frac{d\theta}{dt} = \frac{q_s''}{h} - \theta \quad (3)$$

To get the final solution of the differential equation, apply the assumption for the water temperature which is constant during the experiment. The water temperature is calculated at time zero.

$$T_w = T(0) - \frac{q_s''(0)}{h} \quad (4)$$

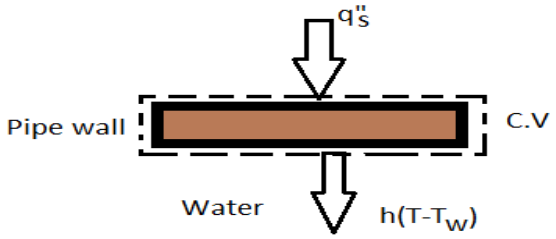

Fig. 5 Energy Balance around the pipe wall.

Where $T(0)$ is the wall pipe temperature at $t = 0$. To find the wall pipe temperature at $t = 0$, applying the energy balance around the sensor by using figure 6. The pipe wall temperature at steady state is

$$T(0) = T_s(0) - R".q_s''(0) \quad (5)$$

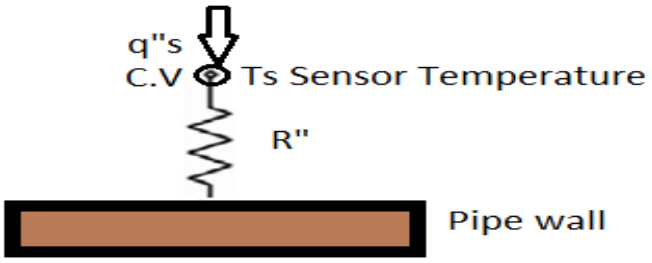

Fig. 6 Energy balance around the sensor.

For a single step input of heat at $t = t_o$ (fig.7), the solution of equation 3 for the wall pipe temperature is

$$T(t) = T_s\,(0) - R".q_s''(0) + \frac{q_{s,1}'' - q_{s,0}''}{h}(1 - e^{\frac{-(t1-t_0)}{\tau}}) \qquad (6)$$

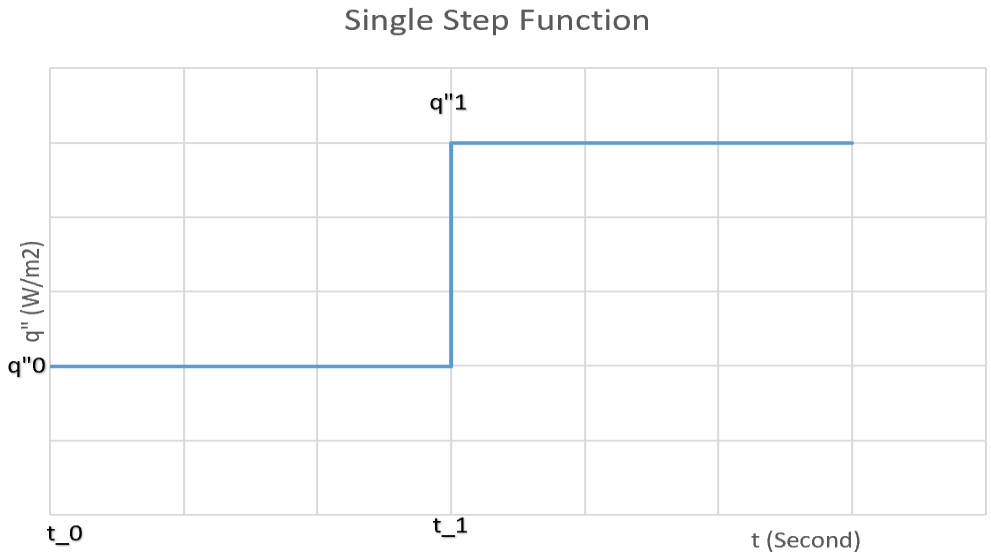

Fig. 7 Single step Function.

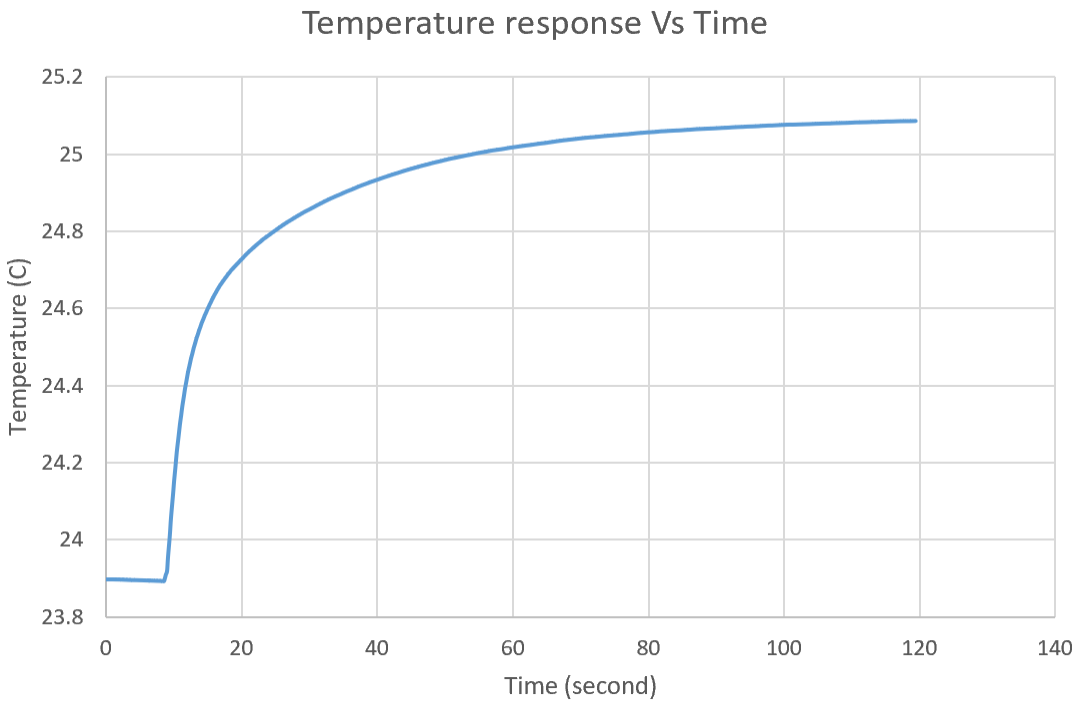

Fig. 8 Corresponding Temperature Solution.

According to the superposition principle, the total solution of the wall pipe temperature is

$$T_{total}(t) = Tsteady\ state(t) + Ttransient(t)$$

The input heat flux can be written as steady state plus transient $q_s''(t)=q_s''(0) + \sum_{j=1}^{k-1} \Delta q_{s,j}''\, H(t-t_j)$,

where $H(t-t_j)$ is the step function and $\Delta q_{s,j}''$ = ($q_{s,j}''$- $q_{s,j-1}''$). Write the total solution with the variable θ

$\theta(t)=\theta(0) + \sum_{j=1}^{k-1} \Delta q_{s,j}''.\Psi(t-t_j)$.

Where $\theta_{transient} = \Delta q_{s,j}''.\Psi(t-t_j)$ and $\theta_{steady\ state} = \theta(0)$. According to the unit source problem solution (table. 1), the governing equation is

$$\rho C\delta \frac{\partial \Psi}{\partial t} = 1 - h\Psi \qquad (7)$$

or

$$\frac{\partial \Psi}{\partial t} = \frac{1}{\rho c \delta} - \frac{1}{\tau}\Psi \tag{8}$$

With the initial condition $\Psi = 0$, t=0, the solution is

$$\Psi(\mathrm{t}) = \frac{1}{\mathrm{h}}(1 - e^{-\frac{t}{\tau}}) \tag{9}$$

For multiple steps (fig.9), the final wall pipe temperature becomes

$$T_k(t) = T_s(0) - R''.q_s''(0) + \sum_{j=1}^{k-1} \frac{\Delta q_{s,j}''}{h}\left(1 - e^{-\frac{(t_k - t_j)}{\tau}}\right).H(t_k - t_j) \tag{10}$$

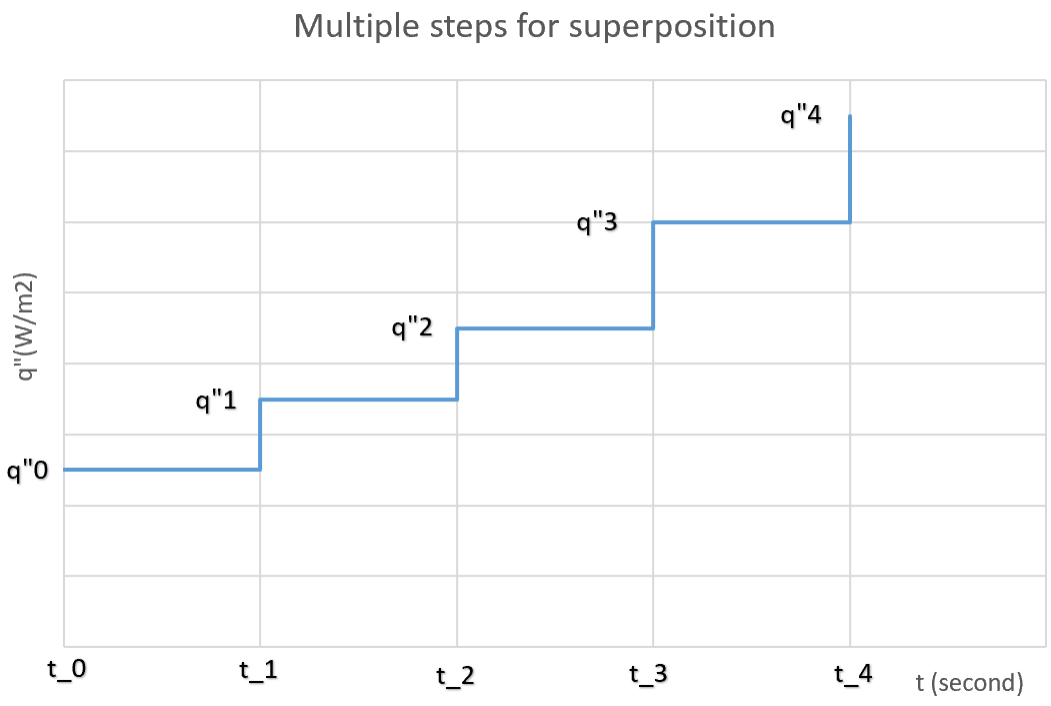

Fig. 9 Multiple steps Function.

Table 1 Unit problem solution.

	Unit Source Problem	Unit Initial condition Problem
Governing Equations	$\frac{\partial \Psi}{\partial t}+\frac{1}{\tau}\Psi=1$ $\Psi=0, \mathrm{t}=0$	$\frac{\partial \Psi}{\partial t}+\frac{1}{\tau}\Psi=0$ $\Psi=1, \mathrm{t}=0$
Solutions	$\Psi(\mathrm{t})=\ \tau\left(1-e^{-\frac{t}{\tau}}\right).H(t)$	$\Psi(\mathrm{t})=\left(e^{-\frac{t}{\tau}}\right).H(t)$

2.4- Parameter Estimation

Three parameters, heat transfer coefficient h, the thermal contact resistance between the pipe surface and thermocouple thickness R", and the time constant τ, were treated as unknown parameters in this problem. They were estimated from the input measurement data, time t in seconds, sensor heat flux $q"_s$ $(W/m2)$, and sensor measured temperature $T_{s,k}$ (℃). The parameters h and τ are estimated independent in of each other. The thermal contact resistance R" is calculated from the previous iteration values.

According to the flow chart in figure 10, a mat-lab parameter estimation code the range of values of h and τ are estimated in two "for loops". For the value of h the code will search for all τ values. For the first iteration the value of R" was estimated as 0.0006 $(m2.℃/W)$. It was then calculated from the data for each subsequent iteration. The wall pipe temperature is calculated based on these parameters. The new estimation of R" for each data point is calculated by

$$R"_k=\frac{T_{s,k}-T_k}{q''_{s,k}} \quad (11)$$

Where $T_{s,k}$ is the sensor measured temperature, T_k is the wall pipe calculated temperature, and $q''_{s,k}$ is the measured heat flux by the sensor. The new average of $R"_k$ values is used as the initial estimation value at the second iteration and it is calculated by

$$R" = \frac{R"_k}{N} \tag{12}$$

Where N is the number of data taken. Now, it is ready to calculate the sensor temperature $T_{SC,k}$ for each data point by using

$$T_{SC,k} = T_k(t) + R" * q''_{s,k} \tag{13}$$

To optimize the model, the root mean square error (RMS) method was used to fit the curve into the model which is giving the minimum error by using

$$RMS = \sqrt{\sum_{K=1}^{N} \frac{\left(T_{SC,k} - T_{s,k}\right)^2}{N}} \tag{14}$$

The overall heat transfer coefficient (U) depends on the optimal parameter values of h and $R"$, which is

$$U = \frac{1}{R" + \frac{1}{h}} \tag{15}$$

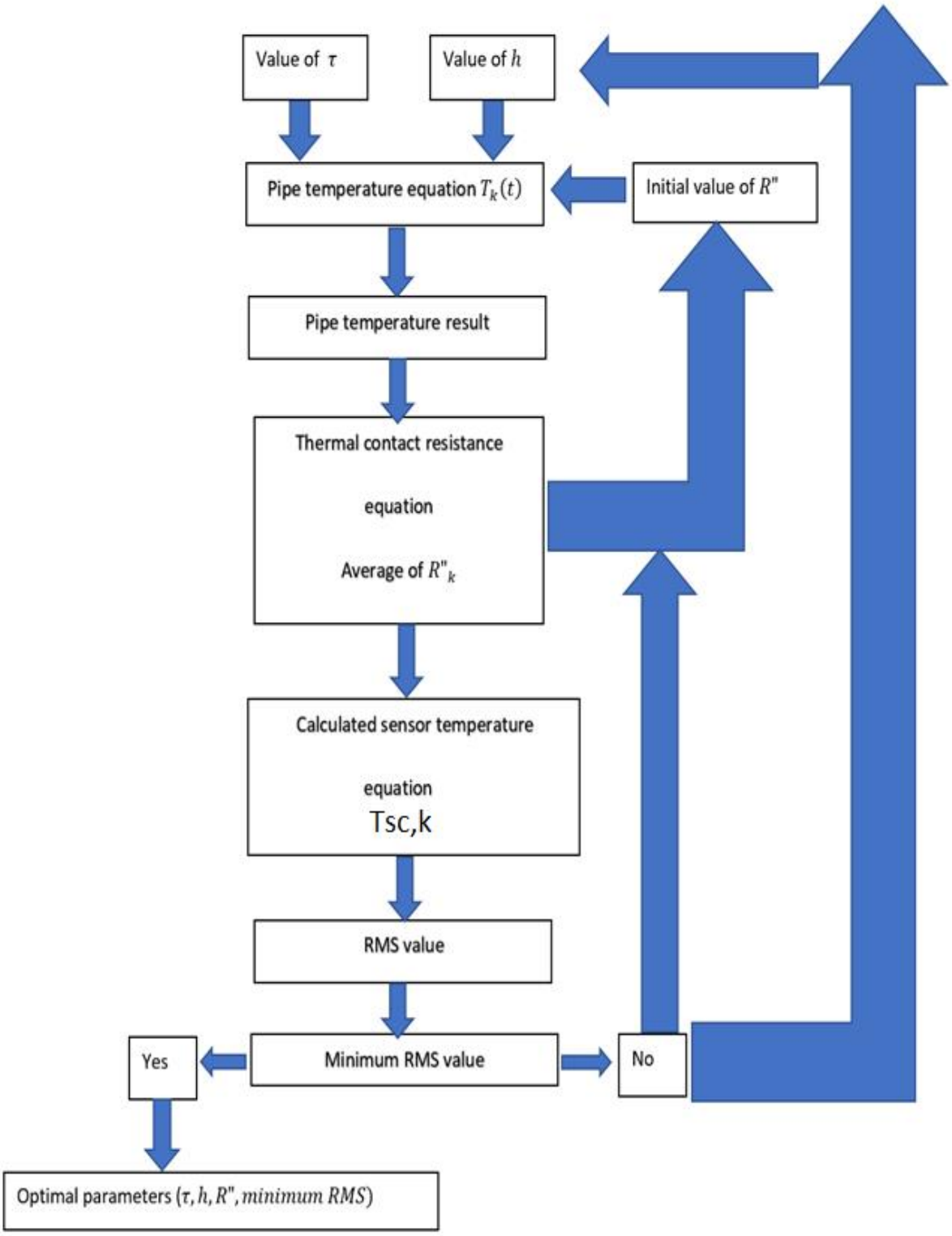

Fig.10 Flow chart for the optimal parameter estimation.

According to figure 11&12, the RMS error for the h and τ calculation will be decreased until the minimum error is achieved and the optimal parameters will be known. If the error does not achieve the minimum error, the code will go back to take the average thermal contact resistance R" and put it as initial estimation value to the next iterations until the minimum error is achieved. After getting the optimal parameters, the water temperature is calculated by using Eq 4&5.

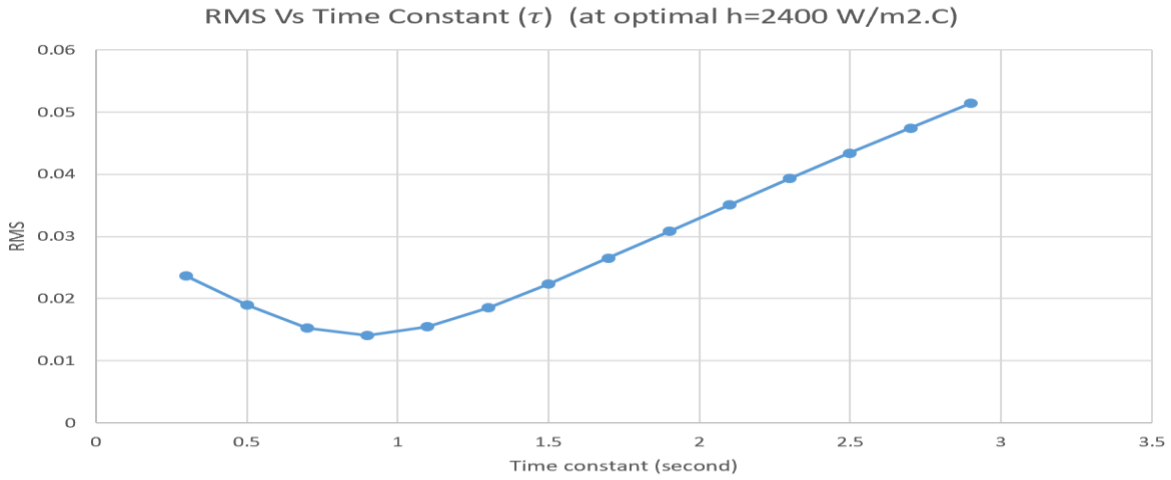

Fig.11 Illustration of minimum RMS value and the optimal time constant for the parallel thermocouple.

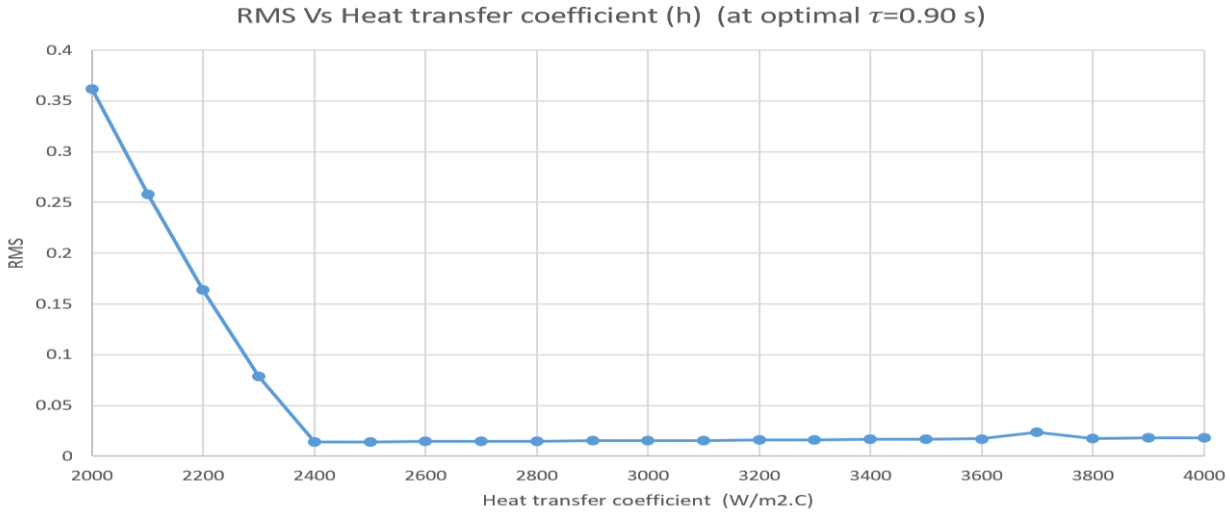

Fig.12 Illustration of minimum RMS value and the optimal heat transfer coefficient for the parallel thermocouple.

According to figure 13, this parameter estimation routine provided a good match temperature curves between the measurement and theoretical sensor temperature. The wall pipe calculated temperature was very close to the sensor calculated temperature which indicates that the thermal contact resistance R" is very small. Numerical values are listed in table 2, for this case of a parallel thermocouple and a flow rate of 5.7 gallon/minute. The results illustrate that the parameter estimation routine gave a small thermal contact resistance R", small time constant τ, small error value RMS, the water temperature T_w, and the heat transfer coefficient h.

Table 2 Optimal Parameters Estimation results for Figure 13.

Flow rate (gallon/minute)	Thermocouple	h (W/m2.℃)	τ (second)	R'' (m2.℃/W)	T_w (℃)	Minimum RMS
5.7	Parallel	2400	0.90	0.0000169	23.84	0.0141

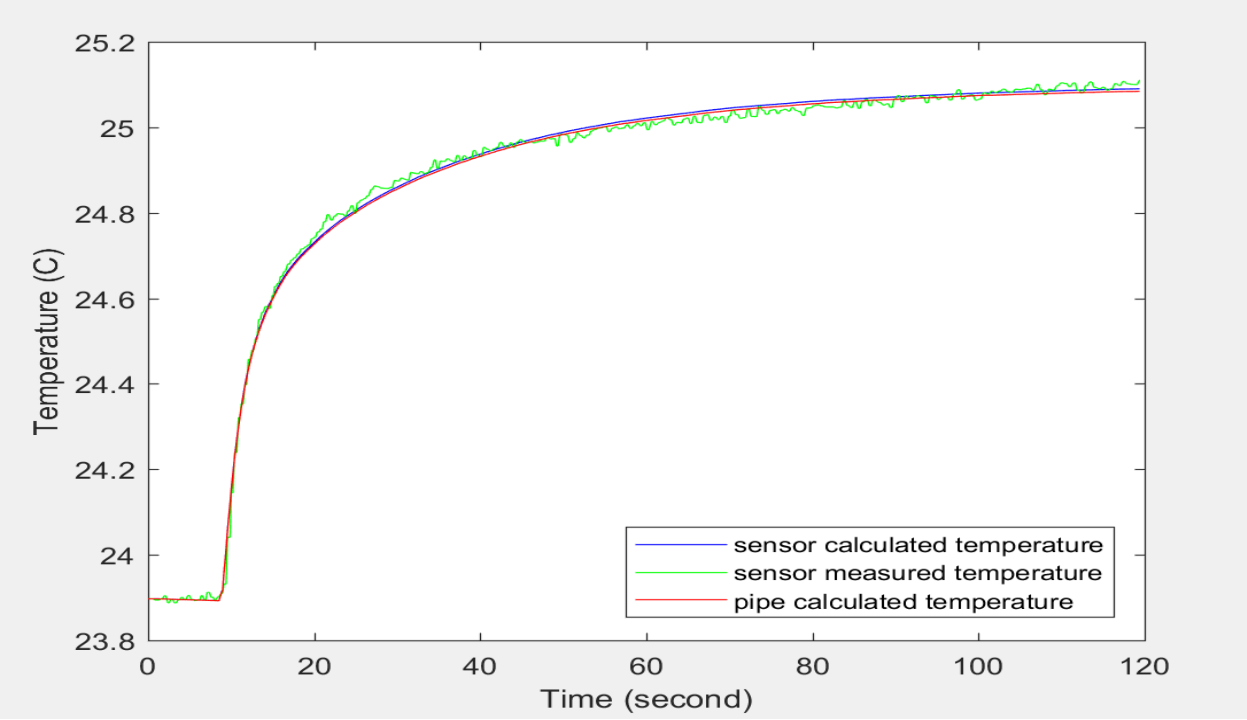

Fig.13 Measured and Analytical temperature curves result.

Chapter 3-Experimental Testing

3.1- Energy Flow Meter (BTU Meter)

A non-invasive BTU meter was designed consisting of three main parts: electric heater, heat flux sensor (PHFS), and T-type thin-foil thermocouples. This was built and tested on a pipe over a range of water flow rates.

3.1.1-Heat Flux Sensor (PHFS)

An inexpensive heat flux sensor (PHFS) was developed in our lab since 2015, and it has been used for many applications to measure the heat flux values. A PHFS-01 (1-inch by 1-inch square) was used with a sensitivity of S=0.77 μV/(W/m2) with a quoted accuracy of 5%. It has an overall thickness of 0.254 mm. It was calibrated by using a conduction calibration system at temperature 25℃ by FluxTeq LLC company and can be used for any operating temperature less than 150 ℃. It was located between the electric heater and the thermocouples on the top of the pipe. It receives heat from the heater which is measured as heat flux through the sensor. According to figure 14, the white and red wires on the left side measure the heat flux values by using a differential thermopile. They are connected to a data acquisition instrument which displays the voltages on the computer screen and then converted into the heat flux values $(W/m2)$ by using equation 16 (fig.15).

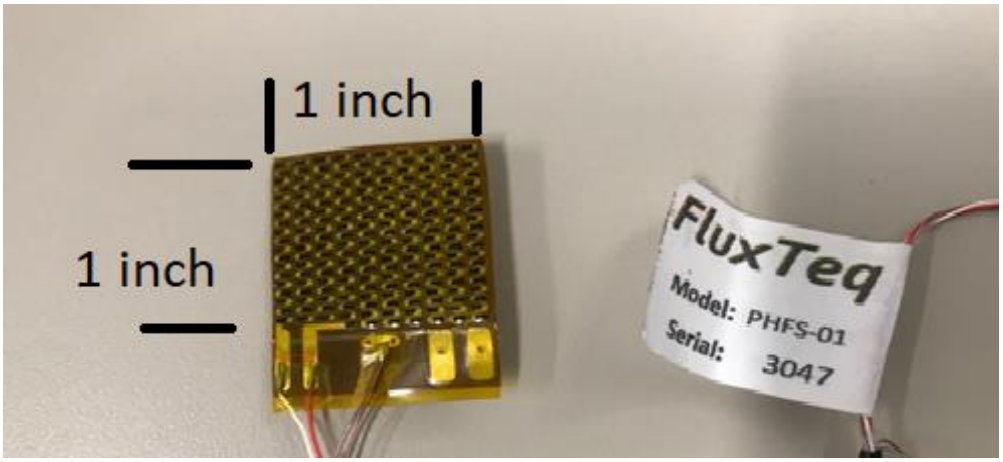

Fig. 14 FluxTeq LCC Heat Flux Sensor (PHFS).

$$q" = \frac{Voltage}{S} \ (W/m2) \tag{16}$$

Where S is the PHFS-01 sensitivity in $\mu V/(W/m2)$.

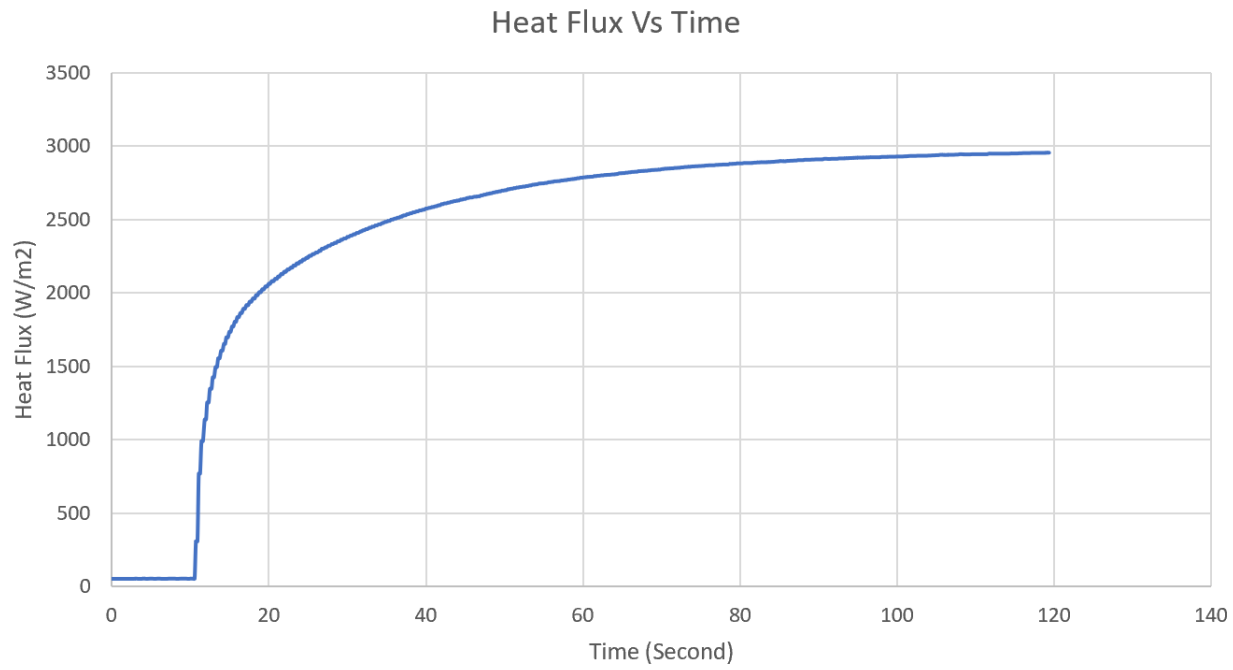

Fig. 15 Typical Heat Flux Values from the Data Acquisition System.

3.1.2- Thermocouples

In this system, different two T-type thin-foil thermocouples, welded and parallel, were tested to minimize the contact resistance between the thermocouple and the pipe surface. They were made in our lab by using thermocouple wires, different material foils, and solder. The thermocouple wire was selected with a diameter of 0.25 mm, and the foils were selected with a thickness of 0.0125 mm, a length of 4.826 mm, and a width of 6.858 mm. The thermocouple wires were soldered with the foils at the end. Thermocouples depend on the Seebeck coefficient (ε) of the two conductors and a material property [7]. According to figure 16, when the wires of two different materials, copper and constantan, are connected, the voltage output that occurs depends on the temperature difference between the free ends of the two wires and the junction between the two wires [7].

$$Voltage\ (E) = \varepsilon(T - T_{Ref}) \tag{17}$$

Where ε is Seebeck coefficient for copper and constantan materials. The two thermocouples are located between the pipe surface and the PHFS.

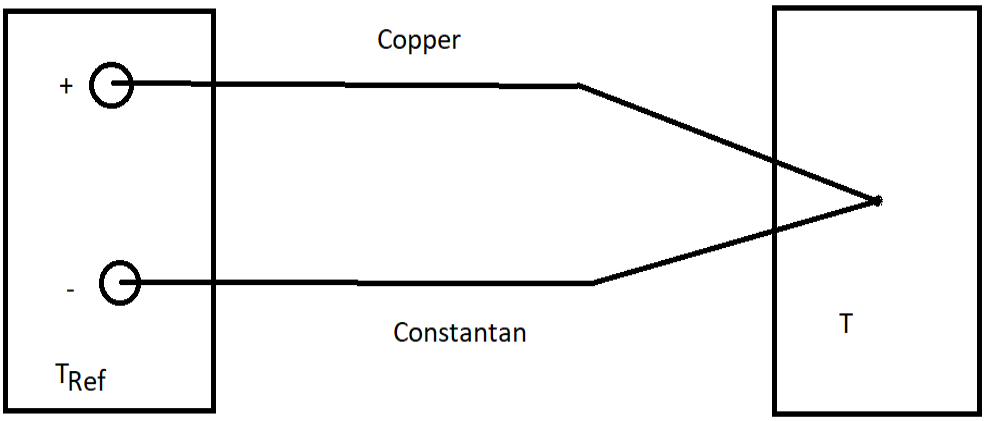

Fig. 16 Net voltage when different materials are connected.

According to figure 17, the welded thermocouple, the foils are welded by using HUGHES welder directly over each other at the end. The resulting thermocouple is mounted directly on the pipe. The other ends are soldered with the thermocouple wire. These junctions are placed on a double side Kapton tape to electrically insulate this end of the thermocouple. A single layer of Kapton tape is placed over top of the thermocouple to keep it in place. Cares taken to ensure that there is no air gap between the foils and the pipe surface.

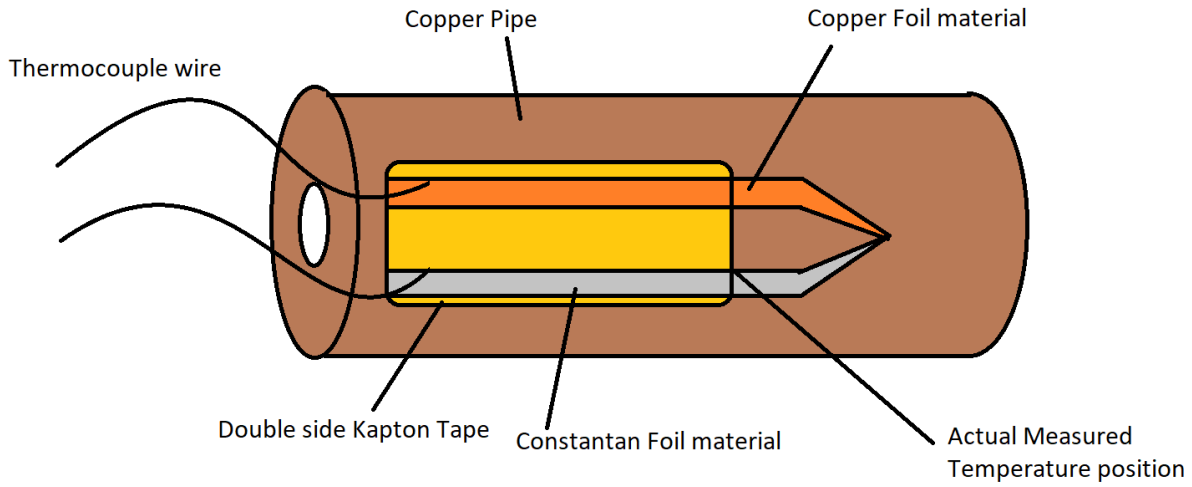

Fig. 17 Actual measured temperature position for the welded thermocouple.

According to figure 18, the parallel thermocouple, the foils are not contacted or welded directly with each other, but they are placed directly on the pipe at the end. The other ends are soldered with the thermocouple wire. These junctions are placed on a double side Kapton tape to electrically insulate this end of the thermocouple. A single layer of Kapton tape is placed over top of the thermocouple to keep it in place. Cares taken to ensure that there is no air gap between the foils and the pipe surface.

To make sure the water temperature is still constant during the experiment a K-type thermocouple was used to measure water temperature. It was plugged in a data acquisition see figure 22 and it was located in the drum water supply directly.

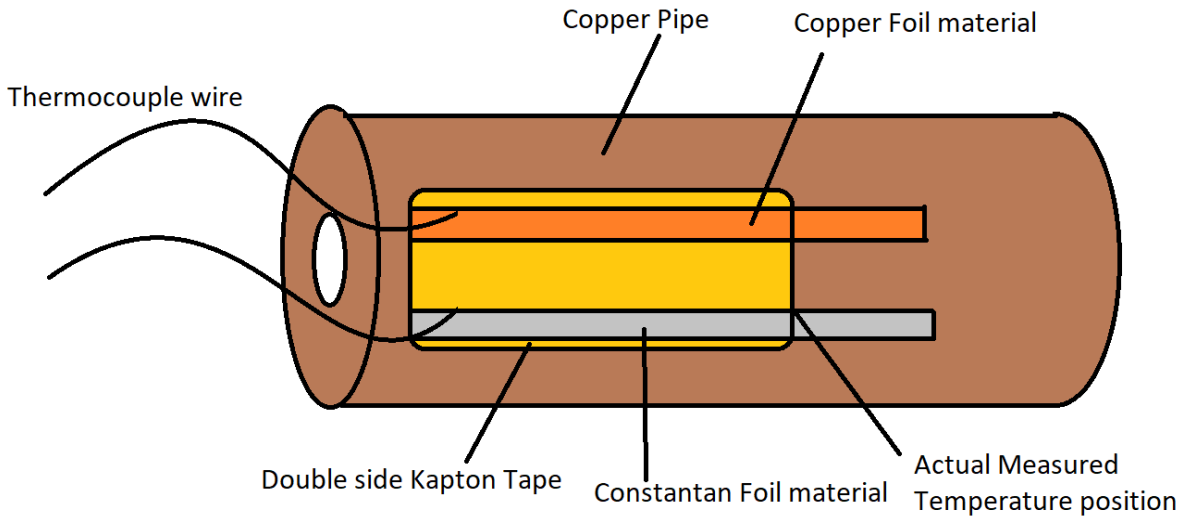

Fig. 18 Actual measured temperature position for the parallel thermocouple.

Fig. 19 HUGHES Welding Machine.

3.1.3- Electric Heater

An Omega electric heater (3 inches by 3 inches square) was purchased and used in this system to provide the input heat flux. It has an electrical resistance of 140 ohms, and it was plugged into a DC power supply which was used to provide 49.38 volts. The heat flux value was calculated using Eq. 18 which gave a maximum value is 3000$W/m2$. When data was taken, the heater was switched on after 10 seconds until it reached at steady state to compare the PHFS temperature before and during the event. Compression wrap was placed over the heater to hold it firmly in position. The heat flux calculation value is

$$q''_{heater} = \frac{E^2}{R}A \tag{18}$$

Where A is the heater area, E is the voltage, q''_{heater} is the heater heat flux $W/m2$, and R is the heater resistance. Only a portion of the heat goes through the sensor to the pipe.

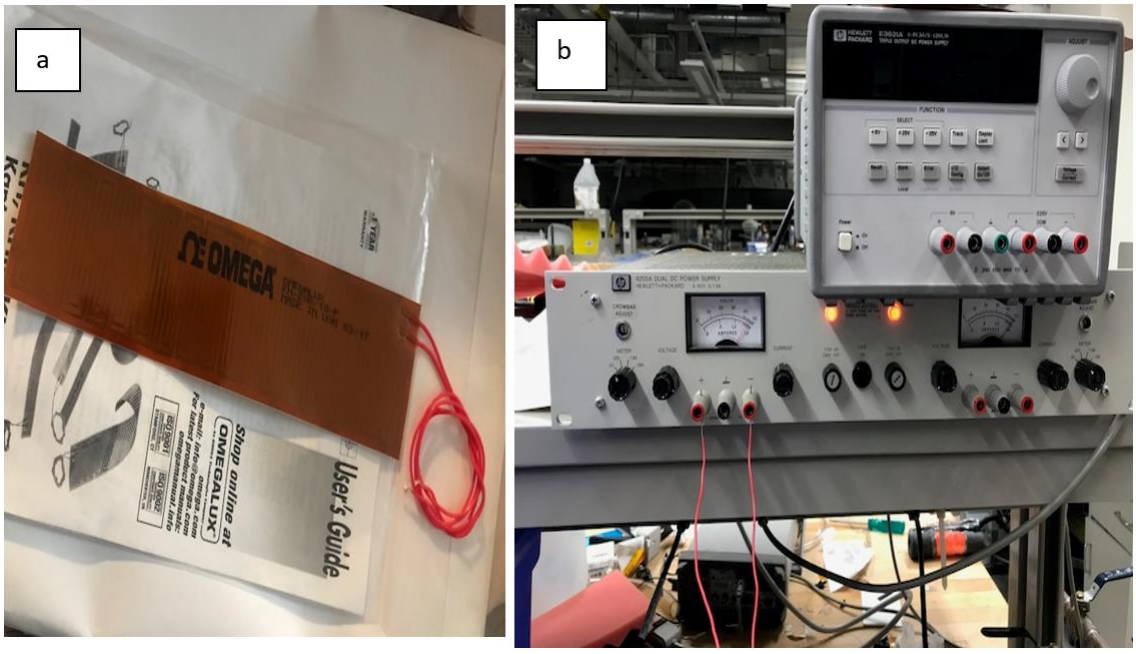

Fig. 20 (a) Omega electric heater. (b) DC power supplier.

3.2- Experimental Test

3.2.1- Experimental Test Apparatus

To test the performance of the BTU meter, an experimental apparatus was designed and constructed as shown in figure 22. The design was selected as a small piping system. To satisfy our assumptions, we selected a thin copper pipe with an internal diameter of $D = 19.5\ mm$ and thickness $\delta = 1.27\ mm$ because it has high thermal conductivity. The pipe was connected to an electric pump which is located in a 20-gallon drum to drive the water inside the system as a closed system. A manual control valve was used to control the flow rate during the experiment. The BTU meter or the energy flow meter was mounted on the top of a polished copper pipe by a compression wrap and an insulation material as shown at the front of the table in figure 21.

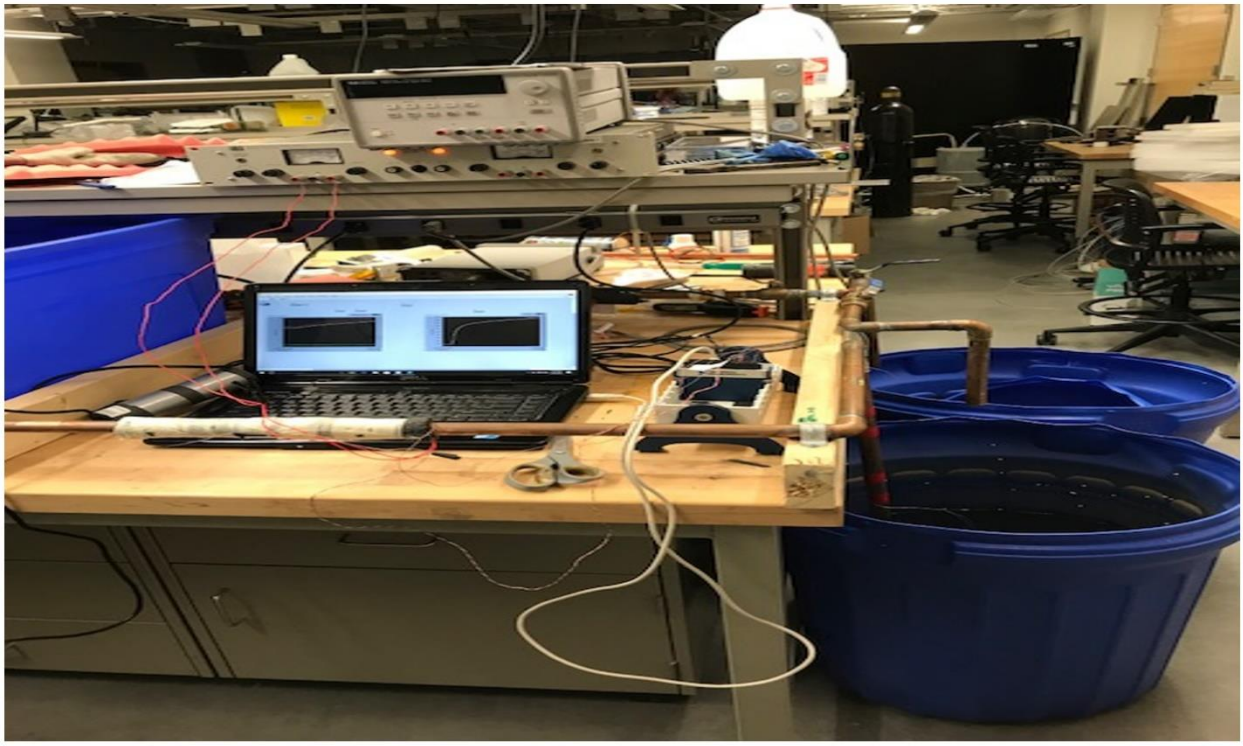

Fig. 21 Experiment set-up when the experiment was taken.

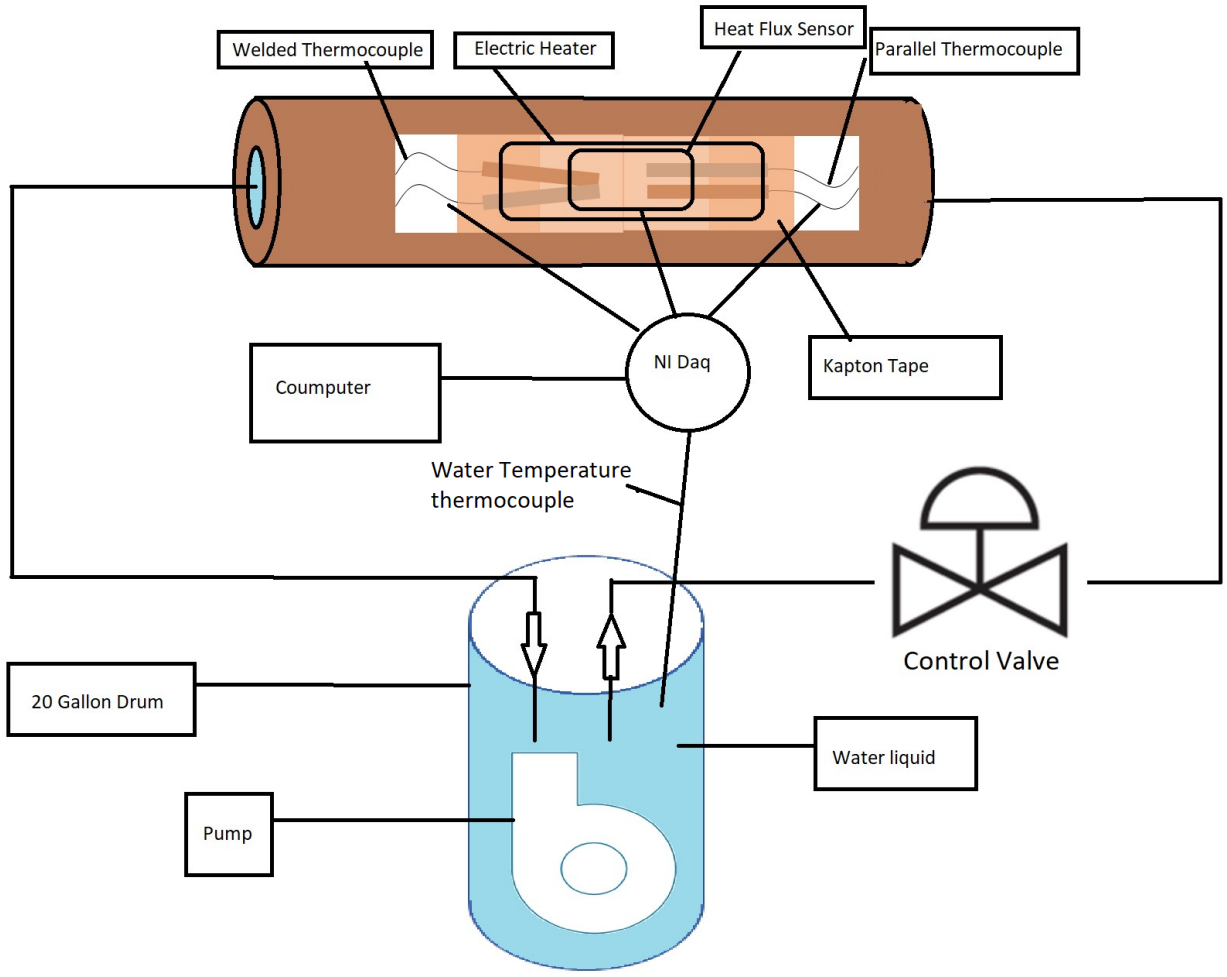

Fig. 22 Schematic of experimental set-up.

3.2.2- Measuring Flow Rate

Before the data was taken, the flow rate was measured by timing the filling of a 20-gallon drum. Two drums, one empty and one filled with water, were divided into four sections of 5-gallon each with 20-gallon total volume for each drum (Fig. 23). The filled drum had an electric pump inside and was filled with water at room temperature. A manual control valve was used to control the flow (fig. 24). Before the pump was switched on, the control valve set to a given flow rate. When the pump was switched on, the flow rate was calculated by the measured rate of change of volume in the drum using Eq. 19&20. The experiments were done over a range of flow rates (1.5 gallon/minute to 14.5 gallon/minute).

$$Flow\ rate = \frac{\Delta Volume}{time} \quad (19)$$

$$Volume = (\pi r^2 * height) \quad (20)$$

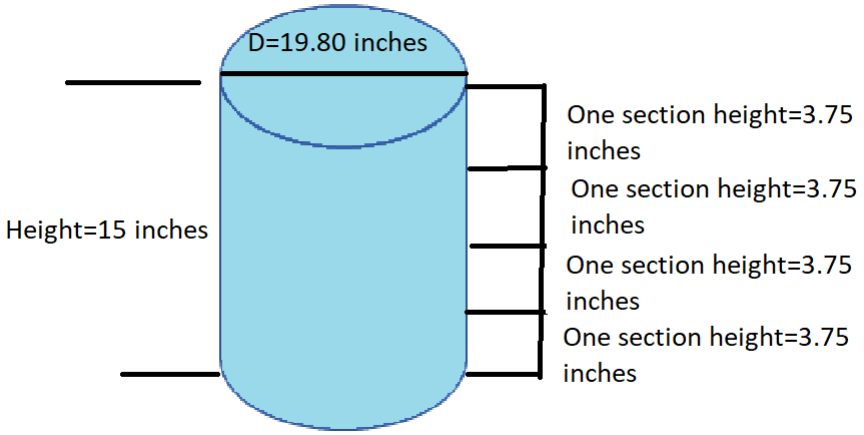

Fig. 23 Drum specifications.

Fig. 24 Manual control valve.

3.2.3- Data Acquisition (DAQ)

The experiments were repeated using three data acquisition systems, Texas instrument (TI), Arduino, and National Instrument (NI) data acquisition. The TI data acquisition was made at Virginia Tech in mechanical engineering labs and it is inexpensive. The results showed that there is noise in the temperature data that makes correlation difficult between the flow rate and the heat transfer coefficient. The Arduino data acquisition was purchased and is also inexpensive. The results indicate that the noise was decreased in the temperature data sometimes, but was not consistent. It was concluded that both the TI and Arduino data acquisition systems do not work well for the parameter estimation routine.

To minimize the noise, a National Instrument (NI) data acquisition was purchased and used to analyze the data in this paper. A lab-view 2017 program was designed for the NI 9213 Daq with a sample rate of 5 samples/second. Four channels were designed for this problem, three channels were for thermocouples, and one channel was for the heat flux values. The three channels were for welded, parallel, and water temperature thermocouples. The program screen showed the two different charts for the curve temperatures and the heat flux curve values. According to figure 25, the thermocouples and the heat flux wires were plugged into NI Daq which was plugged into a computer. The NI Daq gave temperature data that had less noise than the other data acquisitions, and it provided a good correlation between the flow rate and heat transfer coefficient.

Fig. 25 NI9213 Data Acquisition with the thermocouples and the heat flux wires.

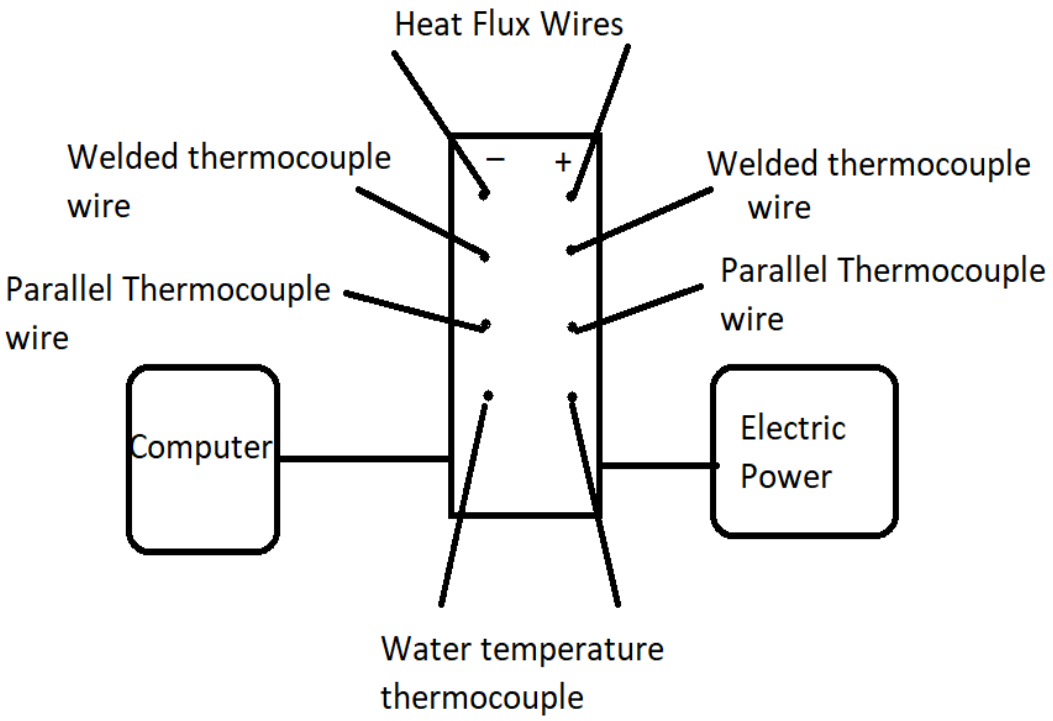

Fig. 26 NI Data acquisition schematic.

3.3- Experimental Procedure

There are five steps to take the data. First, the control valve is manually set to the desired flow rate. Second, at the specified flow rate the electric pump is switched on and the lab-view main page is opened. The water is flowing inside the pipe in the closed cycle at room temperature. Third, the data acquisition is started when the heater is off at steady state from $t = 0\ second$ to $t = 10\ seconds$. Fourth, the heater is switched on and data is taken for a time span of 120 seconds. The data was saved as an excel file with the five columns in the computer. The five columns are time (second), heat flux (W/m2), welded thermocouple temperature (℃), parallel thermocouple temperature (℃), and the measurement water temperature (℃), respectively. The experiments were repeated three times at each flow rate. The data was analyzed by using a parameter estimation routine mat-lab code. The time for processing data to get the parameter estimation values is from three to four minutes.

Chapter 4- Results and Uncertainty Analysis

Before looking at the results, the uncertainty is estimated for the measurements.

4.1-Estimated uncertainty

The sources of estimated uncertainty in the measurement flow rate are listed in Table 3 with respective uncertainty values. This analysis was assumed to be the same for all of the measurements.

Table 3 Uncertainty sources and respective values.

#	Source of uncertainty	Value	Unit
1	Temperature measurement, U_n, ΔT	0.02	% of ℃
2	Heat flux measurement, U_n,q"	0.05%	% of $W/m2$

The measured flow rate for the welded thermocouple was correlated as

$$Q = 0.5101e^{0.00158276*(q"/\Delta T)} \quad (21)$$

And for the parallel thermocouple was correlated as

$$Q = 0.606e^{0.00094*(q"/\Delta T)} \quad (22)$$

Therefore, the estimated uncertainty U_n for the measured flow rate Q was estimated using propagation of uncertainties [14].

$$Un = [(\left(\frac{\partial Q}{\partial q"}\right).(Unq"))^2+(\left(\frac{\partial Q}{\partial \Delta T}\right).(Un\Delta T))^2]^{1/2} \quad (23)$$

An estimated uncertainty of 13% was found for the measured Q with the welded thermocouple. For the parallel thermocouple, an estimated uncertainty of 11.88%, was found for the measured Q.

4.2- Welded thermocouple results for all measured days

Figure 27, shows the correlation between the heat transfer coefficient (h) and the flow rate (Q) for 41 measurements. An exponential curve fit of the data for flow rate was found based on least squared error (RMS). The curve fit illustrates that the heat transfer coefficient increases strongly with increasing flow rate. The measured data points for the heat transfer coefficient have much more variation at high flow rates than at low flow rates. The flow rate can be calculated from equation 24 after when the measured heat transfer coefficient is obtained.

$$Q = 0.4382 * e^{(0.001568*h)} \quad (24)$$

Where Q is the flow rate in (gallon/minute) and h is the heat transfer coefficient in (W/m2.℃). The R squared value is 0.867.

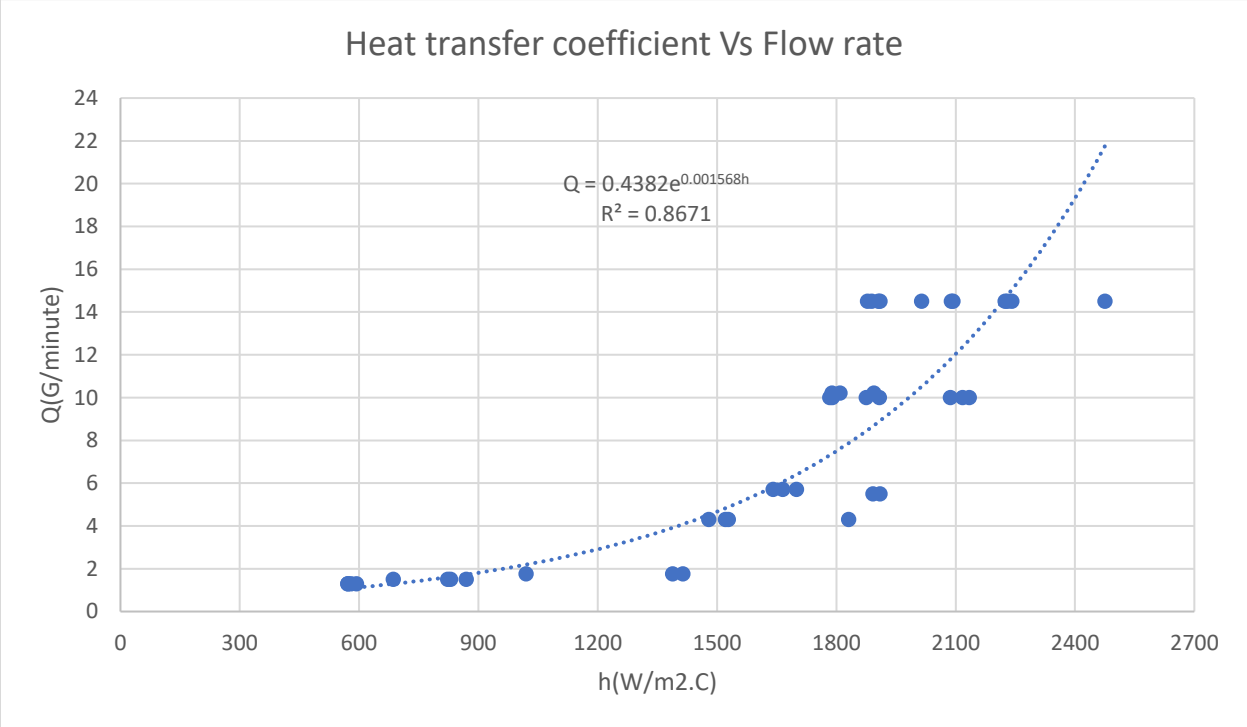

Fig.27 Correlation between Flow rate and heat transfer coefficient for the welded thermocouple.

The corresponding time constant values are shown in figure 28. Although the values increase with increasing flow rate, the heat transfer coefficient in figure 27 gives a better correlation than in figure 28 with flow rate.

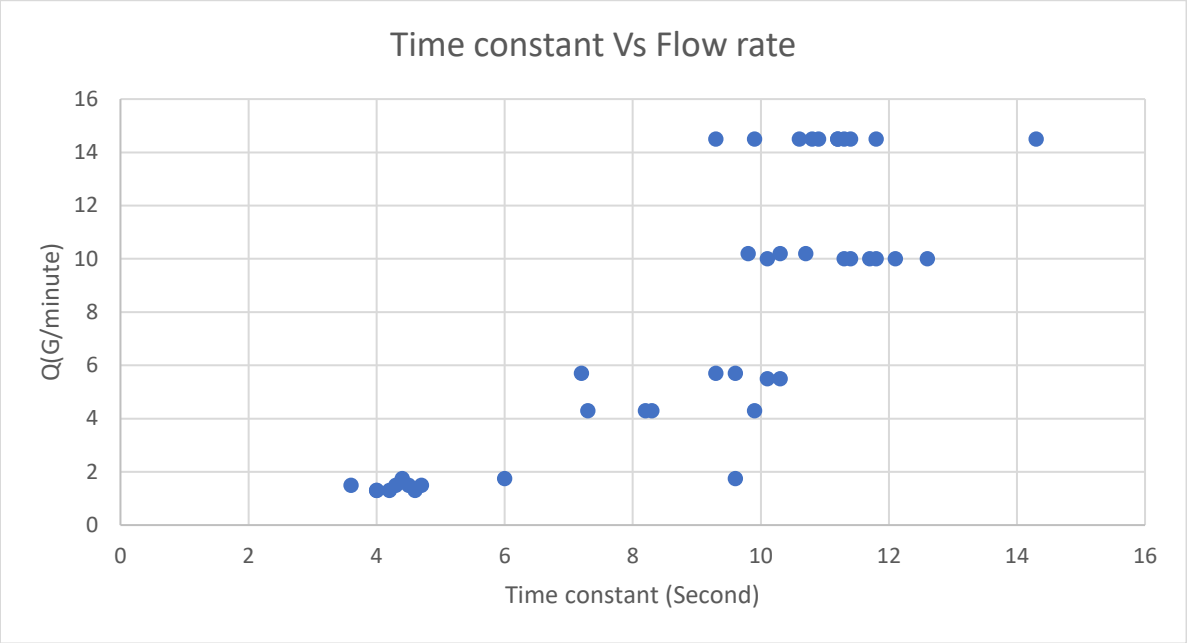

Fig.28 The time constant and flow rates for the welded thermocouple.

The estimated values for the thermal contact resistance are shown in figure 29. The thermal contact resistance is a physical parameter which should be a constant value independent flow rate. The measured thermal contact resistance values scatter around the average $R"\ average = 0.00039\ (m2.℃/W)$, particularly at lower flow rates.

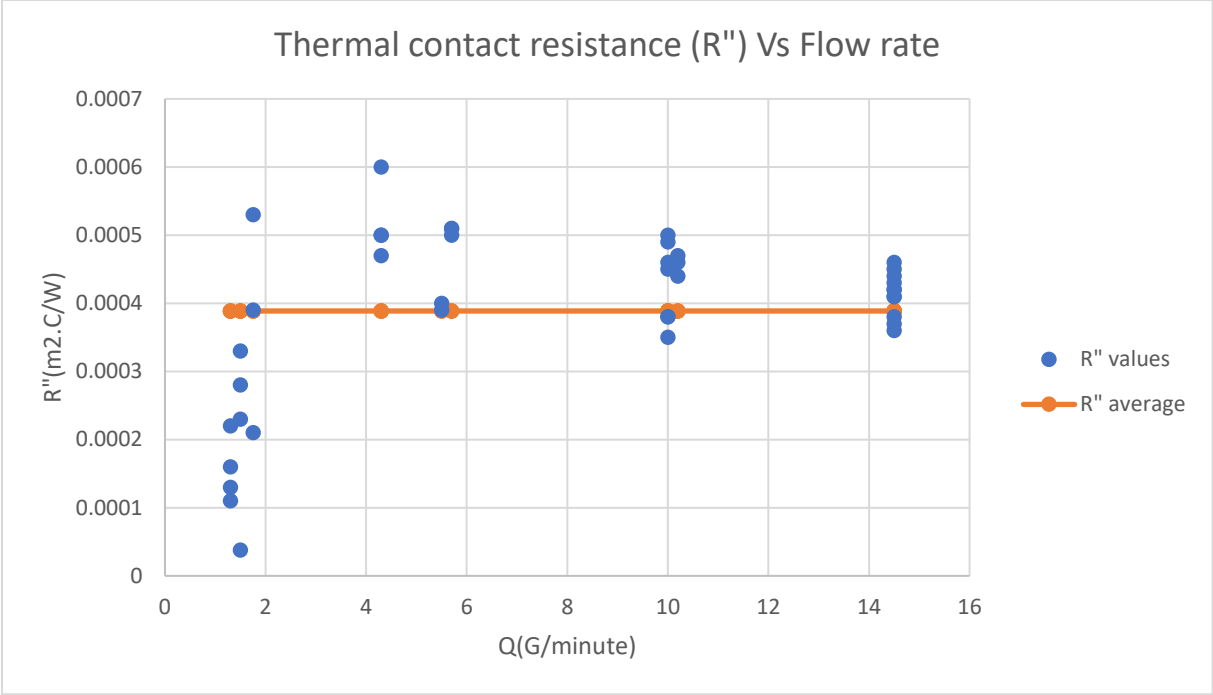

Fig.29 The average thermal contact resistance for the welded thermocouple.

The non-dimensional representation of the data in figure 27 is shown in figure 30 in terms of Reynolds, Re, and Nusselt number, Nu. A power curve fit was obtained with an R squared value of 0.82. The Re was calculated by using equation 25, and the Nu was calculated by using equation 27.

$$Re = \frac{V*D}{\upsilon} \tag{25}$$

$$V = \frac{Q}{A} \tag{26}$$

$$\frac{hD}{k} = Nu = 0.6337Re^{0.4298} \tag{27}$$

Where V is the water velocity in (m/s), D is the pipe diameter in (m), υ is the kinematic viscosity in (m2/s), Q is the flow rate in (m3/s), A is the cross-section area of the pipe in (m2), h is the heat transfer coefficient in (W/m2.℃), and K is the water thermal conductivity in (W/m.℃) at average water temperature.

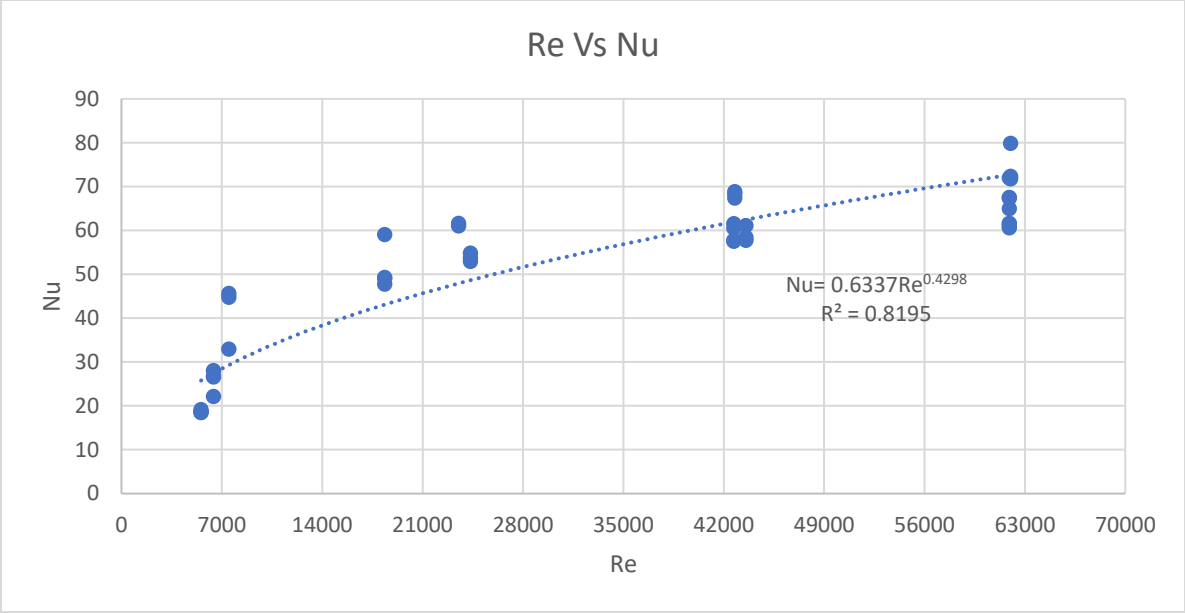

Fig.30 Non-dimension correlation between Re and Nu for the welded thermocouple.

Calculated values of Q based on equation 24 are compared with the measured flow rates in figure 31. An uncertainty analysis was done based on the 95% confidence interval of the average of ($\frac{\Delta Q}{Qm}$), where Qm is the measured flow rate and ΔQ is the difference between the measured and calculated flow rate. Based on all 41 measurements of $\frac{\Delta Q}{Qm}$ the observed 95% confidence interval was 57.1% based on student, t, distribution. These values are much higher than the estimated uncertainty of 13%, indicating the presence of uncontrolled variables in the experiments.

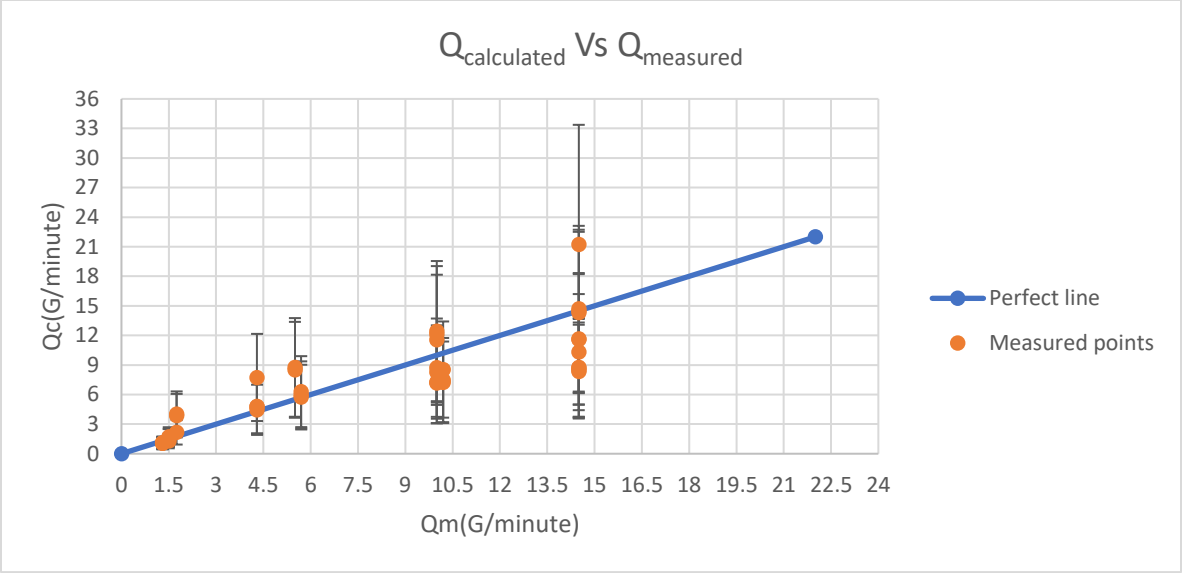

Fig.31 Variation of $Q_{measured}$ Vs $Q_{calculated}$ for the welded thermocouple.

4.3- Welded thermocouple results for an individual day

It was observed that these was more variation in results from day-to-day than for single day. Therefore, typical results are presented for the testing on a single day. The heat transfer coefficient values are shown in figure 32 with a flow rate correlation with an R squared value of 0.97. The exponential curve fit similar to that of equation 24, but the R square values was much higher.

$$Q = 0.5101 * e^{(0.00158276*h)} \quad (28)$$

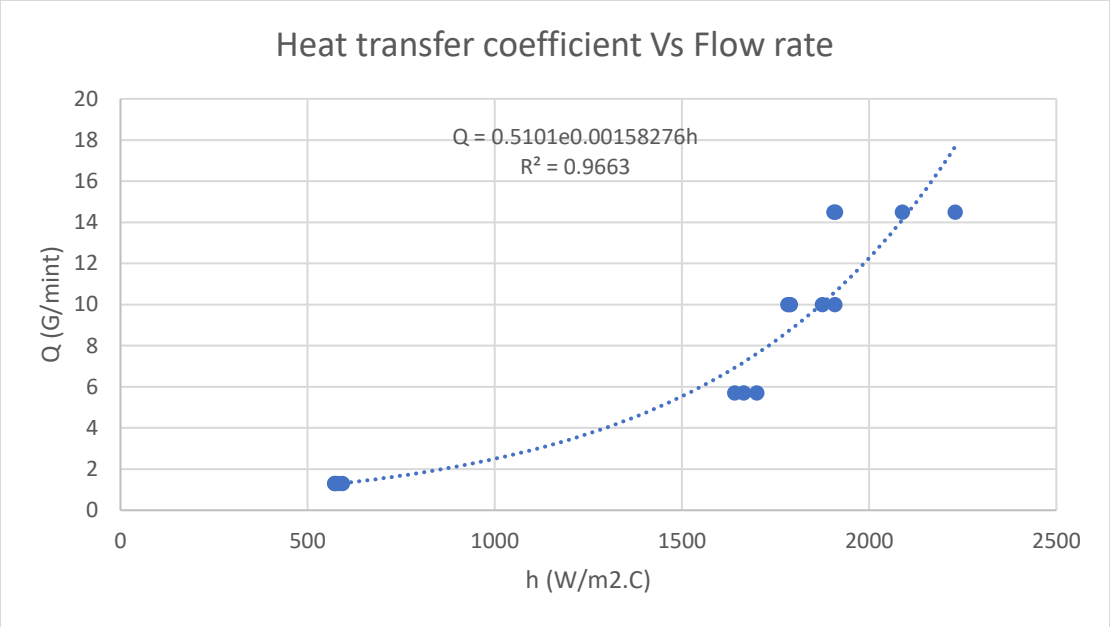

Fig.32 Correlation between Flow rate and heat transfer coefficient for an individual day for the welded thermocouple.

The corresponding values of thermal contact resistance and time constant are shown in figure 33 and 34. The scatter, however, is still typical of the full data set.

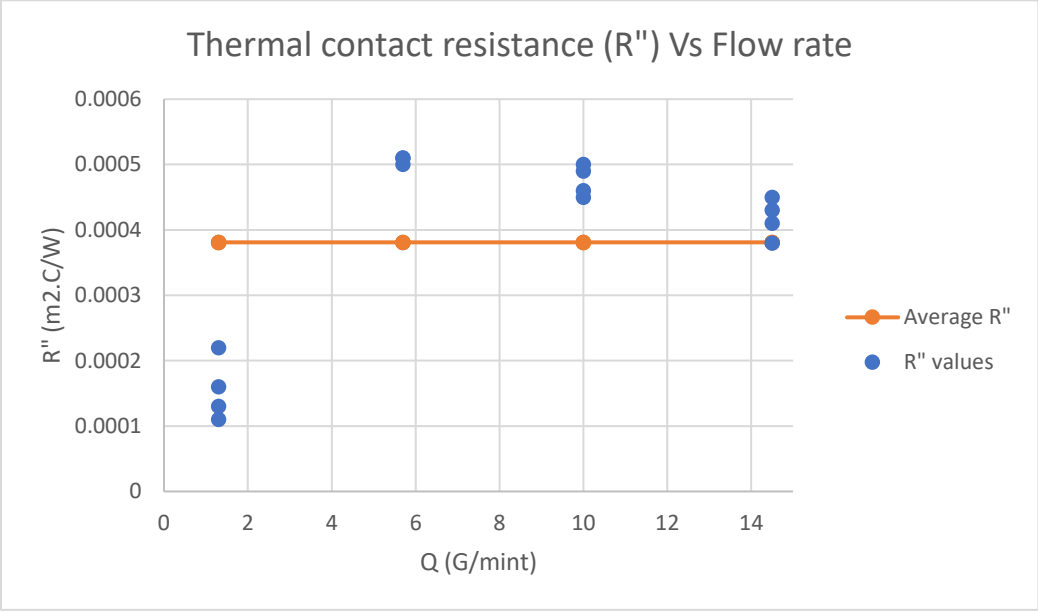

Fig.33 The average thermal contact resistance for an individual day for the welded thermocouple.

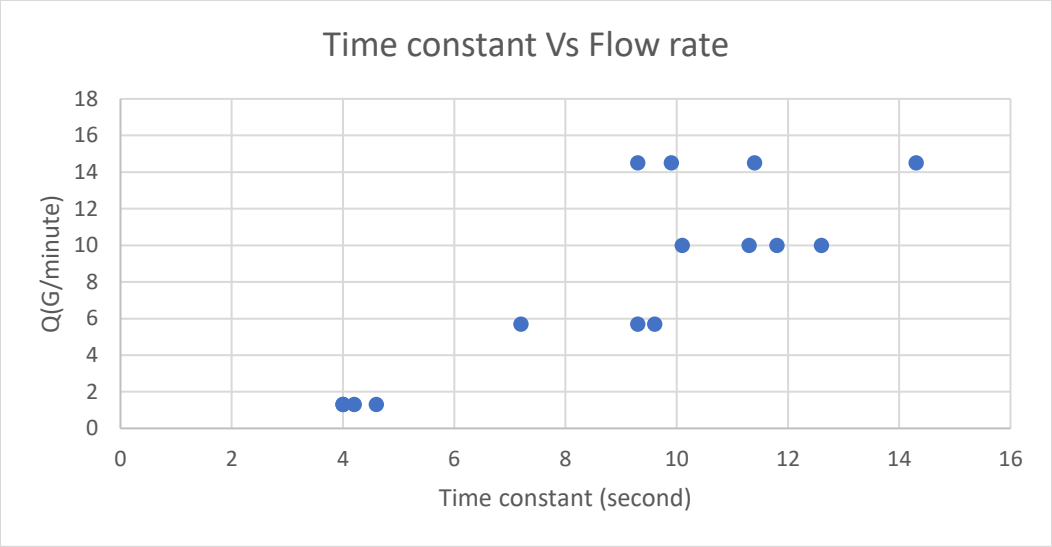

Fig.34 The time constant values and flow rates for an individual day for the welded thermocouple.

The non-dimensional correlation of heat transfer coefficient for a single day of testing is shown in figure 35. The correlation is slightly different than equation 27 and has a higher R squared value of 0.95.

$$Nu = 0.1968Re^{0.5364} \quad (29)$$

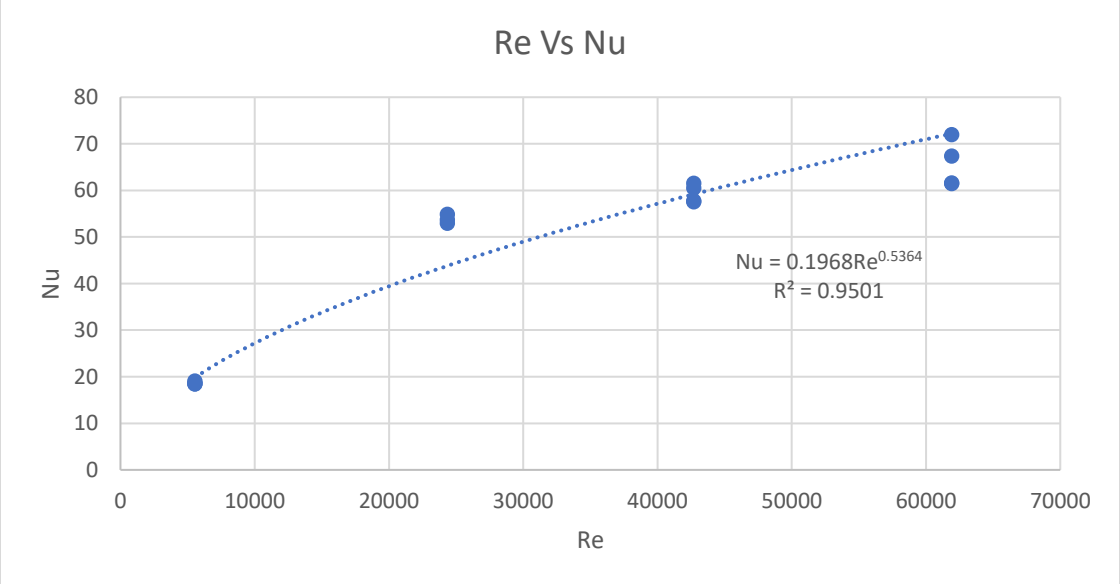

Fig.35 Non-dimension correlation between Re and Nu for individual day for the welded thermocouple.

The Calculated values of Q based on equation 28 are compared with the directly measured values in figure 36. The 95% confidence interval of these 14 measurements is 24.5% which is much lower than using all 41 measurements, again indicating some day-to-day variability in the results.

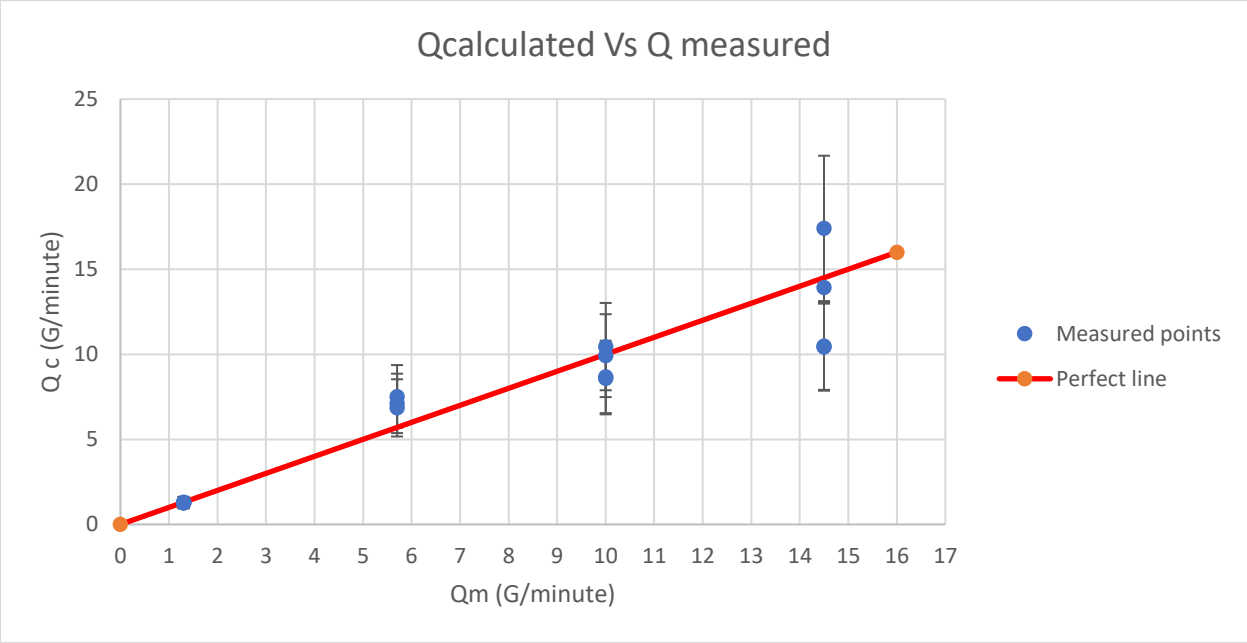

Fig.36 Variation of Q $_{measured}$ Vs Q $_{calculated}$ for an individual day for the welded thermocouple.

4.4- Parallel thermocouple results for all measured days

Figure 37, shows the correlation between the heat transfer coefficient (h) and the flow rate (Q) for 43 measurements using the parallel thermocouple arrangement. The data was taken over three days. The exponential curve fit

$$Q = 0.5073 e^{0.0009860*h} \quad (30)$$

is much better than the curve fit for the welded thermocouple with an R squared value of 0.98, the heat transfer coefficient shows a greater range of values and more consistency.

The measured data points for the heat transfer coefficient have more variation at high flow rates than at low flow rates. The flow rate can be calculated from equation 30 after when the measured heat transfer coefficient is obtained.

Where Q is the flow rate in (gallon/minute) and h is the heat transfer coefficient in (W/m2.℃). The R squared value is 0.985 which is better than the welded thermocouple.

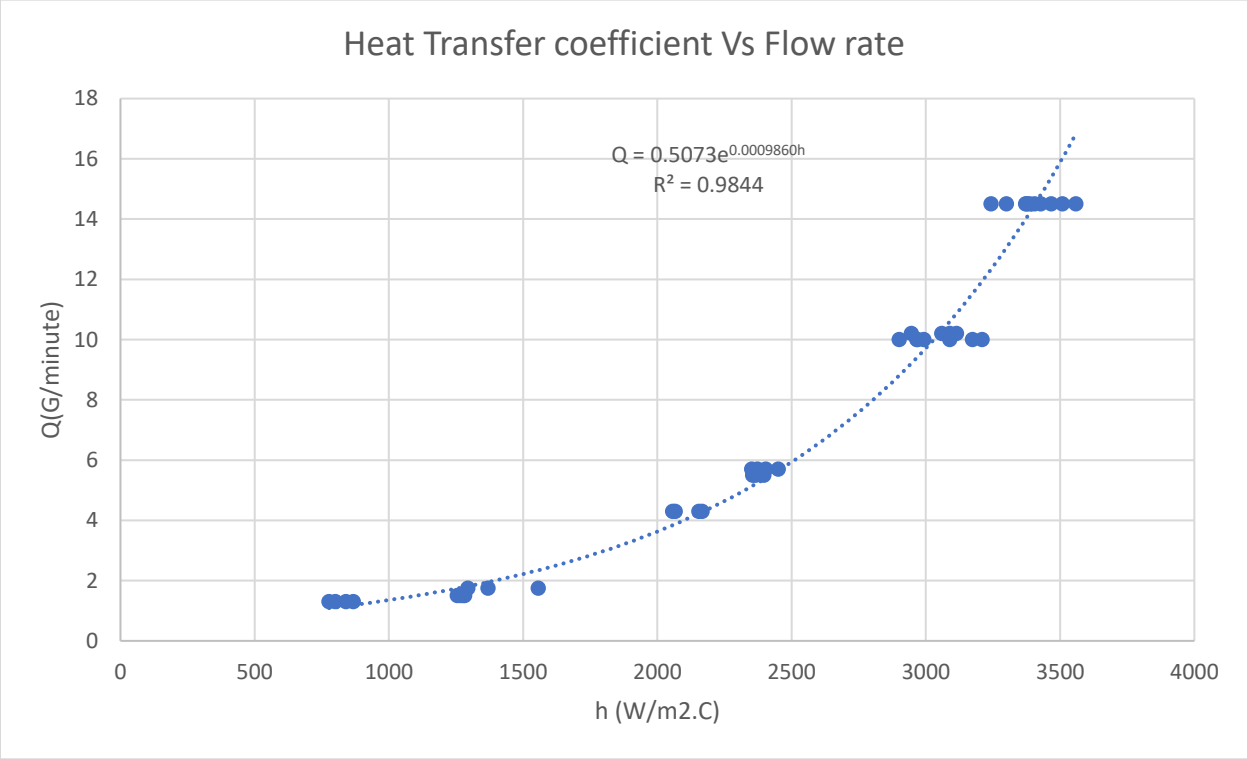

Fig.37 Correlation between Flow rate and heat transfer coefficient for the parallel thermocouple.

The corresponding time constant values are shown in figure 38. Unlike the welded thermocouple, the values decrease with increasing flow rate. Consequently, values are more reasonable than for the welded thermocouple. These results are encouraging and satisfy the theoretical relationship between h and τ in equation 31, the theoretical time constant range is from 1.20 to 4.64 second. Overall, the time constant

values in the parallel thermocouple are lower than in the welded thermocouple. The heat transfer coefficient in figure 37 gives a better correlation than in figure 38 with flow rate.

$$\tau = \frac{\rho C \delta}{h} \tag{31}$$

Where ρ is the copper pipe density, 8933 kg/m3, C is heat capacity of copper pipe, 385 J/Kg.℃, and δ is the copier pipe thickness, 0.00129 m.

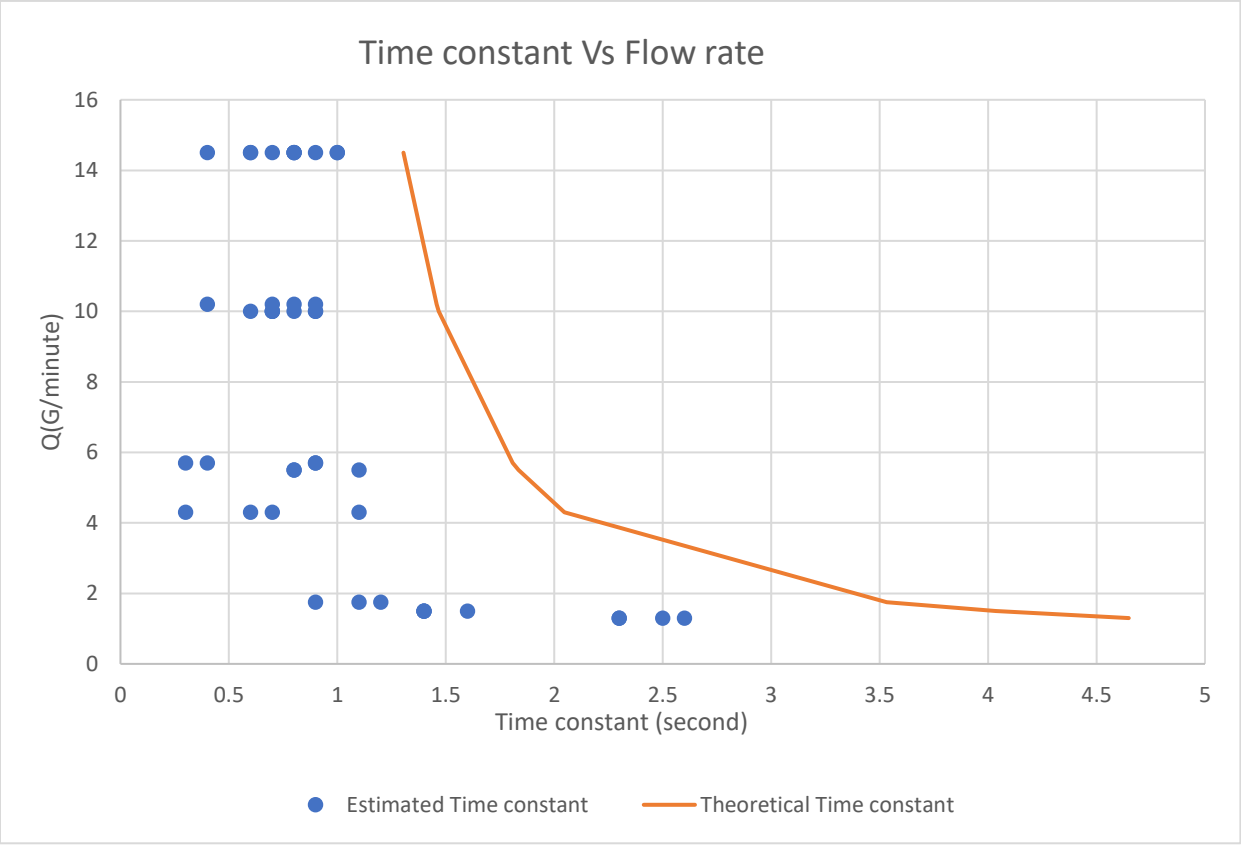

Fig.38 The time constant values and flow rates for the parallel thermocouple.

The estimated values for the thermal contact resistance are shown in figure 39. The thermal contact resistance is a physical parameter which should be a constant value independent of flow rate. The measured thermal contact resistance values scatter around the average $R"\ average = 0.00001\ (m2.℃/$

W), particularly at lower flow rates. The average thermal contact resistance in the parallel thermocouple is much smaller than in the welded thermocouple. This helps give a better discrimination of flow rate from the heat transfer coefficient.

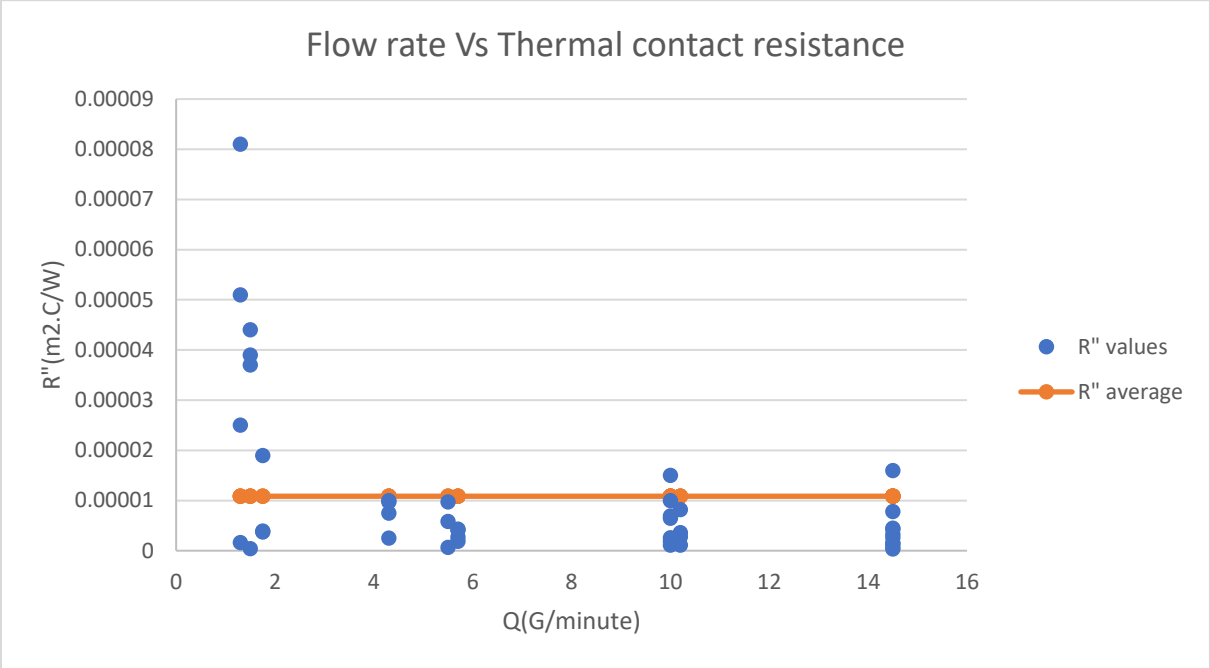

Fig.39 The average thermal contact resistance for the parallel thermocouple.

The non-dimensional representation of the data in figure 37 is shown in figure 40 in terms of Reynolds, Re, and Nusselt number, Nu. A power curve fit was obtained with an R squared value of 0.944 which is much better than the welded thermocouple.

$$Re = \frac{V*D}{\upsilon} \quad (32)$$

$$V = \frac{Q}{A} \quad (33)$$

$$\frac{hD}{k} = Nu = 0.4394Re^{0.5059} \quad (34)$$

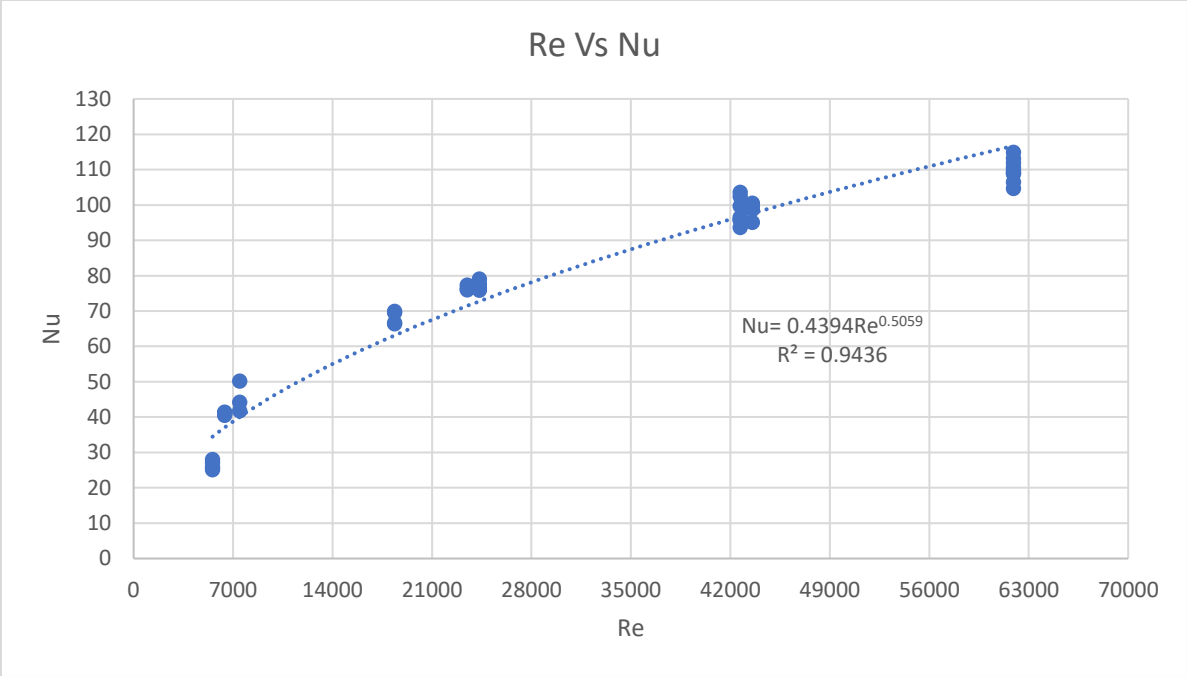

Fig.40 Non-dimension correlation between Re and Nu for the parallel thermocouple.

Calculated values of Q based on equation 30 are compared with the measured flow rates in figure 41. An uncertainty analysis was done based on the 95% confidence interval of the average of $(\frac{\Delta Q}{Qm})$, where Qm is the measured flow rate and ΔQ is the difference between the measured and calculated flow rate. Based on all 43 measurements of $\frac{\Delta Q}{Qm}$ the observed 95% confidence interval was 15.45% which is lower than in the welded thermocouple based on student normal distribution, t. These uncertainties are shown on the figure 41. These values are slightly higher than the estimated uncertainty of 11.88%, indicating the presence of uncontrolled variables in the experiments.

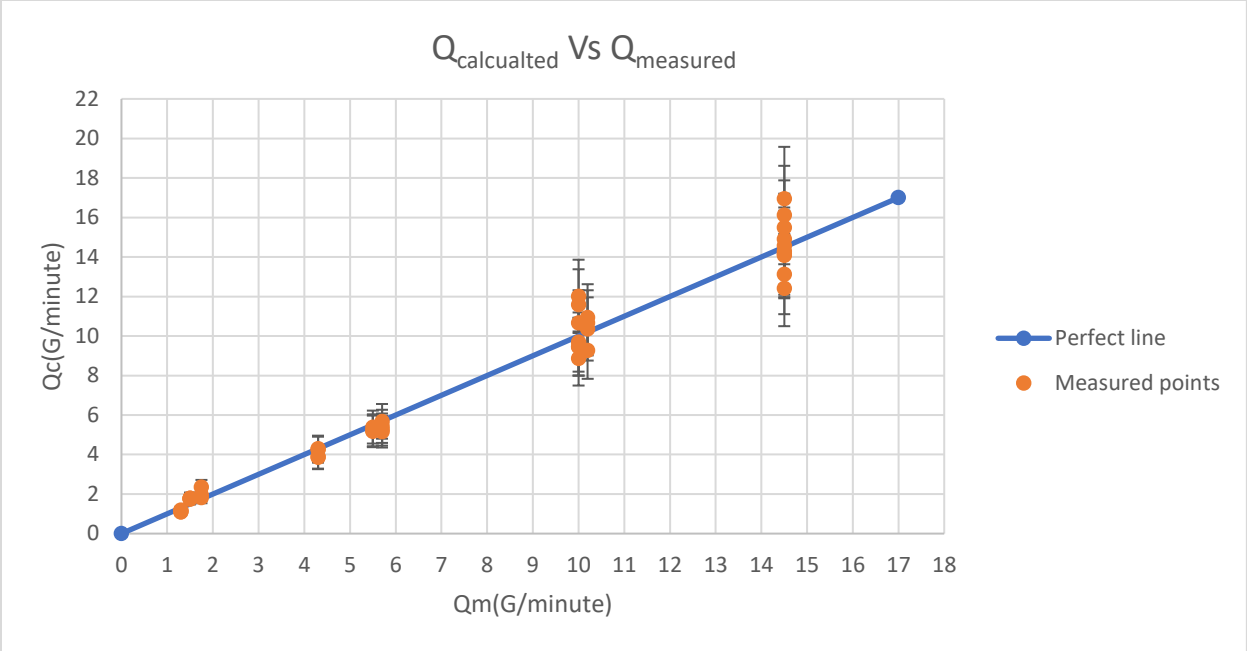

Fig.41 Variation of $Q_{measured}$ Vs $Q_{calculated}$ for the parallel thermocouple.

4.5- Parallel thermocouple results for an individual day

To provide another comparison of the data, results are presented for the testing on a single day. The heat transfer coefficient values are shown in figure 42 with a flow rate correlation with an R squared value of 0.996 which is better than the results of all three days of testing. The better curve fit indicates that there was substantial day-to-day variability.

$$Q = 0.606 * e^{(0.00094*h)} \quad (35)$$

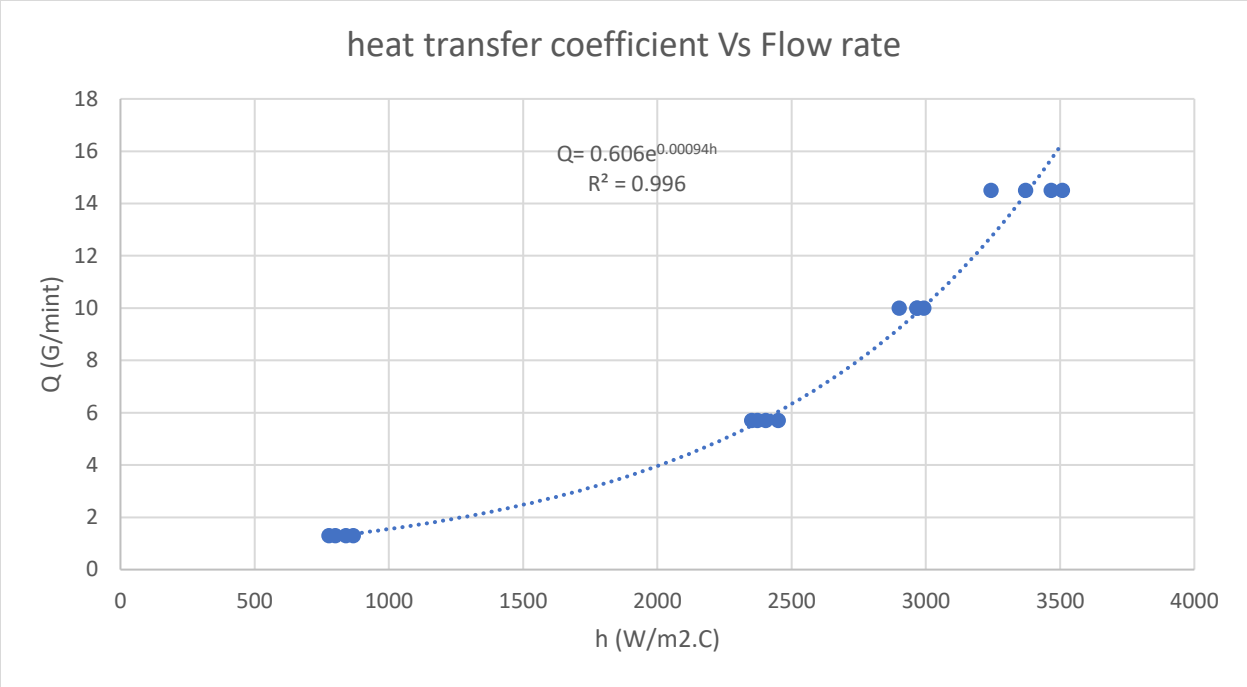

Fig.42 Correlation between the Flow rate and the heat transfer coefficient for an individual day for the parallel thermocouple.

The corresponding values of thermal contact resistance and time constant are shown in figure 43 and 44. The scatter, however, is still typical of the full data set.

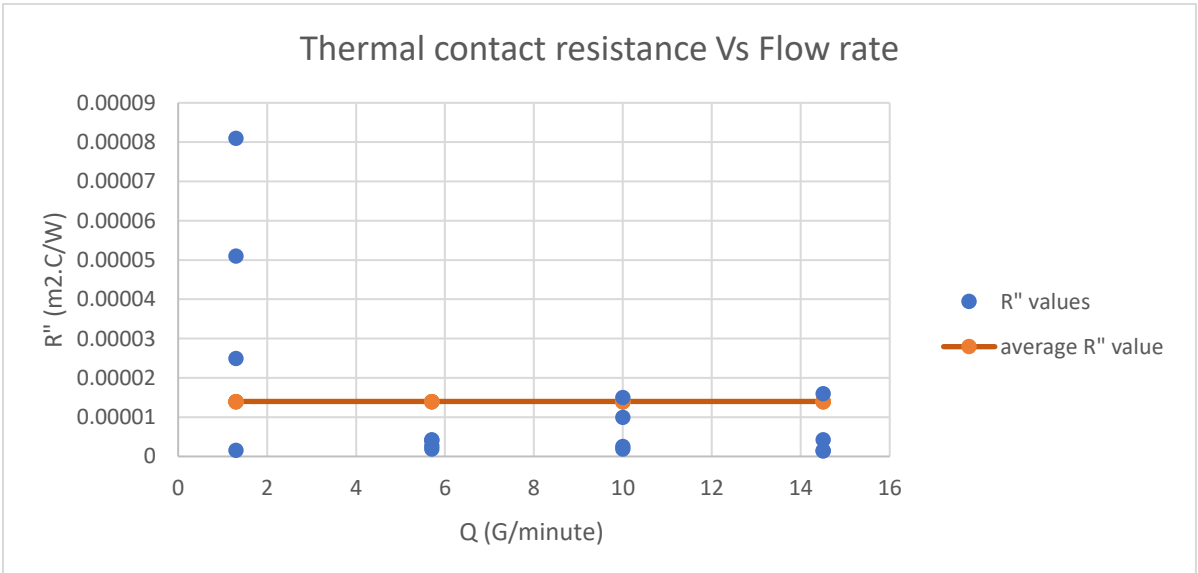

Fig.43 The average thermal contact resistance for an individual day for the parallel thermocouple.

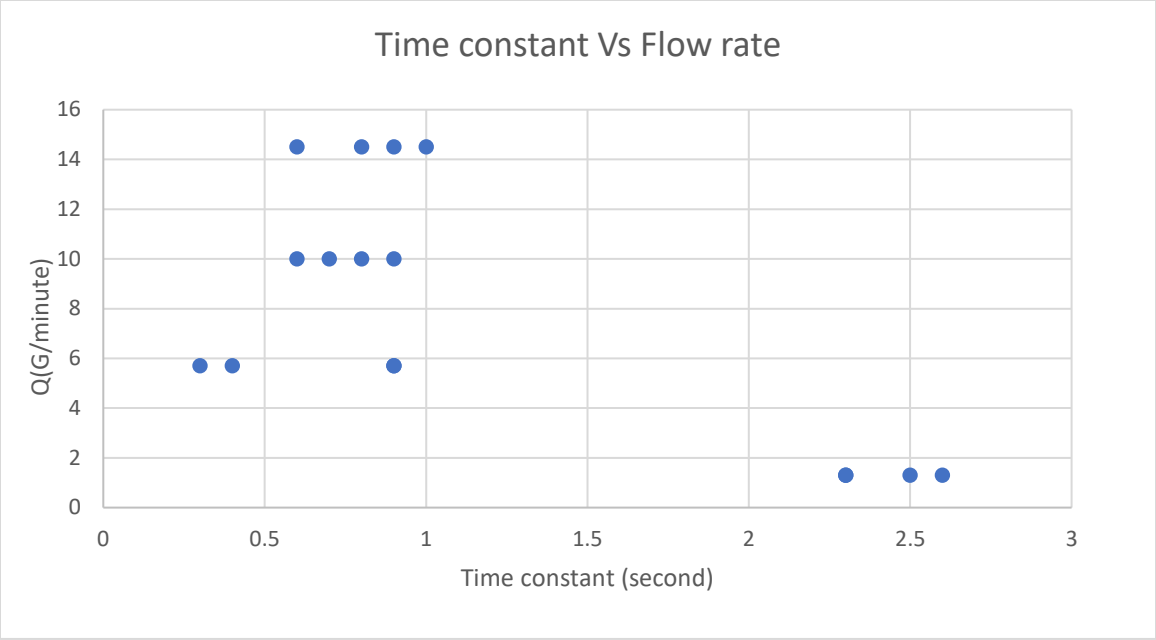

Fig.44 The time constant values and flow rates for an individual day for the parallel thermocouple.

The non-dimensional correlation of heat transfer coefficient for a single day of testing is shown in figure 45. The correlation is substantially different than equation 34 and has a high R squared value of 0.98 which is lightly better than from all of the data.

$$Nu = 0.1551Re^{0.60175} \quad (36)$$

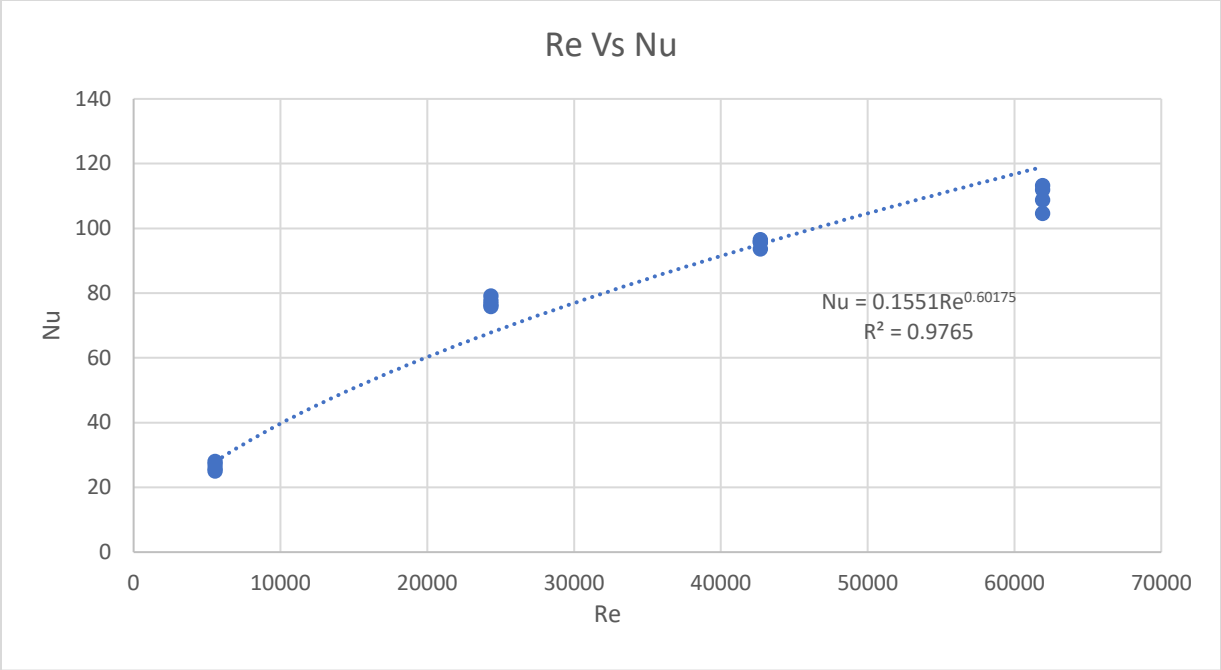

Fig.45 Non-dimension correlation between Re and Nu for an individual day for the parallel thermocouple.

The Calculated values of Q based on equation 35 are compared with the directly measured values in figure 46. The 95% confidence interval of these 16 measurements is 8.55% which is smaller than in the welded thermocouple and slightly lower than the estimated uncertainty. This is much lower than using all 43 measurements, again indicating some day-to-day variability in the results.

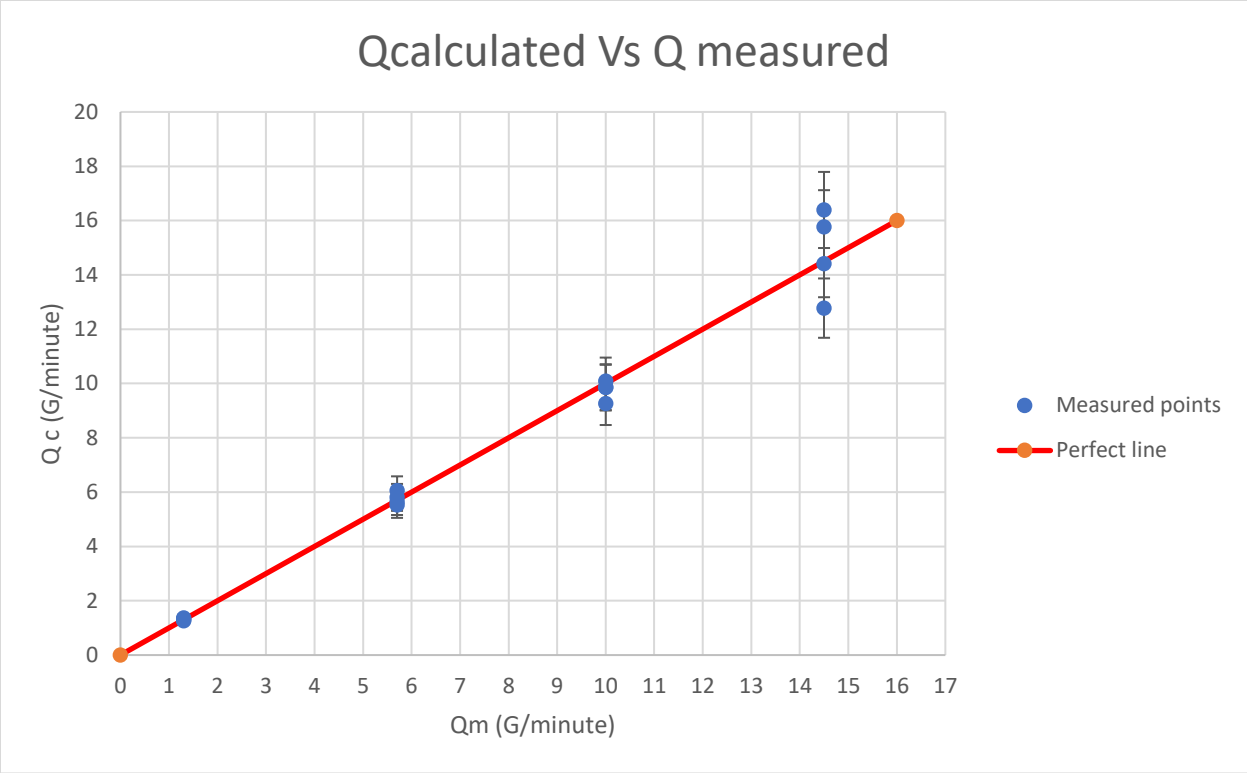

Fig.46 Variation of $Q_{measured}$ Vs $Q_{calculated}$ for an individual day for the parallel thermocouple.

4.6- Water temperature results

Calculated values of water temperature based on equation 4 are compared with the measured water temperatures in figure 47 for 16 measurements for both welded and parallel thermocouple. The measurements were done for one day. The calculated water temperature is assumed constant during the experiments. The difference between the measured and calculated water temperature is very small. The perfect line represents zero error between the calculated and measured water temperature.

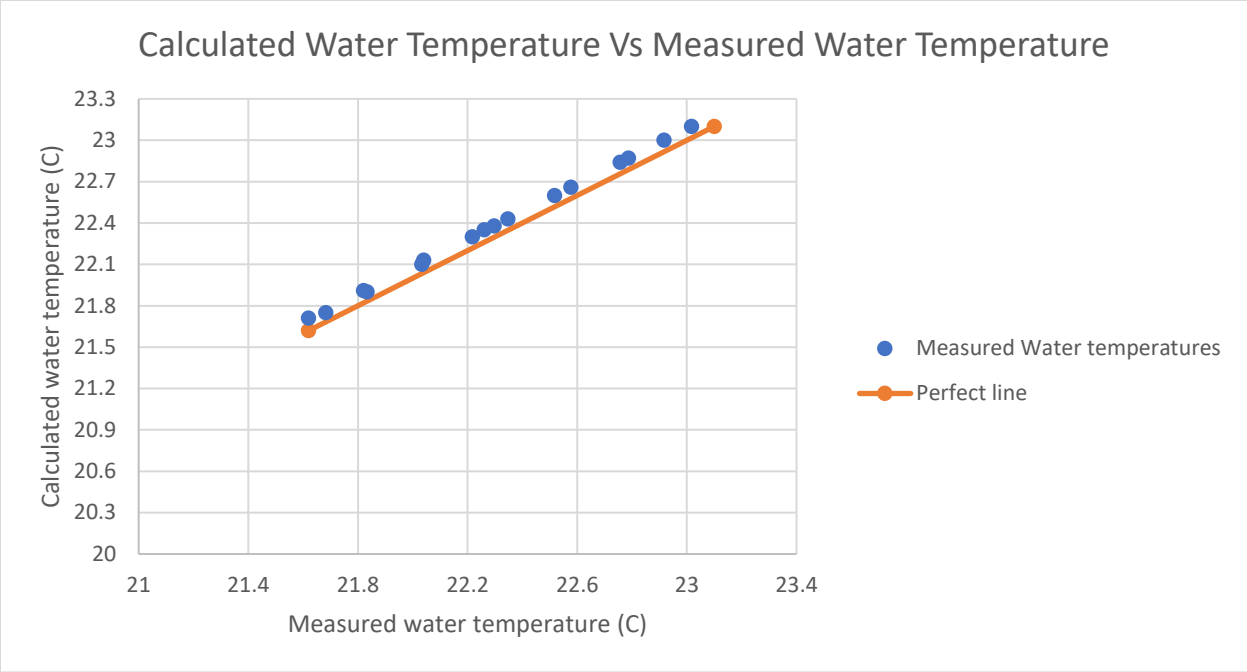

Fig.47 Variation of water temperature $_{measured}$ Vs water temperature $_{calculated}$ for both welded and parallel thermocouples.

The water temperature was measured for each time interval, from t=0 to t=120 second. The difference between the measured water temperature at t=0 second and at t=120 second is less than 0.15 ℃. Then the average measured water temperature was considered as a final measured water temperature. Table 4 shows a few of the measurement and calculated results for both welded and parallel thermocouple.

Table 4 Measured and Calculated Water flow rate and Temperature for 10 gallon/minute.

Measured flow rate (gallon/minute)	Calculated flow rate (gallon/minute)	h (W/m2.℃)	$Measured\ T_w$(℃)	$Calculated\ T_w$(℃)	Type
10	9.86	2968	22.51	22.57	Parallel
10	8.67	1790	22.63	22.72	Welded

4.7- Sensitivity Analysis

Table 6 shows the sensitivity range values between the parallel and the welded thermocouple. The analysis was done for all measured days from low flow rate to high flow rate, sensitivity = ($\Delta h/\Delta Q$) (figure 48). The results show that the parallel thermocouple sensitivity range is from 35.50 to 343 ($W.minute/m2.℃.gallon$) and the welded thermocouple sensitivity range is 19.27 to 186 ($W.minute/m2.℃.gallon$). Therefore, the parallel thermocouple is more sensitive than the welded thermocouple.

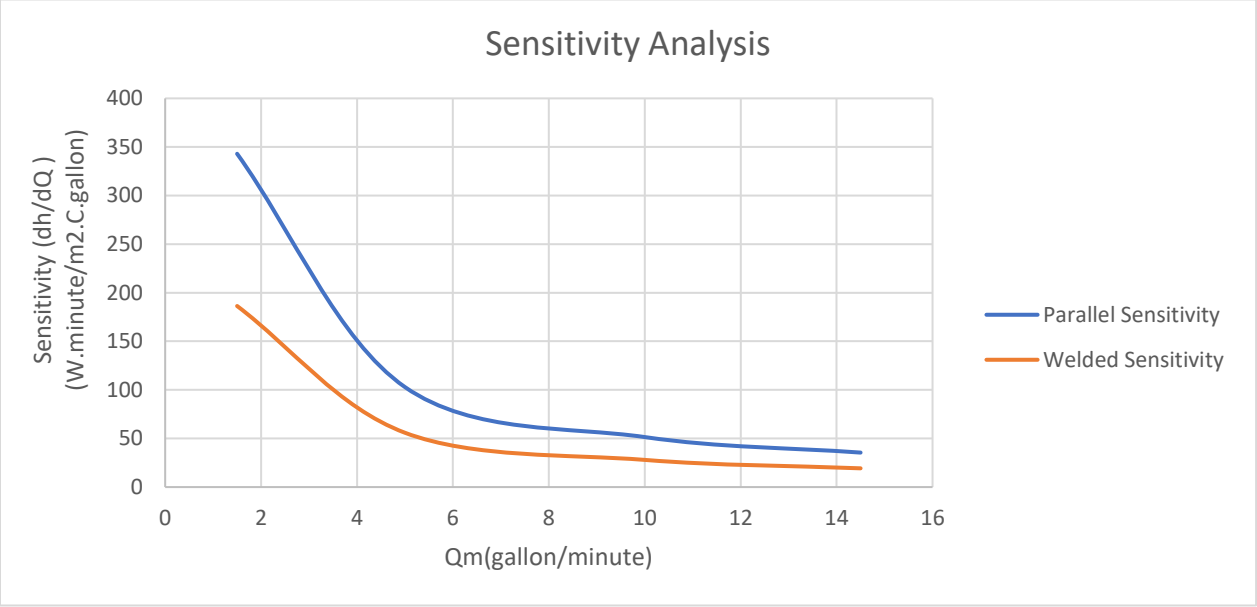

Fig.48 Sensitivity Analysis for the parallel and welded thermocouple.

Table 5 Sensitivity range values for the parallel and the welded thermocouple.

Thermocouple	Qm (gallon/minute)	Qm(gallon/minute)	Sensitivity Range (Watt. Minute/m2.℃. $gallon$)
Parallel	1.50	186	343
Welded	14.5	19.27	35.50

Chapter 5- Conclusion

A new approach, non-invasive thermal interrogation using heat flux and temperature measurements, was successfully tested to estimate the water temperature and flow rate in a pipe. A lumped capacitance method (LCM) was used to analyze the system as a transient conduction problem. It is simple and more efficient method to estimate the heat transfer coefficient h, the thermal contact resistance $R"$, the time constant τ, and the water temperature ℃. The heat transfer and temperature measurements were made on a copper pipe using heat flux sensor (PHFS) and thin film thermocouples. The temperature measurement of the pipe is a crucial measurement in a non-invasive system. Therefore, two different thermocouples, welded and parallel, were tested together in the same set-up. A correlation between the heat transfer coefficient h and the flow rate Q was done for both the parallel and the welded thermocouples. The average thermal contact resistance was estimated for both thermocouples. The results show that the parallel thermocouple is better than the welded thermocouple. The parallel thermocouple gives a good match of sensor temperature curves, small average thermal contact resistance $average\ R" = 0.000010\ (m2.℃/W)$, water temperature T_w= 22.57 ℃, range of heat transfer coefficient values h from 700 to 3500 $(W/m2.℃)$, and good repeatability, 15.45%, and more sensitivity. Based on these encouraging results, future study will be done on different pipe sizes and different types of fluid, including two- phase fluid.

References

[1] A. Venugopal, A. Agrawal, S. V. Prabhu, Review on vortex flowmeter - Designer perspective, Sensors and Actuators, A: Physical. 170 (2011) 8–23. doi:10.1016/j.sna.2011.05.034.

[2] M. Reik, R. Höcker, C. Bruzzese, M. Hollmach, O. Koudal, T. Schenkel, H. Oertel, Flow rate measurement in a pipe flow by vortex shedding, Forschung Im Ingenieurwesen. 74 (2010) 77–86. doi:10.1007/s10010-010-0117-0.

[3] S. Kong, F. Application, P. Data, (12) United States Patent, 2 (2011) 12–15. doi:10.1016/j.(73).

[4] F.J. Weber, W.W. Durgin, H. Johari, Ultrasonic Beam Propagation in Turbulent Flow, Proceedings of ASME FEDSM'01. (2001) 85–91.

[5] https://www.omega.com/prodinfo/vortex-flow-meter.html

[6] https://www.omega.com/pptst/FMC-5000.html?_vsrefdom=mca&mchxkw=c:232865952,k:,m:b,p:1t4,d:c,ai:24221907552,ad:240953947873,s:g&gclid=EAIaIQobChMIgqeNzvuc3AIVx42zCh2_6QwrEAAYBCAAEgIJ9PD_BwE

[7] T. Beckwith, R. Marangoni, J. Lienhard V, Mechanical Measurments 6th Ed, Pearson Prentice Hall, Upper Saddle River, NJ 07458, 2007, PP. 533,534,545,547,548,549,550, 578,579,580,581,582,583.584.585,586

[8] R. Thorn, et al.,"Flow Measurments" Ch.9 in Mechanical Variables Measurement, Eds.J.G.Webster, CRC Press, Boca Raton, New York, Washington, D.C, 1999, PP.9-2,9-40,9-63,9-74,9-89,9-118

[9] A.I.K. Al-Khwaji, Computational and experimental modeling of the bioheat transfer process of perfusion in tissue applied to burn wounds.pdf, (2013) 90.

[10] ASHRAE (2015) *ASHRAE Guideline 13-2015. Specifying Direct Digital Control Systems,* American Society of Heating, Refrigerating and Air-Conditioning Engineers, Atlanta, GA.

[11] ASHRAE (2012) *ASHRAE Guideline 22-2012. Instrumentation of Monitoring Central Chilled-Water Plant Efficiency,* American Society of Heating, Refrigerating and Air-Conditioning Engineers, Atlanta, GA.

[12] U.S. Energy Information Administration (EIA) (2016) 2012 Commercial Buildings Energy Consumption Survey (CBECS) http://www.eia.gov/consumption/commercial/

[13] U.S. Environmental Protection Agency (EPA) (2012) Solar Heating and Cooling: Best Practices in State Policies to Support Commercial and Industrial Market Development. https://www.epa.gov/sites/production/files/2014-11/documents/solar-heating-cooling-state-policy-paper.pdf

[14] R.Figliola, D. Beasly, "Uncertainty Analysis" Ch.5 in Therory And Design For Mechanical Measurments, John Eilly &Sons, New Yourk/Chichster/ Brisbane/ Toronto/ Singapore,1991, PP.5-144,5-145,5-146,5-147,5-148,5-149,5-150,5-151,5-152,5-153,5-154,5-155

Appendixes

Appendix A- Mathematical Model Solution

The lumped capacitance method was used to solve the transient problem. The mathematical model has been investigated from energy balance on the control volume around the thickness of the pipe, therefore reduced to

$$\frac{mC}{A}\frac{dT}{dt} = q_s'' - h(T - T_w)$$

assume that, $\theta = T - T_w$ and $\tau = \frac{mC}{Ah}$. In terms of the variables θ and τ the model become

$$\tau\frac{d\theta}{dt} = \frac{q_s''}{h} - \theta$$

With the initial condition, t=0, the solution of the differential equation is

$$\theta(t) = \frac{q_s''}{h} - \frac{B}{h}e^{-(\frac{t}{\tau})}$$

Where B is constant

$$B = q_s'' - \theta(t = 0).h$$

And $\theta(t = 0)$ is

$$\theta(t = 0) = T(0) - T_w(0)$$

Assume that the water temperature is constant at steady state during the experiment. Therefore, the water temperature at t=0 is

$$T_w = T(0) - \frac{q_s''(0)}{h}$$

And $\theta(t=0)$ become

$$\theta(t=0)=\frac{q_s''(0)}{h}$$

The pipe temperature at t=0 is

$$T(0)=T_s\,(0)-R".q_s''(0)$$

The final pipe temperature, mathematical model, for multi-steps is

$$T_k(t)=T_s(0)-R".q_s''(0)+\sum_{j=1}^{k-1}\frac{\Delta q_{s,j}''}{h}\left(1-e^{-\frac{(t_k-t_j)}{\tau}}\right)$$

Appendix B- Texas Instrument (TI) and Arduino Data Acquisition Results

In fact, in hypothetically the pipe temperature at $t=0$ is,$T(0)=T_s\,(0)-R"*q_s''(0)$, where T_s is measured sensor temperature, $R"$ is thermal contact resistance, and q_s'' is sensor heat flux measured. Initially, we assumed that the wall pipe temperature at $t=0$,$T(0)$, is the same measured sensor temperature, $T_s\,(0)$, at $t=0,T(0)=T_s\,(0)$. Therefore, we neglected the heat flux measured, $q_s''(0)$=0 because the heat flux is very small compared to the remaining data. This assumption is not valid as long as neglecting the heat flux value at $t=0$ because the parameter estimation routine does not work well and does not give a good sensitivity in the results (see the below results). It illustrated that considering the heat flux value at $t=0$ is important in the parameter estimation.

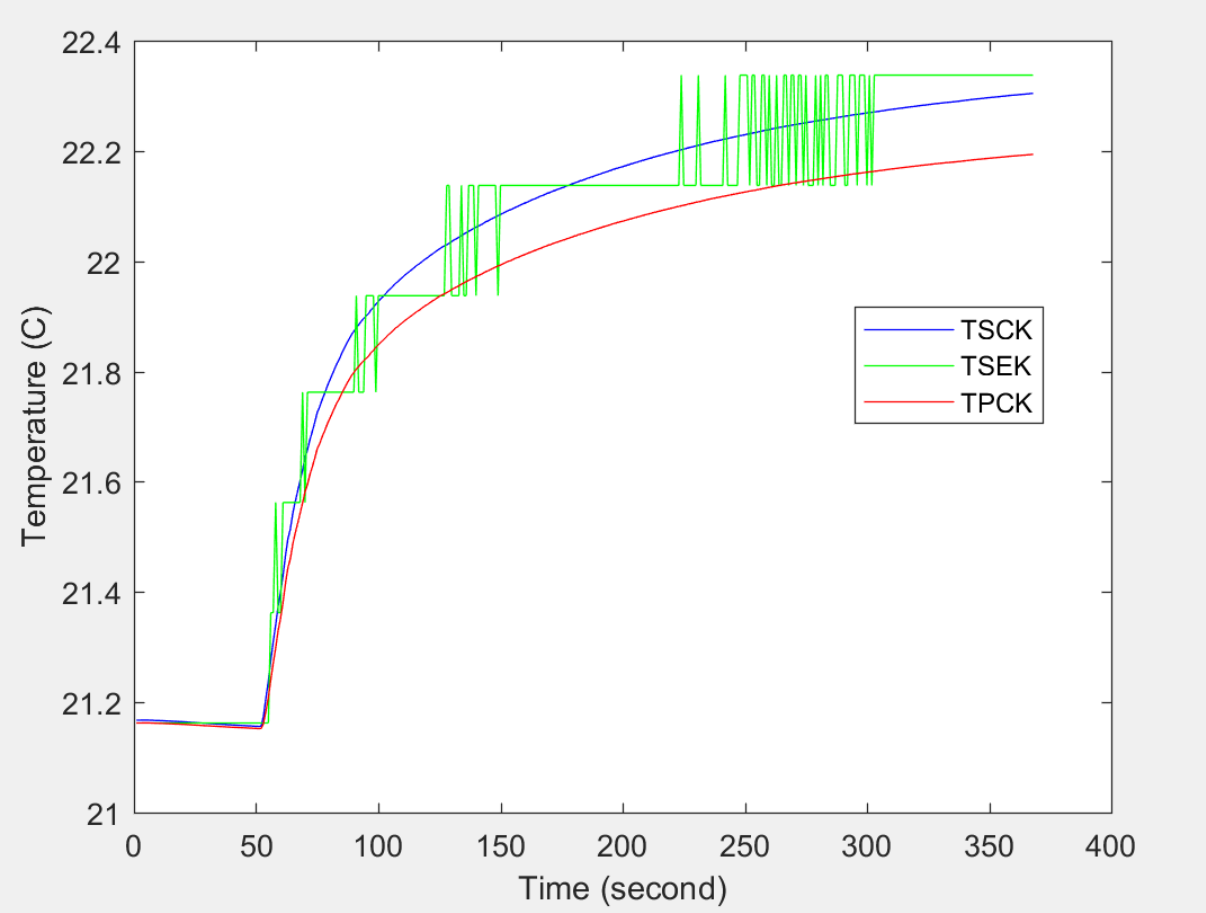

Fig.B1 TI data acquisition temperature curves for the paralleled thermocouple.

TSCK: Sensor calculated temperature.

TSEK: Sensor measured temperature.

TPCK: Pipe calculated temperature.

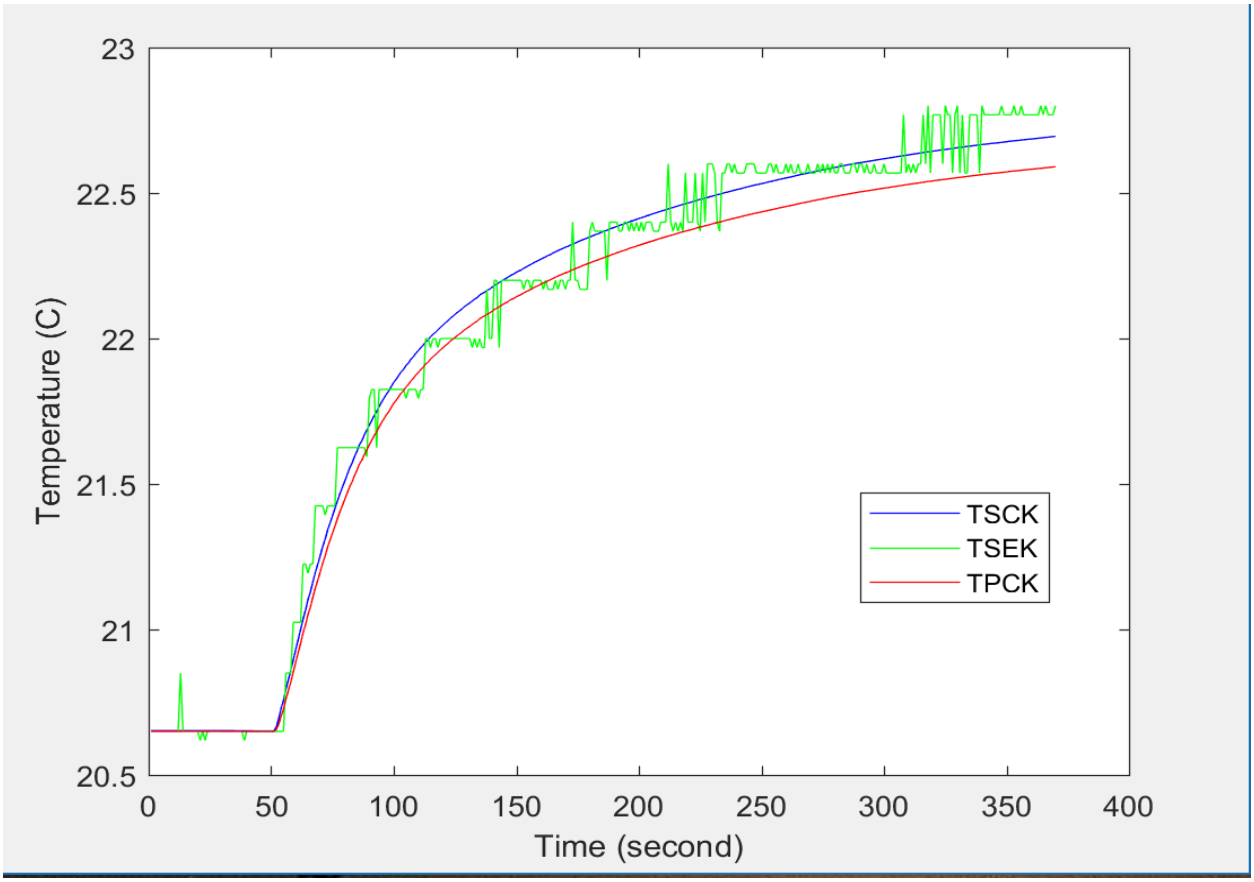

Fig.B2 TI data acquisition temperature curves for the welded thermocouple.

Flow rate (gal/mint)	Iteration	h (w/m2.C)	taw (second)	R" (C.m2/W)	T_water (C)	D (m)	Viscosity (N.S.m2/Kg)	U (m/s)	Re	Min error	Nu	K- water (w/m.C)
max 14.5	1	9901	0.3	2.31E-04	20.92734269	0.019558	9.609E-07	3.039911	61873.84	0.0651	319.5442	0.606
	2	3001	1.1	5.68E-06	21.06296901	0.019558	9.609E-07	3.039911	61873.84	0.0698	96.85406	0.606
	3	2901	1.3	3.35E-05	21.27310583	0.019558	9.609E-07	3.039911	61873.84	0.0512	93.62666	0.606
11	1	2801	0.6	2.63E-05	20.69848625	0.019558	9.609E-07	2.103007	42804.25	0.052	90.39927	0.606
	2	2801	0.7	2.84E-05	20.93455552	0.019558	9.609E-07	2.103007	42804.25	0.0522	90.39927	0.606
	3	3001	1.6	4.09E-05	21.18861046	0.019558	9.609E-07	2.103007	42804.25	0.0569	96.85406	0.606
7.9	1	8601	3.2	2.67E-04	20.74800837	0.019558	9.609E-07	1.661377	33815.39	0.0755	277.588	0.606
	2	2701	0.7	4.90E-05	20.89445391	0.019558	9.609E-07	1.661377	33815.39	0.0658	87.17188	0.606
	3	2601	1.5	3.92E-05	21.11004614	0.019558	9.609E-07	1.661377	33815.39	0.0651	83.94449	0.606
4.9	1	2701	0.8	3.29E-06	20.96550167	0.019558	9.609E-07	1.051503	21402.13	0.0566	87.17188	0.606
	3	2701	1.7	1.40E-04	21.15960015	0.019558	9.609E-07	1.051503	21402.13	0.0607	87.17188	0.606
2.5	1	1701	1.9	6.45E-05	20.61470312	0.019558	9.609E-07	0.315433	6420.278	0.0739	54.89795	0.606
	2	1501	1.2	2.26E-05	20.72398401	0.019558	9.609E-07	0.315433	6420.278	0.0724	48.44317	0.606
	3	1501	0.6	3.44E-05	20.99034644	0.019558	9.609E-07	0.315433	6420.278	0.0785	48.44317	0.606

Fig.B3 TI data acquisition result for the parallel thermocouple.

Flow rate (gal/mint)	Iteration	h (w/m2.C)	taw (second)	R" (C.m2/W)	T_water C	D (m)	Viscosity (N.S.m2/Kg)	U (m/s)	Re	Min error	Nu	K -water (w/m.C)
max 14.5	1	3401	5.7	1.53E-04	21.05403999	0.019558	9.609E-07	3.039911	61873.84	0.067	109.7636	0.606
	2	7301	9.8	3.49E-04	21.0847788	0.019558	9.609E-07	3.039911	61873.84	0.0664	235.6319	0.606
	3	2501	4.7	4.78E-05	21.38040384	0.019558	9.609E-07	3.039911	61873.84	0.0645	80.71709	0.606
11	1	2301	4.7	1.75E-05	20.89598435	0.019558	9.609E-07	2.103007	42804.25	0.069	74.26231	0.606
	2	2301	5.4	2.42E-05	21.12662755	0.019558	9.609E-07	2.103007	42804.25	0.0709	74.26231	0.606
	3	2401	6.9	4.53E-05	21.37826739	0.019558	9.609E-07	2.103007	42804.25	0.0803	77.4897	0.606
7.9	1	2101	2.5	2.22E-05	20.74184674	0.019558	9.609E-07	1.661377	33815.39	0.0693	67.80752	0.606
	2	9901	20	6.54E-04	20.920303	0.019558	9.609E-07	1.661377	33815.39	0.4684	319.5442	0.606
	3	9901	20	4.94E-04	21.14687708	0.019558	9.609E-07	1.661377	33815.39	0.1418	319.5442	0.606
4.9	1	9901	20	4.65E-04	20.98331684	0.019558	9.609E-07	1.051503	21402.13	0.161	319.5442	0.606
	2	1901	3.3	6.31E-05	20.9564808	0.019558	9.609E-07	1.051503	21402.13	0.0711	61.35274	0.606
	3	4001	13.1	4.14E-04	21.16947763	0.019558	9.609E-07	1.051503	21402.13	0.0689	129.128	0.606
2.5	1	1401	3.2	3.73E-05	20.6071449	0.019558	9.609E-07	0.315433	6420.278	0.0805	45.21577	0.606
	2	1501	3	1.25E-04	20.72398401	0.019558	9.609E-07	0.315433	6420.278	0.0744	48.44317	0.606
	3	1601	4.1	1.05E-04	21.19219863	0.019558	9.609E-07	0.315433	6420.278	0.0777	51.67056	0.606

Fig.B4 TI data acquisition result for the welded thermocouple.

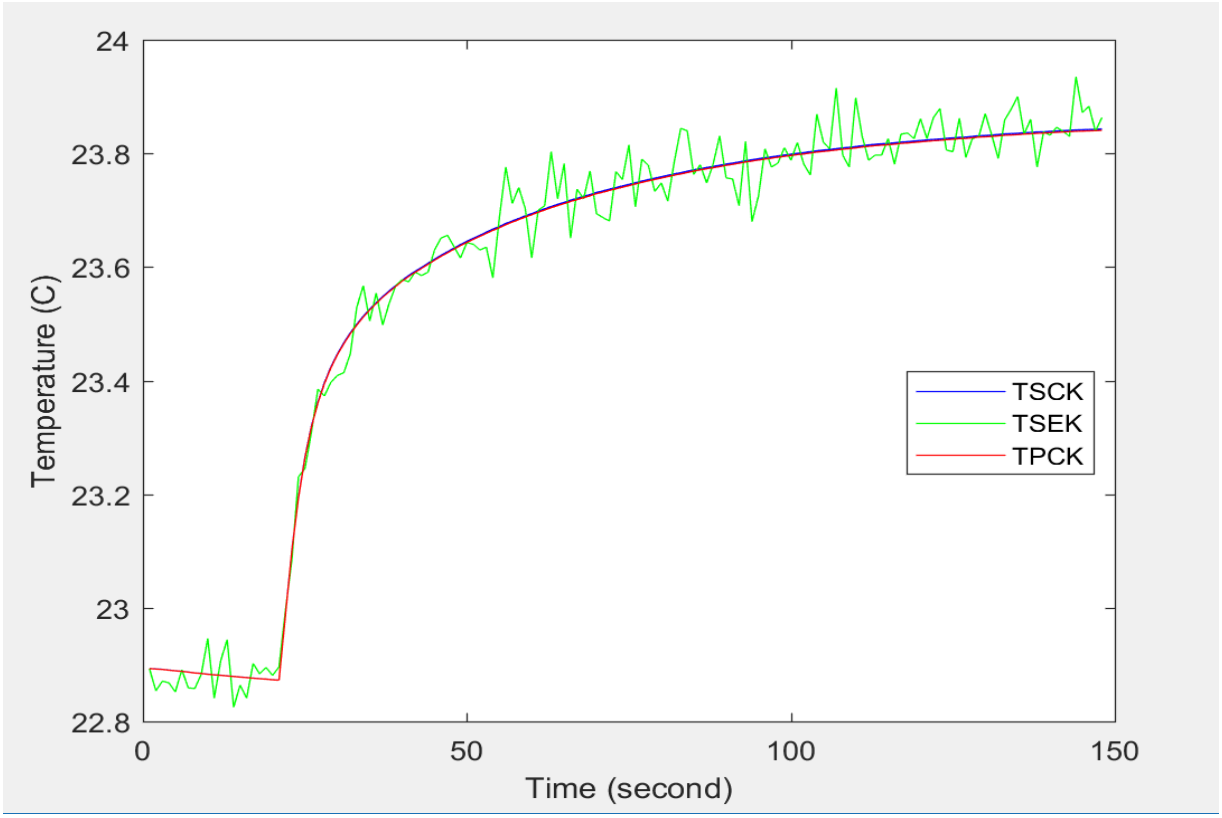

Fig.B5 Arduino data acquisition temperature curves for the paralleled thermocouple.

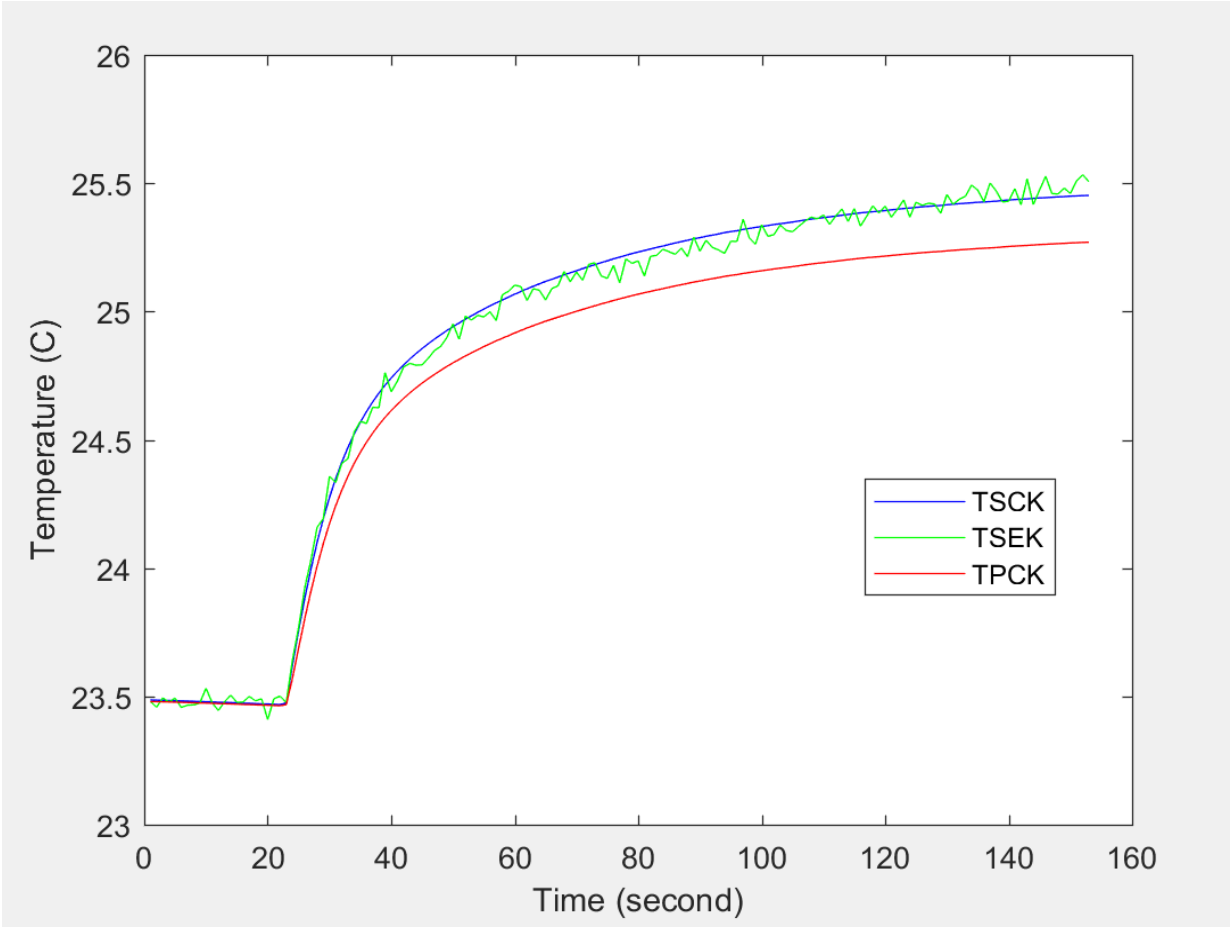

Fig.B6 Arduino data acquisition temperature curves for the welded thermocouple.

Flow rate (gal/mint)	Iteration	h (w/m2.C)	taw (second)	R" (C.m2/W)	T_water (C)	D (m)	Viscosity (N.S.m2/Kg)	U (m/s)	Re	Min error	Nu	K- water (w/m.C)
max 14.5	1	9901	0.5	3.56E-04	22.247004	0.019558	9.609E-07	3.039911	61873.84	0.0427	319.5442	0.606
	2	3801	1.5	2.04E-04	22.536746	0.019558	9.609E-07	3.039911	61873.84	0.0386	122.6732	0.606
	3	2201	0.9	1.1147e-06	22.821536	0.019558	9.609E-07	3.039911	61873.84	0.0384	71.03491	0.606
10	1	2901	0.9	1.51E-04	22.622175	0.019558	9.609E-07	2.103007	42804.25	0.0371	93.62666	0.606
	2	2901	0.9	1.51E-04	22.903812	0.019558	9.609E-07	2.103007	42804.25	0.0371	93.62666	0.606
	3	2901	0.9	1.51E-04	23.313857	0.019558	9.609E-07	2.103007	42804.25	0.0371	93.62666	0.606
8.8	1	2101	0.8	1.3907e-05	22.607568	0.019558	9.609E-07	1.661377	33815.39	0.0378	67.80752	0.606
	2	2101	0.8	1.3907e-05	22.817335	0.019558	9.609E-07	1.661377	33815.39	0.0378	67.80752	0.606
	3	2501	0.6	6.11E-05	23.187233	0.019558	9.609E-07	1.661377	33815.39	0.0403	80.71709	0.606
5.5	1	2101	0.6	1.14E-04	22.760733	0.019558	9.609E-07	1.051503	21402.13	0.0394	67.80752	0.606
	2	2001	0.8	1.01E-04	23.013513	0.019558	9.609E-07	1.051503	21402.13	0.0375	64.58013	0.606
	3	1801	0	6.37E-06	23.260589	0.019558	9.609E-07	1.051503	21402.13	0.0503	58.12534	0.606
2.7	1	1301	1.6	5.27E-05	23.141422	0.019558	9.609E-07	0.315433	6420.278	0.0568	41.98838	0.606
	2	2001	1.4	3.21E-04	23.37084	0.019558	9.609E-07	0.315433	6420.278	0.0395	64.58013	0.606
	3	1401	0.2	4.98E-05	23.642755	0.019558	9.609E-07	0.315433	6420.278	0.074	45.21577	0.606

Fig.B7 Arduino data acquisition result for the parallel thermocouple.

Flow rate (gal/mint)	Iteration	h (w/m2.C)	taw (second)	R" (C.m2/W)	T_water C	D (m)	Viscosity (N.S.m2/Kg)	U (m/s)	Re	Min error	Nu	K -water (w/m.C)
max 14.5	1	1701	6.7	1.57E-05	22.262563	0.019558	9.609E-07	3.039911	61873.84	0.0601	54.89795	0.606
	2	2801	10.5	2.34E-04	22.604873	0.019558	9.609E-07	3.039911	61873.84	0.04	90.39927	0.606
	3	1901	4.9	2.61E-05	22.910731	0.019558	9.609E-07	3.039911	61873.84	0.05	61.35274	0.606
10	1	1801	5	3.86E-05	22.667396	0.019558	9.609E-07	2.103007	42804.25	0.0492	58.12534	0.606
	2	1801	5	3.86E-05	23.00171	0.019558	9.609E-07	2.103007	42804.25	0.0492	58.12534	0.606
	3	1801	5	3.86E-05	23.360105	0.019558	9.609E-07	2.103007	42804.25	0.0492	58.12534	0.606
8.8	1	1701	2.7	1.02E-05	22.604644	0.019558	9.609E-07	1.661377	33815.39	0.05	54.89795	0.606
	2	1701	2.7	1.02E-05	22.91495	0.019558	9.609E-07	1.661377	33815.39	0.05	54.89795	0.606
	3	1801	3.8	4.59E-05	23.228384	0.019558	9.609E-07	1.661377	33815.39	0.0433	58.12534	0.606
5.5	1	1601	3.2	8.92E-05	22.767839	0.019558	9.609E-07	1.051503	21402.13	0.0404	51.67056	0.606
	2	1601	3.2	8.92E-05	23.0694	0.019558	9.609E-07	1.051503	21402.13	0.0404	51.67056	0.606
	3	1401	4.5	1.60E-05	0.0166952	0.019558	9.609E-07	1.051503	21402.13	0.0619	45.21577	0.606
2.7	1	1201	2.5	8.17E-05	23.139434	0.019558	9.609E-07	0.315433	6420.278	0.0375	38.76099	0.606
	2	1201	2.5	8.17E-05	23.414754	0.019558	9.609E-07	0.315433	6420.278	0.0375	38.76099	0.606
	3	1201	1.3	3.86E-05	23.663222	0.019558	9.609E-07	0.315433	6420.278	0.0656	38.76099	0.606

Fig.B8 Arduino data acquisition result for the welded thermocouple.

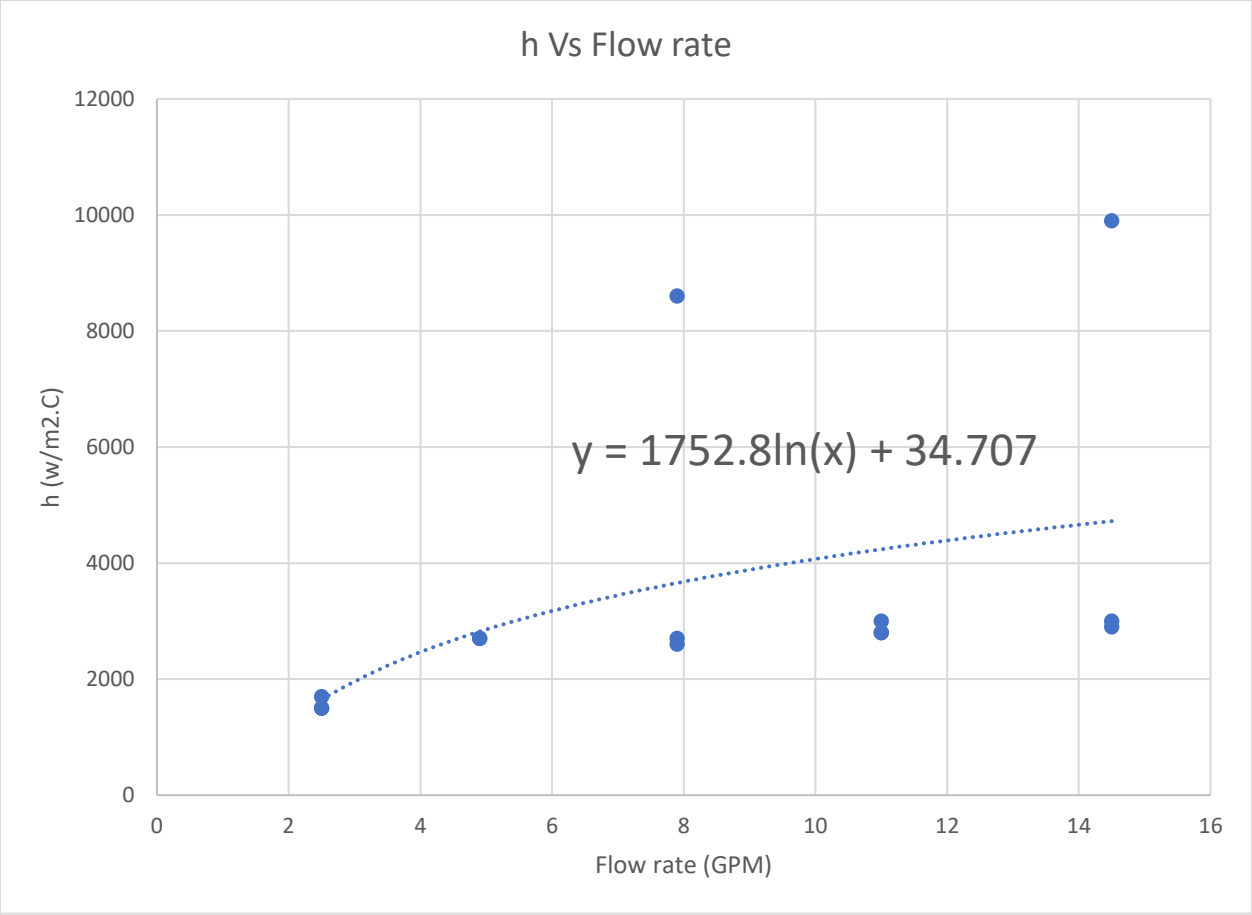

Fig.B9 TI data acquisition correlation for the parallel thermocouple.

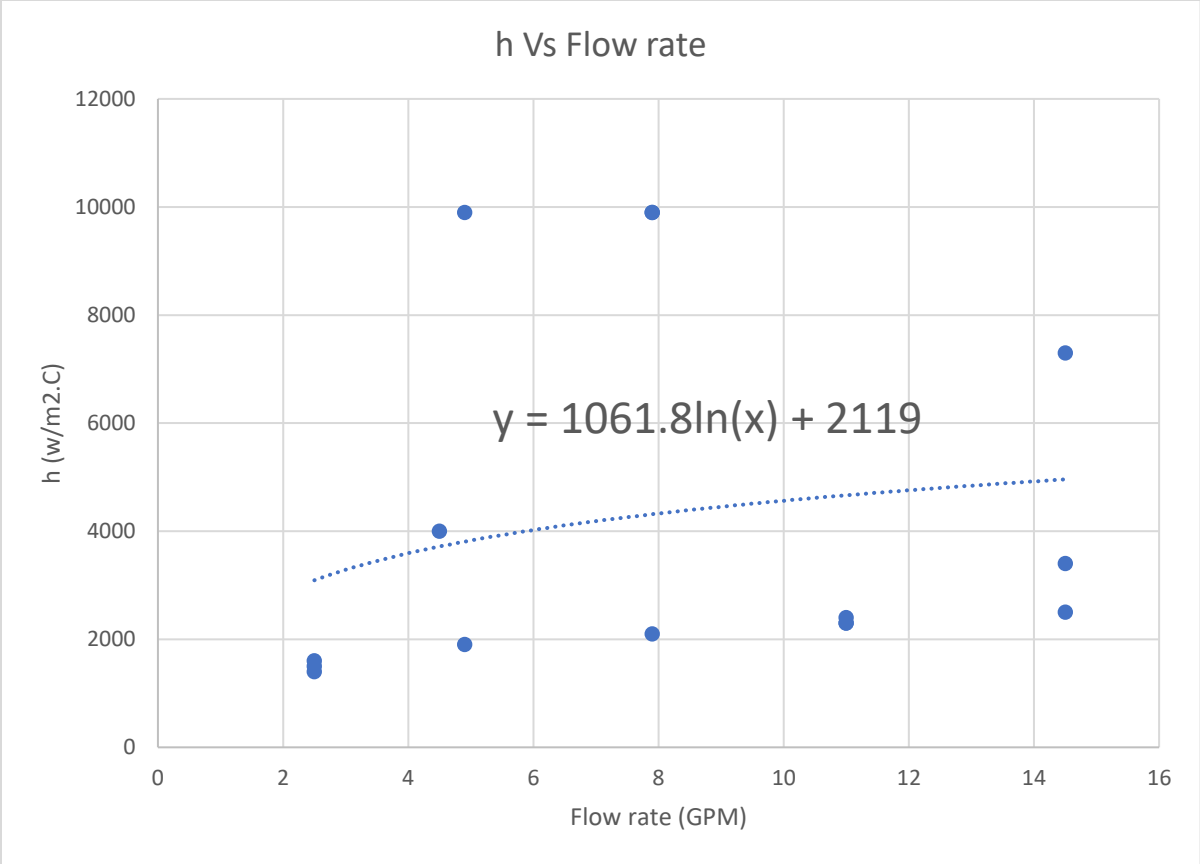

Fig.B10 TI data acquisition correlation for the welded thermocouple.

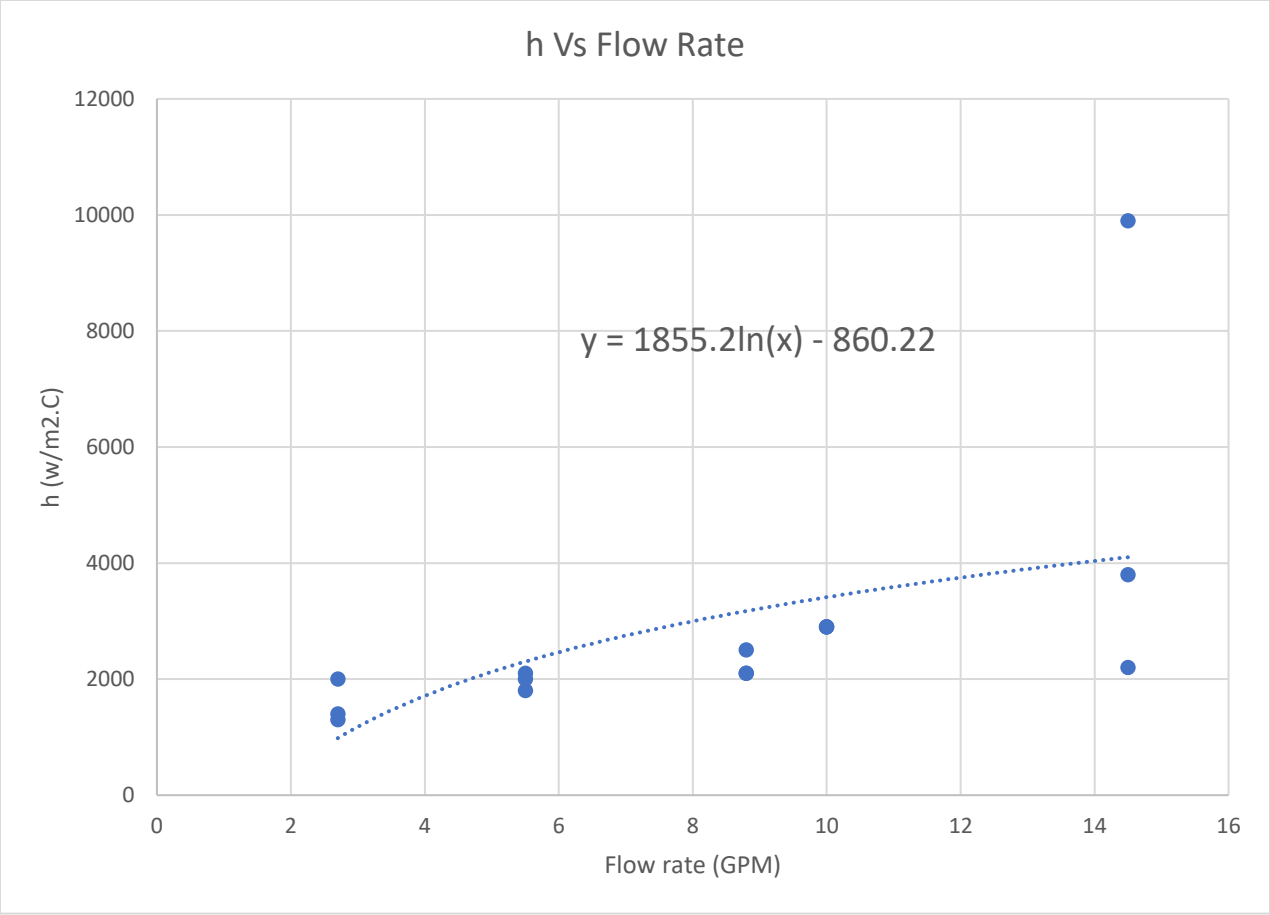

Fig.B11 Arduino data acquisition correlation for the parallel thermocouple.

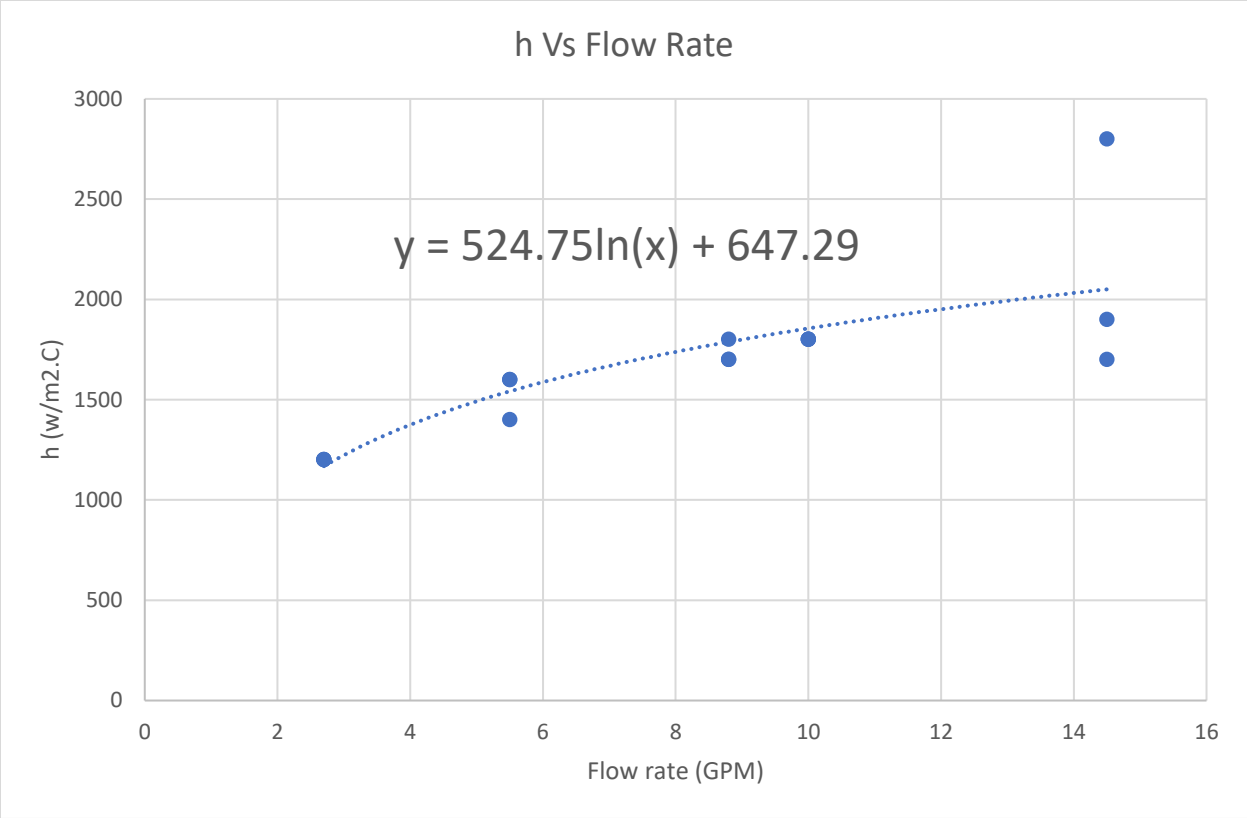

Fig.B12 Arduino data acquisition correlation for the welded thermocouple.

Appendix C- National Instrument (NI) Data Acquisition Results

To minimize the noise, a National Instrument (NI) data acquisition was purchased and used to analyze the data in this paper. For multiple steps, the final wall pipe temperature is

$$T_k(t) = T_s(0) - R".q_s''(0) + \sum_{j=1}^{k-1} \frac{\Delta q_{s,j}''}{h}\left(1 - e^{-\frac{(t_k - t_j)}{\tau}}\right).H(t - t_j)$$

The results were analyzed for three days for both parallel and welded thermocouples. Please see the figures below.

								at 298 K						
Flow rate (G/mint)	h(W/m2.C)	tau (S)	R" (C.m2/W)	U (W/C.m2)	Tw©	Min RMS Value	h*tau (W.S/m2.C)	D (m)	Viscosity (N.S.m2/Kg)	Velocity (m/s)	K- water (w/m.C)	Re	Nu	R" average
14.5	2475	11.8	0.00044	1177	25.35	0.0422	29205	0.019558	9.609E-07	3.046561779	0.606	62009.22	79.87797	0.000382
14.5	2241	10.6	0.00036	1227	25.52	0.0375	23754.6	0.019558	9.609E-07	3.046561779	0.606	62009.22	72.32587	0.000382
14.5	2224	11.2	0.00037	1214	25.67	0.0379	24908.8	0.019558	9.609E-07	3.046561779	0.606	62009.22	71.77721	0.000382
10	2134	11.4	0.00038	1170	24.83	0.0458	24327.6	0.019558	9.609E-07	2.101077089	0.606	42764.98	68.87256	0.000382
10	2117	11.7	0.00035	1202	25	0.0597	24768.9	0.019558	9.609E-07	2.101077089	0.606	42764.98	68.3239	0.000382
10	2087	12.1	0.00038	1158	25.19	0.0561	25252.7	0.019558	9.609E-07	2.101077089	0.606	42764.98	67.35569	0.000382
5.5	1892	10.1	0.00039	1078	24.54	0.053	19109.2	0.019558	9.609E-07	1.155592399	0.606	23520.74	61.06227	0.000382
5.5	1910	10.3	0.0004	1073	24.71	0.0556	19673	0.019558	9.609E-07	1.155592399	0.606	23520.74	61.6432	0.000382
1.75	1020	4.4	0.00021	838	23.64	0.0601	4488	0.019558	9.609E-07	0.367688491	0.606	7483.871	32.91941	0.000382
1.75	1414	9.6	0.00053	802	23.71	0.0779	13574.4	0.019558	9.609E-07	0.367688491	0.606	7483.871	45.63533	0.000382
1.75	1388	6	0.00039	900	23.89	0.0663	8328	0.019558	9.609E-07	0.367688491	0.606	7483.871	44.79621	0.000382

Fig.C1 NI data acquisition results for the welded thermocouple Day 1.

								at 297					
Flow rate (G/mint)	h(W/m2.C)	tau (S)	R" (C.m2/W)	U (W/C.m2)	Tw©	Min RMS Value	h*tau (W.S/m2.C)	D (m)	Viscosity (N.S.m2/Kg)	Velocity (m/s)	K- water (w/m.C)	Re	Nu
14.5	2230	14.3	0.00045	1112	21.71	0.0417	31889	0.019558	9.609E-07	3.042215757	0.606	61920.76	71.97086
14.5	2089	11.4	0.00043	1089	21.91	0.0393	23814.6	0.019558	9.609E-07	3.042215757	0.606	61920.76	67.42023
14.5	1906	9.9	0.00041	1064	22.13	0.0386	18869.4	0.019558	9.609E-07	3.042215757	0.606	61920.76	61.51411
14.5	1910	9.3	0.00038	1106	22.35	0.0551	17763	0.019558	9.609E-07	3.042215757	0.606	61920.76	61.6432
10	1908	10.1	0.00049	980	22.56	0.0412	19270.8	0.019558	9.609E-07	2.098079832	0.606	42703.97	61.57865
10	1790	12.6	0.00045	991	22.72	0.0448	22554	0.019558	9.609E-07	2.098079832	0.606	42703.97	57.77033
10	1783	11.8	0.00046	980	22.96	0.0458	21039.4	0.019558	9.609E-07	2.098079832	0.606	42703.97	57.54441
10	1875	11.3	0.0005	964	23.21	0.042	21187.5	0.019558	9.609E-07	2.098079832	0.606	42703.97	60.51361
5.7	1641	9.6	0.00051	888	23.82	0.045	15753.6	0.019558	9.609E-07	1.195905504	0.606	24341.26	52.96151
5.7	1665	9.3	0.0005	906	24	0.0436	15484.5	0.019558	9.609E-07	1.195905504	0.606	24341.26	53.73609
5.7	1700	7.2	0.00051	907	24.3	0.0466	12240	0.019558	9.609E-07	1.195905504	0.606	24341.26	54.86568
1.3	593	4.2	0.00022	524	24.72	0.0579	2490.6	0.019558	9.609E-07	0.272750378	0.606	5551.516	19.13844
1.3	572	4.6	0.00016	523	24.87	0.0562	2631.2	0.019558	9.609E-07	0.272750378	0.606	5551.516	18.46069
1.3	572	4	0.00011	535	25.14	0.0539	2288	0.019558	9.609E-07	0.272750378	0.606	5551.516	18.46069
1.3	580	4	0.00013	537	25.37	0.0348	2320	0.019558	9.609E-07	0.272750378	0.606	5551.516	18.71888

Fig.C2 NI data acquisition results for the welded thermocouple Day 2.

								at297						
Flow rate (G/mint)	h(W/m2.C)	tau (S)	R" (C.m2/W)	U (W/C.m2)	Tw©	Min RMS Value	h*tau (W.S/m2.C)	D (m)	Viscosity (N.S.m2/Kg)	Velocity (m/s)	K- water (w/m.C)	Re	Nu	R" Average
14.5	2014	10.9	0.00042	1082	22.38	0.0372	21952.6	0.019558	9.609E-07	3.042215757	0.606	61920.76	64.99969	0.000402
14.5	2093	11.3	0.00046	1056	22.6	0.0397	23650.9	0.019558	9.609E-07	3.042215757	0.606	61920.76	67.54933	0.000402
14.5	1878	11.2	0.00041	1057	22.84	0.0486	21033.6	0.019558	9.609E-07	3.042215757	0.606	61920.76	60.61044	0.000402
14.5	1889	10.8	0.00042	1045	23	0.0452	20401.2	0.019558	9.609E-07	3.042215757	0.606	61920.76	60.96545	0.000402
10.2	1894	10.7	0.00047	994	23.58	0.0398	20265.8	0.019558	9.609E-07	2.140041429	0.606	43558.05	61.12682	0.000402
10.2	1789	10.3	0.00044	994	23.81	0.044	18426.7	0.019558	9.609E-07	2.140041429	0.606	43558.05	57.73806	0.000402
10.2	1809	9.8	0.00046	984	24	0.0422	17728.2	0.019558	9.609E-07	2.140041429	0.606	43558.05	58.38353	0.000402
4.3	1831	9.9	0.0006	866	24.33	0.0544	18126.9	0.019558	9.609E-07	0.902174328	0.606	18362.71	59.09356	0.000402
4.3	1528	8.3	0.0005	868	24.56	0.0493	12682.4	0.019558	9.609E-07	0.902174328	0.606	18362.71	49.31456	0.000402
4.3	1521	8.2	0.0005	864	24.79	0.0543	12472.2	0.019558	9.609E-07	0.902174328	0.606	18362.71	49.08864	0.000402
4.3	1479	7.3	0.00047	866	25.3	0.0446	10796.7	0.019558	9.609E-07	0.902174328	0.606	18362.71	47.73314	0.000402
1.5	823	3.6	0.00023	688	25.63	0.0411	2962.8	0.019558	9.609E-07	0.314711975	0.606	6405.596	26.56144	0.000402
1.5	869	4.7	0.00033	673	25.78	0.0484	4084.3	0.019558	9.609E-07	0.314711975	0.606	6405.596	28.04604	0.000402
1.5	830	4.5	0.00028	672	26	0.0511	3735	0.019558	9.609E-07	0.314711975	0.606	6405.596	26.78736	0.000402
1.5	686	4.3	0.000038	668	26.2	0.0419	2949.8	0.019558	9.609E-07	0.314711975	0.606	6405.596	22.13991	0.000402

Fig.C3 NI data acquisition results for the welded thermocouple Day 3.

								at 298 K					
Flow rate (G/mint)	h(W/m2.C)	tau (S)	R" (C.m2/W)	U (W/C.m2)	Tw©	Min RMS Value	h*tau (W.S/m2.C)	D (m)	Viscosity (N.S.m2/Kg)	Velocity (m/s)	K- water (w/m.C)	Re	Nu
14.5	3559	0.6	0.0000045	3502	25.47	0.0143	2135.4	0.019558	9.609E-07	3.042215757	0.606	61920.75738	114.8629
14.5	3386	0.4	0.00000033	3382	25.6	0.0256	1354.4	0.019558	9.609E-07	3.042215757	0.606	61920.75738	109.2795
10	3209	0.7	0.0000011	3197	24.81	0.012	2246.3	0.019558	9.609E-07	2.098079832	0.606	42703.97061	103.567
10	3089	0.9	0.0000065	3027	24.92	0.0114	2780.1	0.019558	9.609E-07	2.098079832	0.606	42703.97061	99.69416
10	3173	0.7	0.0000069	3104	25.14	0.0131	2221.1	0.019558	9.609E-07	2.098079832	0.606	42703.97061	102.4052
5.5	2397	0.8	0.00000067	2393	24.28	0.0156	1917.6	0.019558	9.609E-07	1.153943908	0.606	23487.18383	77.3606
5.5	2366	1.1	0.0000058	2333	24.41	0.0114	2602.6	0.019558	9.609E-07	1.153943908	0.606	23487.18383	76.36011
5.5	2355	0.8	0.0000097	2302	24.51	0.0163	1884	0.019558	9.609E-07	1.153943908	0.606	23487.18383	76.0051
1.75	1369	1.1	0.000019	1332	23.59	0.0357	1505.9	0.019558	9.609E-07	0.367163971	0.606	7473.194856	44.18301
1.75	1294	1.2	0.0000039	1287	23.7	0.0491	1552.8	0.019558	9.609E-07	0.367163971	0.606	7473.194856	41.76246
1.75	1556	0.9	0.0000037	1547	24	0.0339	1400.4	0.019558	9.609E-07	0.367163971	0.606	7473.194856	50.21823

Fig.C4 NI data acquisition results for the parallel thermocouple Day 1.

								at 297						
Flow rate (G/mint)	h(W/m2.C)	tau (S)	R" (C.m2/W)	U (W/C.m2)	Tw©	Min RMS Value	h*tau (W.S/m2.C)	D (m)	Viscosity (N.S.m2/Kg)	Velocity (m/s)	K- water (w/m.C)	Re	Nu	R" average
14.5	3467	0.9	0.0000015	3448	21.75	0.0122	3120.3	0.019558	9.609E-07	3.042215757	0.606	61920.76	111.8937063	0.000014
14.5	3508	1	0.000016	3322	21.9	0.0107	3508	0.019558	9.609E-07	3.042215757	0.606	61920.76	113.2169373	0.000014
14.5	3243	0.6	0.0000014	3245	22.1	0.0195	1945.8	0.019558	9.609E-07	3.042215757	0.606	61920.76	104.6643465	0.000014
14.5	3371	0.8	0.0000043	3322	22.3	0.0112	2696.8	0.019558	9.609E-07	3.042215757	0.606	61920.76	108.7954092	0.000014
10	2968	0.7	0.0000026	2944	22.57	0.0153	2077.6	0.019558	9.609E-07	2.098079832	0.606	42703.97	95.7890165	0.000014
10	2992	0.8	0.000015	2864	22.73	0.0141	2393.6	0.019558	9.609E-07	2.098079832	0.606	42703.97	96.56359076	0.000014
10	2966	0.9	0.00001	2880	22.96	0.0128	2669.4	0.019558	9.609E-07	2.098079832	0.606	42703.97	95.72446865	0.000014
10	2901	0.6	0.0000019	2885	23.24	0.023	1740.6	0.019558	9.609E-07	2.098079832	0.606	42703.97	93.62666337	0.000014
5.7	2373	0.3	0.0000041	2349	23.63	0.0421	711.9	0.019558	9.609E-07	1.195905504	0.606	24341.26	76.5860297	0.000014
5.7	2404	0.9	0.0000019	2392	23.84	0.0144	2163.6	0.019558	9.609E-07	1.195905504	0.606	24341.26	77.58652145	0.000014
5.7	2450	0.9	0.0000027	2433	24	0.0134	2205	0.019558	9.609E-07	1.195905504	0.606	24341.26	79.07112211	0.000014
5.7	2351	0.4	0.0000043	2327	24.29	0.0346	940.4	0.019558	9.609E-07	1.195905504	0.606	24341.26	75.8760033	0.000014
1.3	800	2.5	0.000025	785	24.71	0.0663	2000	0.019558	9.609E-07	0.272750378	0.606	5551.516	25.81914191	0.000014
1.3	777	2.6	0.0000016	776	24.83	0.0682	2020.2	0.019558	9.609E-07	0.272750378	0.606	5551.516	25.07684158	0.000014
1.3	840	2.3	0.000051	805	25.14	0.09	1932	0.019558	9.609E-07	0.272750378	0.606	5551.516	27.11009901	0.000014
1.3	867	2.3	0.000081	810	25.38	0.0766	1994.1	0.019558	9.609E-07	0.272750378	0.606	5551.516	27.98149505	0.000014

Area

Fig.C5 NI data acquisition results for the parallel thermocouple Day 2.

								at 297						
Flow rate (G/mint)	h(W/m2.C)	tau (S)	R" (C.m2/W)	U (W/C.m2)	Tw©	Min RMS Value	h*tau (W.S/m2.C)	D (m)	Viscosity (N.S.m2/Kg)	Velocity (m/s)	K- water (w/m.C)	Re	Nu	R" average
14.5	3405	1	0.00000073	3396	22.43	0.0097	3405	0.019558	9.609E-07	3.042215757	0.606	61920.76	109.8927228	0.00001126
14.5	3428	0.8	0.0000078	3338	22.66	0.0114	2742.4	0.019558	9.609E-07	3.042215757	0.606	61920.76	110.6350231	0.00001126
14.5	3300	0.7	0.0000026	3272	22.87	0.0163	2310	0.019558	9.609E-07	3.042215757	0.606	61920.76	106.5039604	0.00001126
14.5	3376	0.8	0.0000033	3337	23.1	0.0124	2700.8	0.019558	9.609E-07	3.042215757	0.606	61920.76	108.9567789	0.00001126
10.2	3089	0.4	0.00000822	3012	23.43	0.029	1235.6	0.019558	9.609E-07	2.140041429	0.606	43558.05	99.69416172	0.00001126
10.2	2946	0.7	0.0000036	2914	23.57	0.0193	2062.2	0.019558	9.609E-07	2.140041429	0.606	43558.05	95.0789901	0.00001126
10.2	3059	0.8	0.0000011	3047	23.83	0.0117	2447.2	0.019558	9.609E-07	2.140041429	0.606	43558.05	98.72594389	0.00001126
10.2	3114	0.9	0.0000028	3086	24	0.0115	2802.6	0.019558	9.609E-07	2.140041429	0.606	43558.05	100.5010099	0.00001126
4.3	2057	0.3	0.0000097	2016	24.35	0.0699	617.1	0.019558	9.609E-07	0.902174328	0.606	18362.71	66.38746865	0.00001126
4.3	2066	0.6	0.0000025	2055	24.56	0.0326	1239.6	0.019558	9.609E-07	0.902174328	0.606	18362.71	66.67793399	0.00001126
4.3	2166	1.1	0.0000075	2131	24.79	0.0198	2382.6	0.019558	9.609E-07	0.902174328	0.606	18362.71	69.90532673	0.00001126
4.3	2155	0.7	0.00001	2106	25.31	0.0289	1508.5	0.019558	9.609E-07	0.902174328	0.606	18362.71	69.55031353	0.00001126
1.5	1254	1.4	0.00000038	1253	25.61	0.035	1755.6	0.019558	9.609E-07	0.314711975	0.606	6405.596	40.47150495	0.00001126
1.5	1266	1.4	0.000037	1208	25.74	0.0399	1772.4	0.019558	9.609E-07	0.314711975	0.606	6405.596	40.85879208	0.00001126
1.5	1277	1.4	0.000039	1216	25.94	0.0419	1787.8	0.019558	9.609E-07	0.314711975	0.606	6405.596	41.21380528	0.00001126
1.5	1282	1.6	0.000044	1213	26.18	0.0548	2051.2	0.019558	9.609E-07	0.314711975	0.606	6405.596	41.37517492	0.00001126

Fig.C6 NI data acquisition results for the parallel thermocouple Day 3.

Appendix D- National Instrument (NI) Data Acquisition correlations between the overall heat transfer coefficient and the flow rate

Another correlation between the overall heat transfer coefficient (U) and the flow rate (Q) was done for both welded and parallel thermocouples. The correlations presented in the appendix because there are no advantages to use these in the results section. Please see the correlations below.

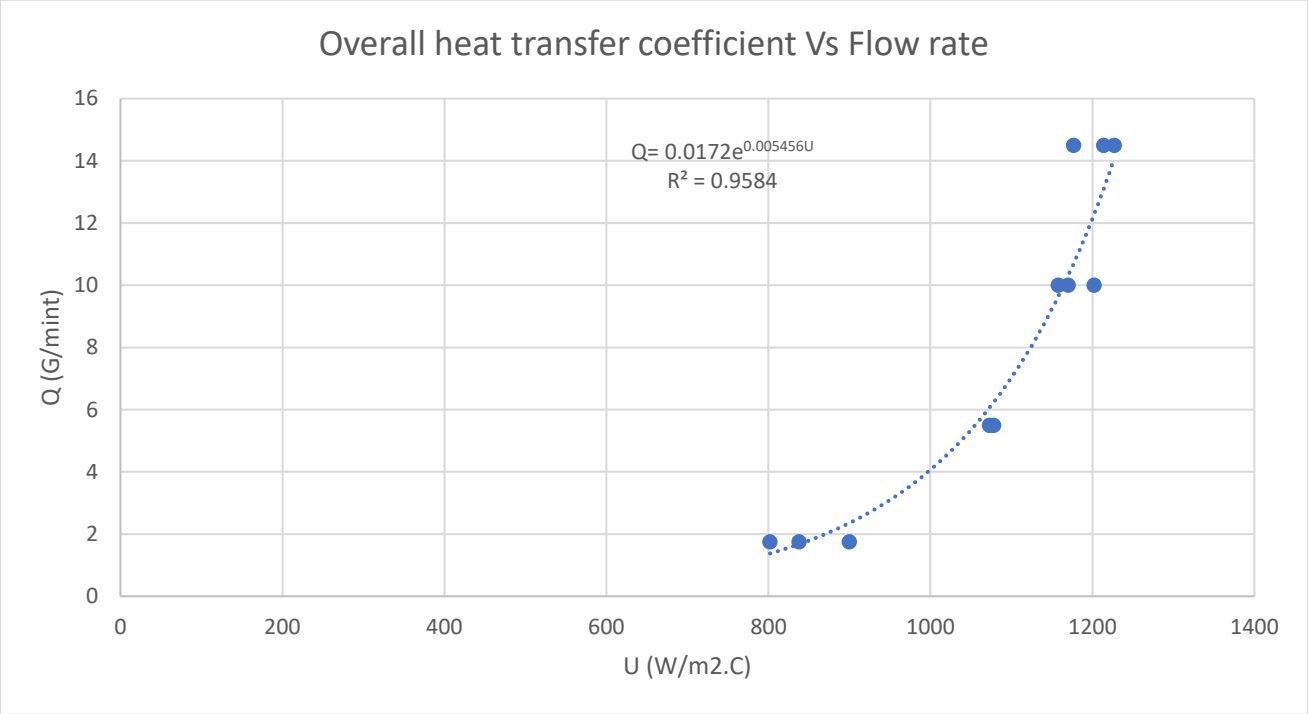

Fig.D1 NI data acquisition correlation for the welded thermocouple Day 1.

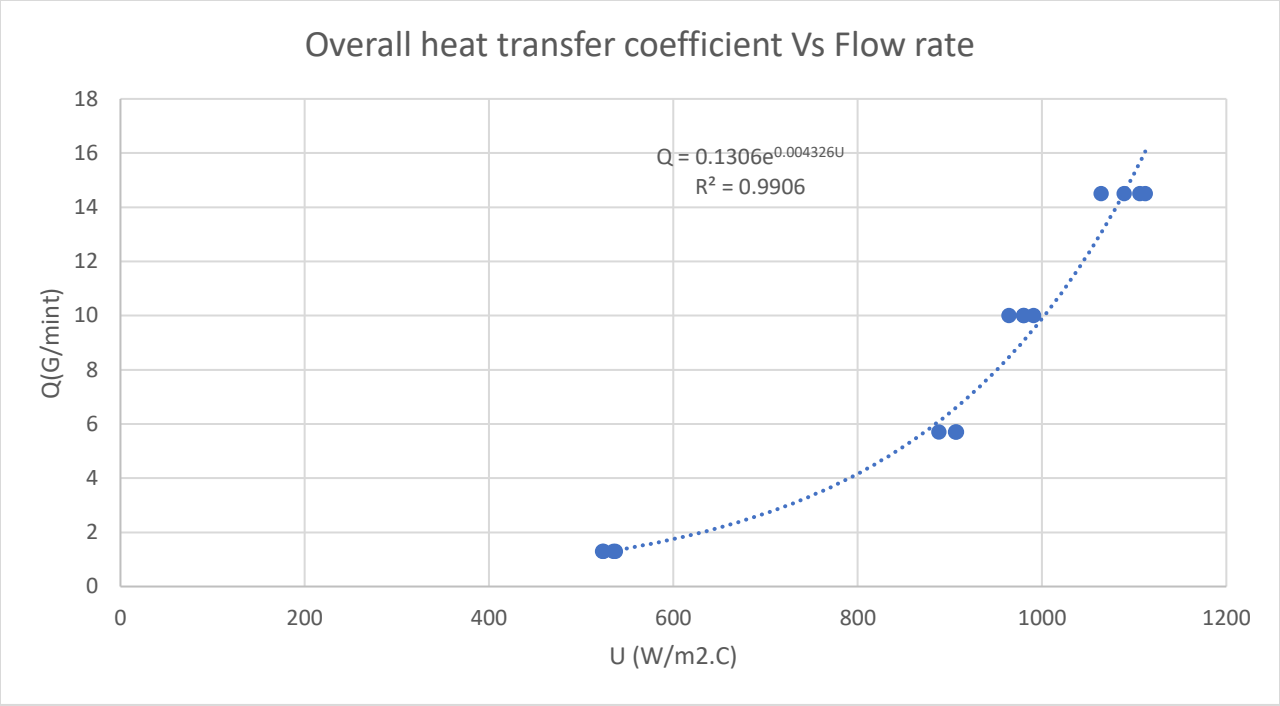

Fig.D2 NI data acquisition correlation for the welded thermocouple Day 2.

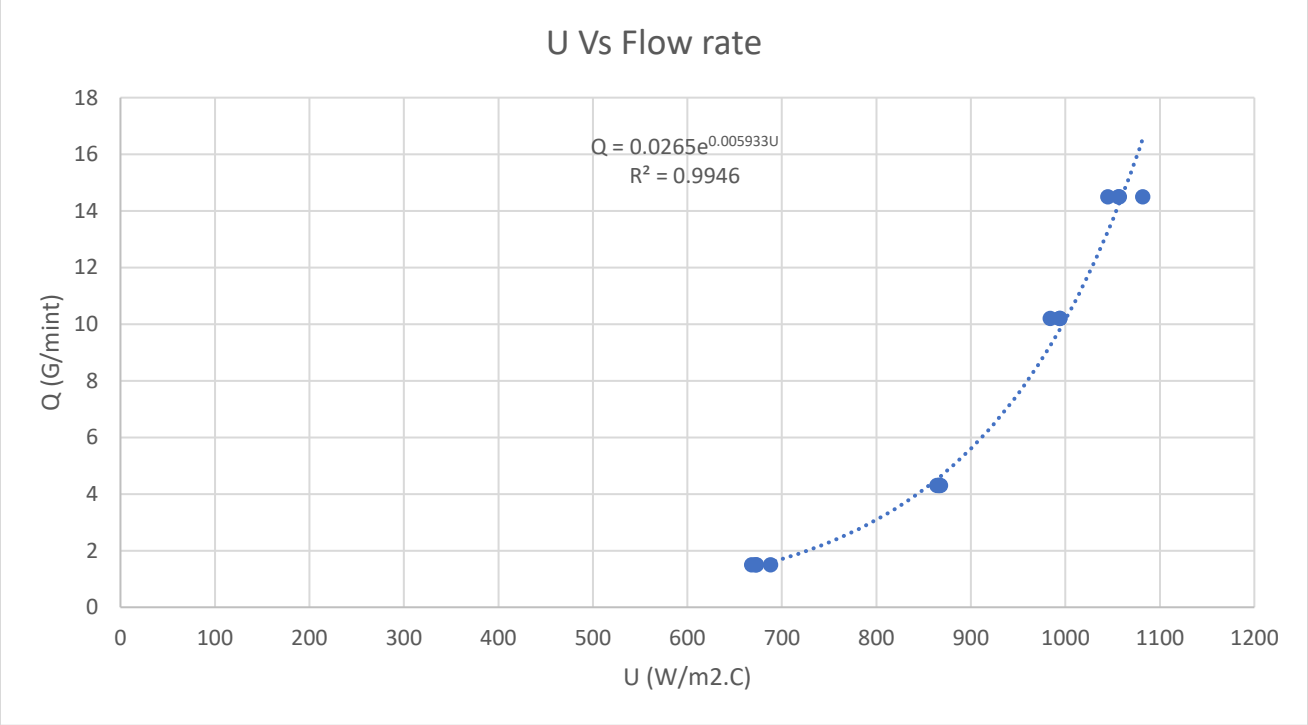

Fig.D3 NI data acquisition correlation for the welded thermocouple Day 3.

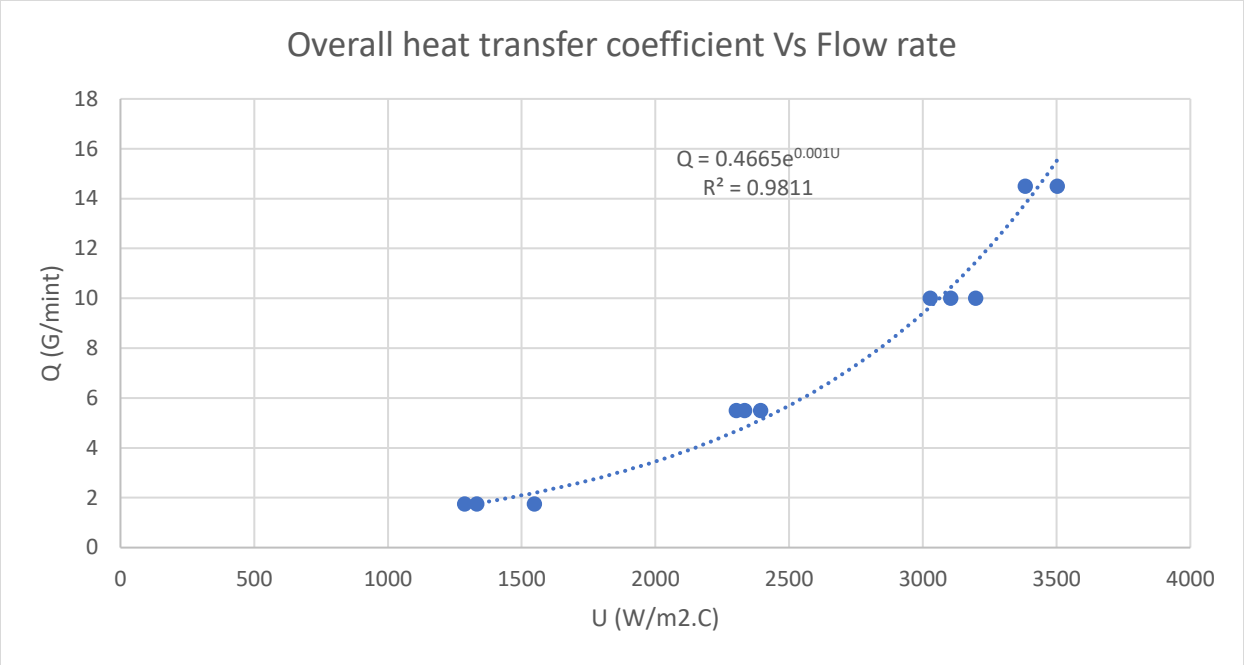

Fig.D4 NI data acquisition correlation for the parallel thermocouple Day 1.

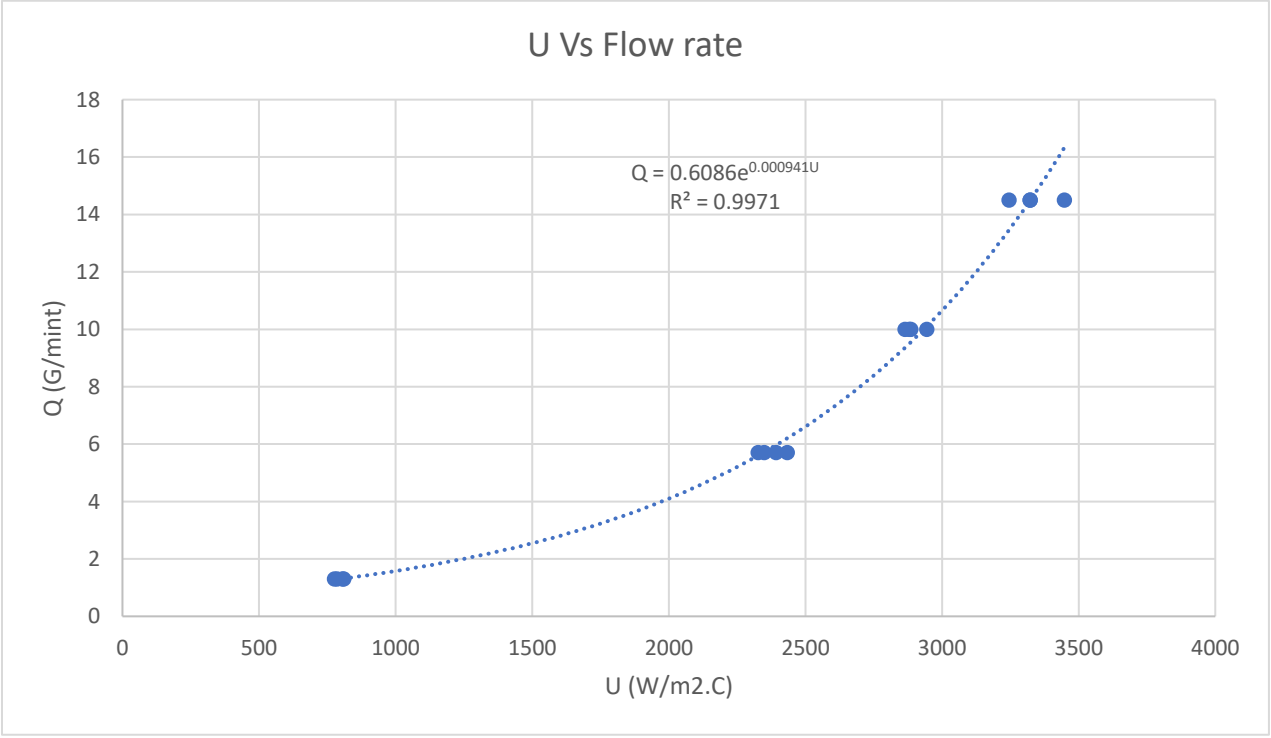

Fig.D5 NI data acquisition correlation for the parallel thermocouple Day 2.

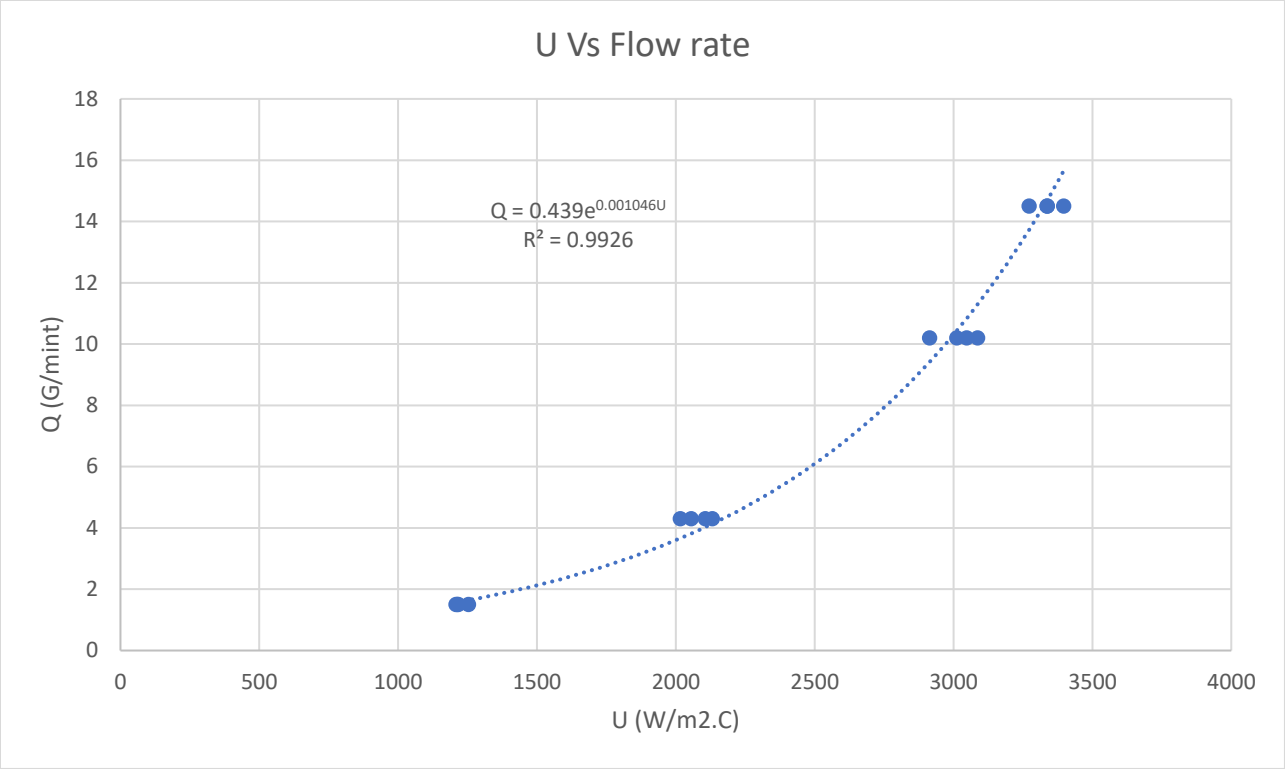

Fig.D6 NI data acquisition correlation for the parallel thermocouple Day 3.

Appendix E- Root Mean Sequard error (RMS) Vs h, R", and Time constant curves for National Instrument (NI) Data Acquisition for Both Parallel and Welded Thermocouples

Depend on the parameter estimation routine the curves between RMS and optimal parameters were plotted for the parallel and welded thermocouples. They are helpful to distinguish better estimation routine in the future.

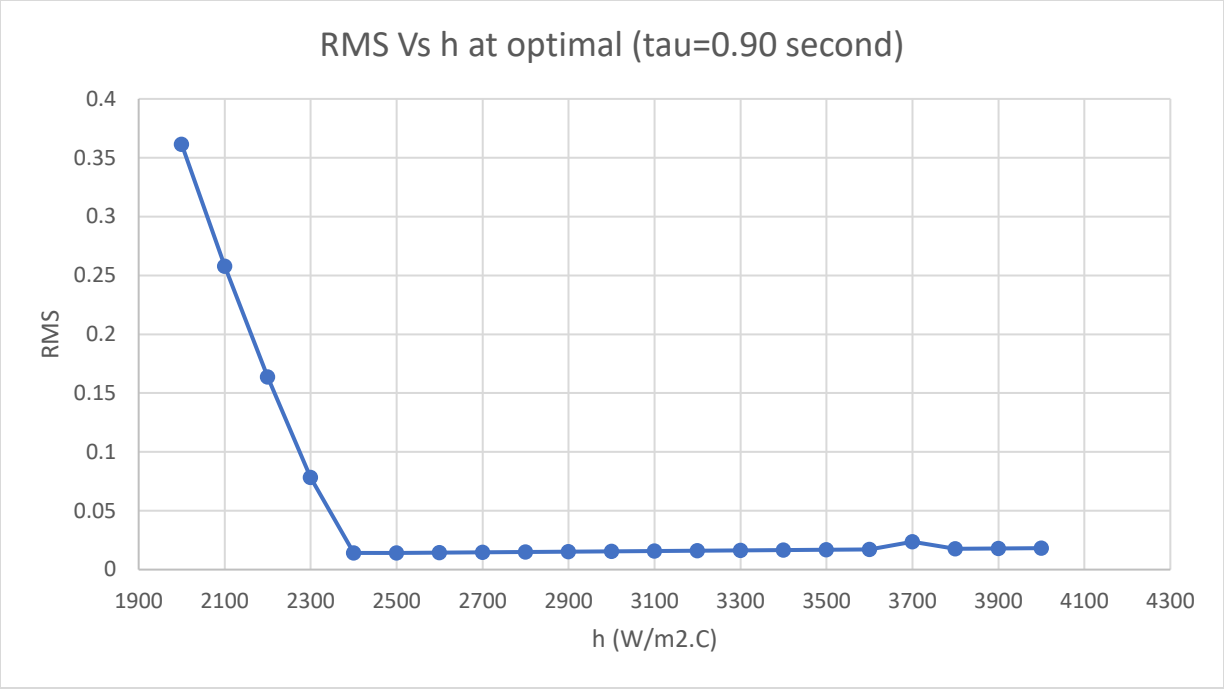

Fig.E1 NI data acquisition RMS Vs h at optimal time constant for the parallel thermocouple.

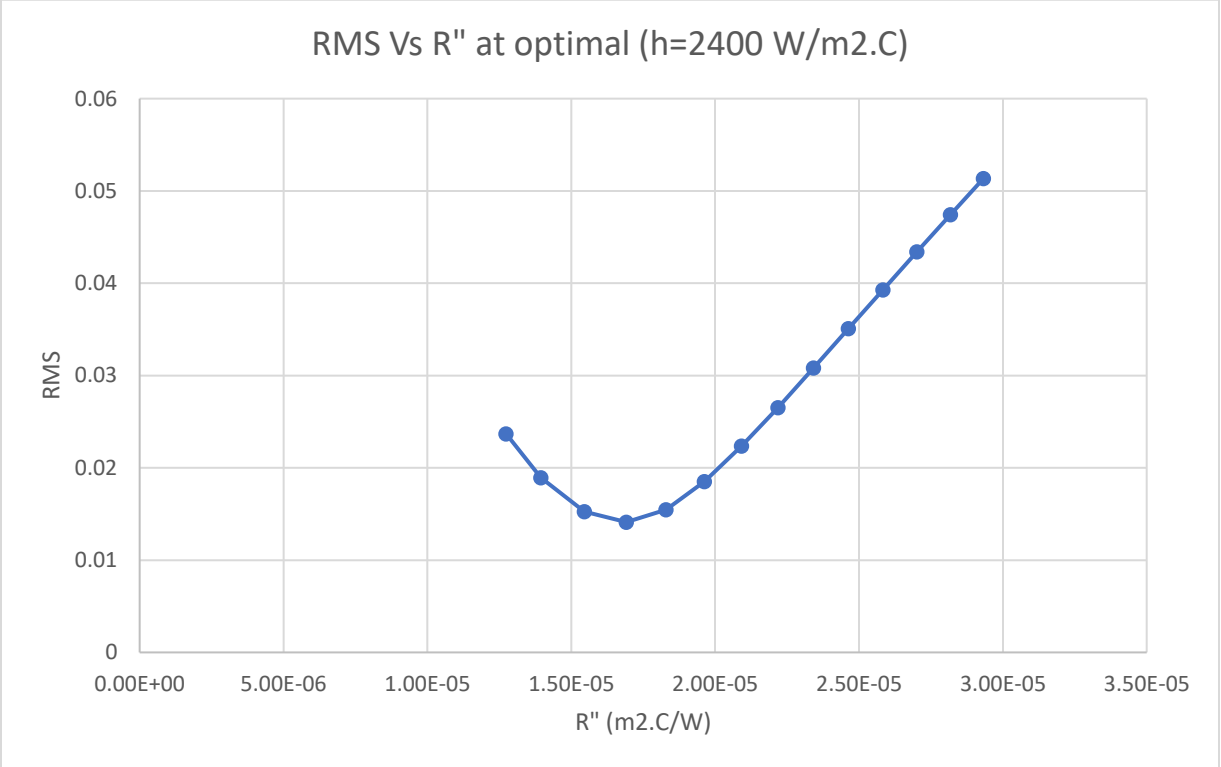

Fig.E2 NI data acquisition RMS Vs R" at optimal h for the parallel thermocouple.

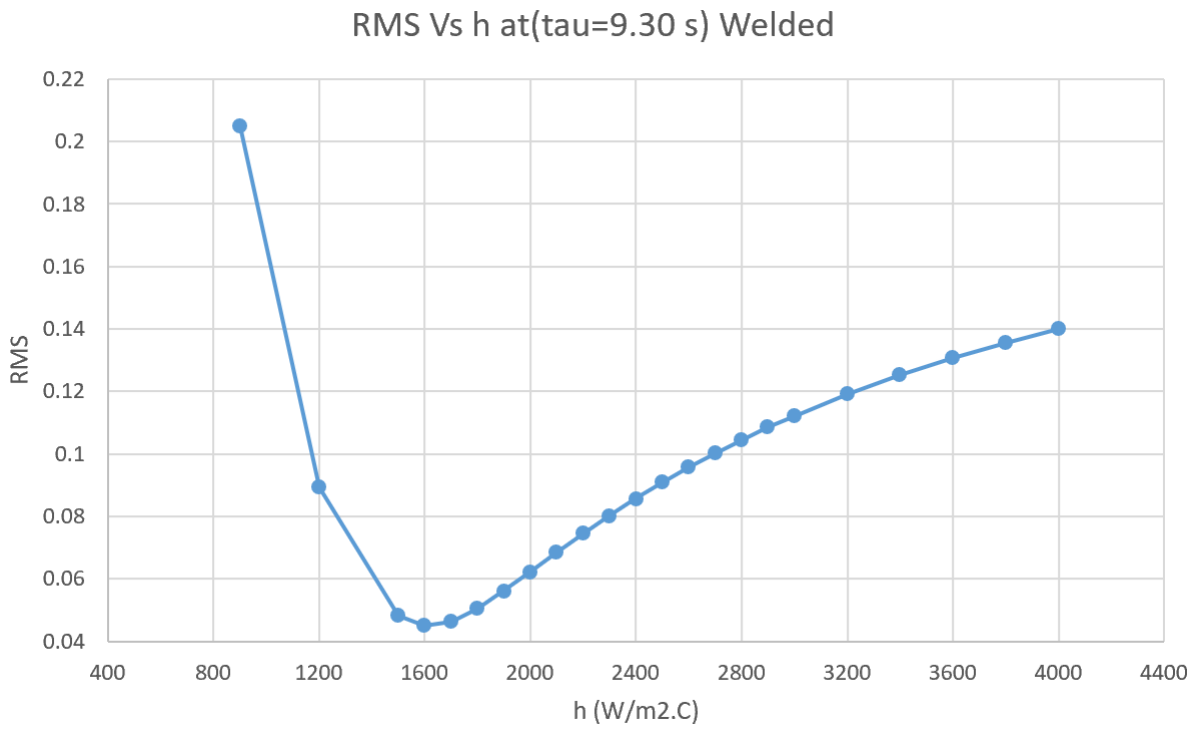

Fig.E3 NI data acquisition RMS Vs h at optimal time constant for the welded thermocouple.

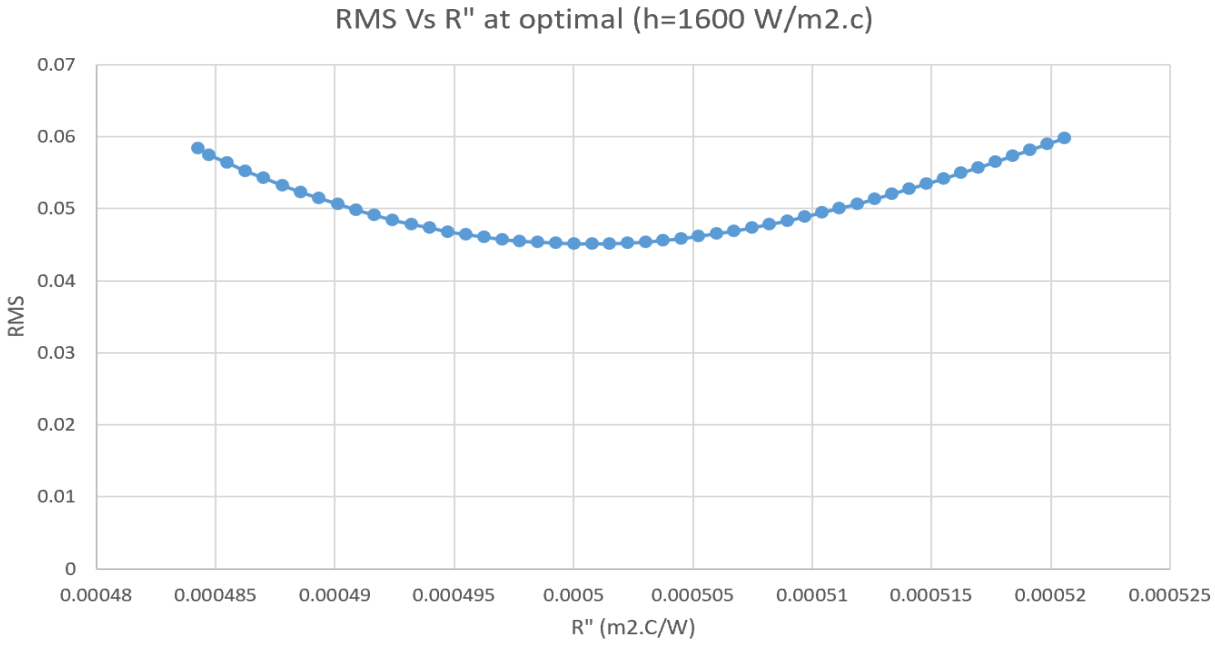

Fig.E4 NI data acquisition RMS Vs R" at optimal h for the welded thermocouple.

Appendix F- Lab-View 2017 Design for NI data Acquisition

The lab-view 2017 program was designed for NI data acquisition. Pleas see the below pictures.

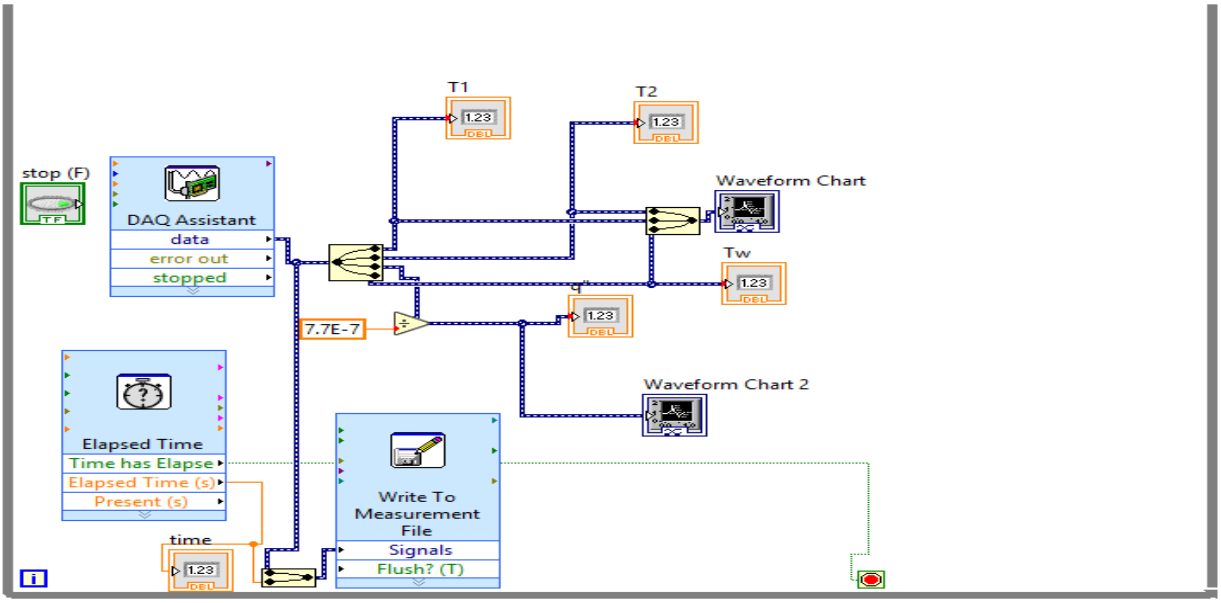

Fig.F1 Lab-View Design Program.

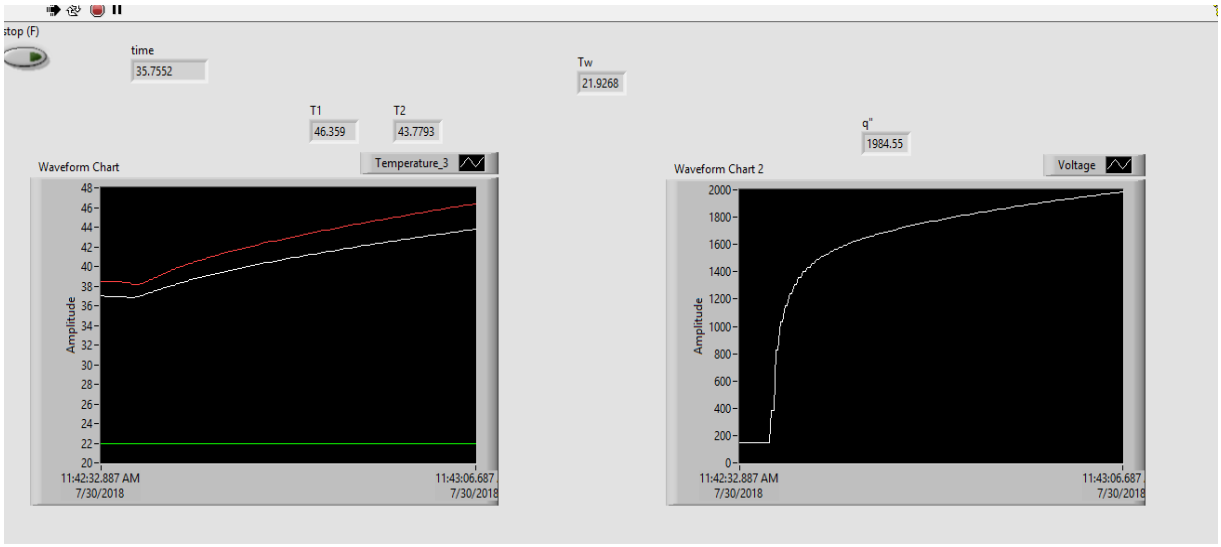

Fig.F2 Measurement data curves in the main board Lab-view when the experiment was taken.

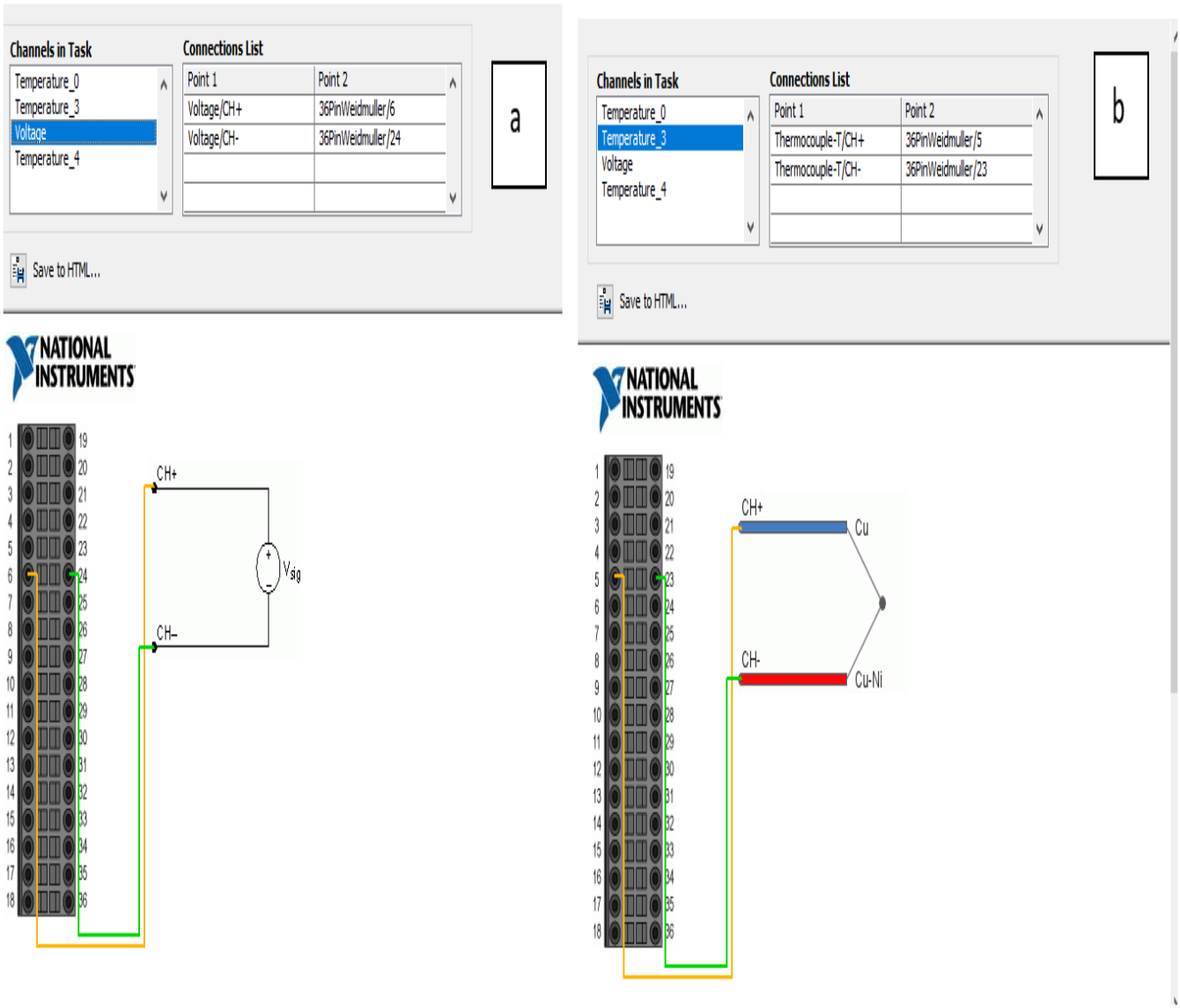

Fig.F3 (a) Plugin Heat Flux wire in a channel. (b) Plugin a Thermocouple wire in a channel.

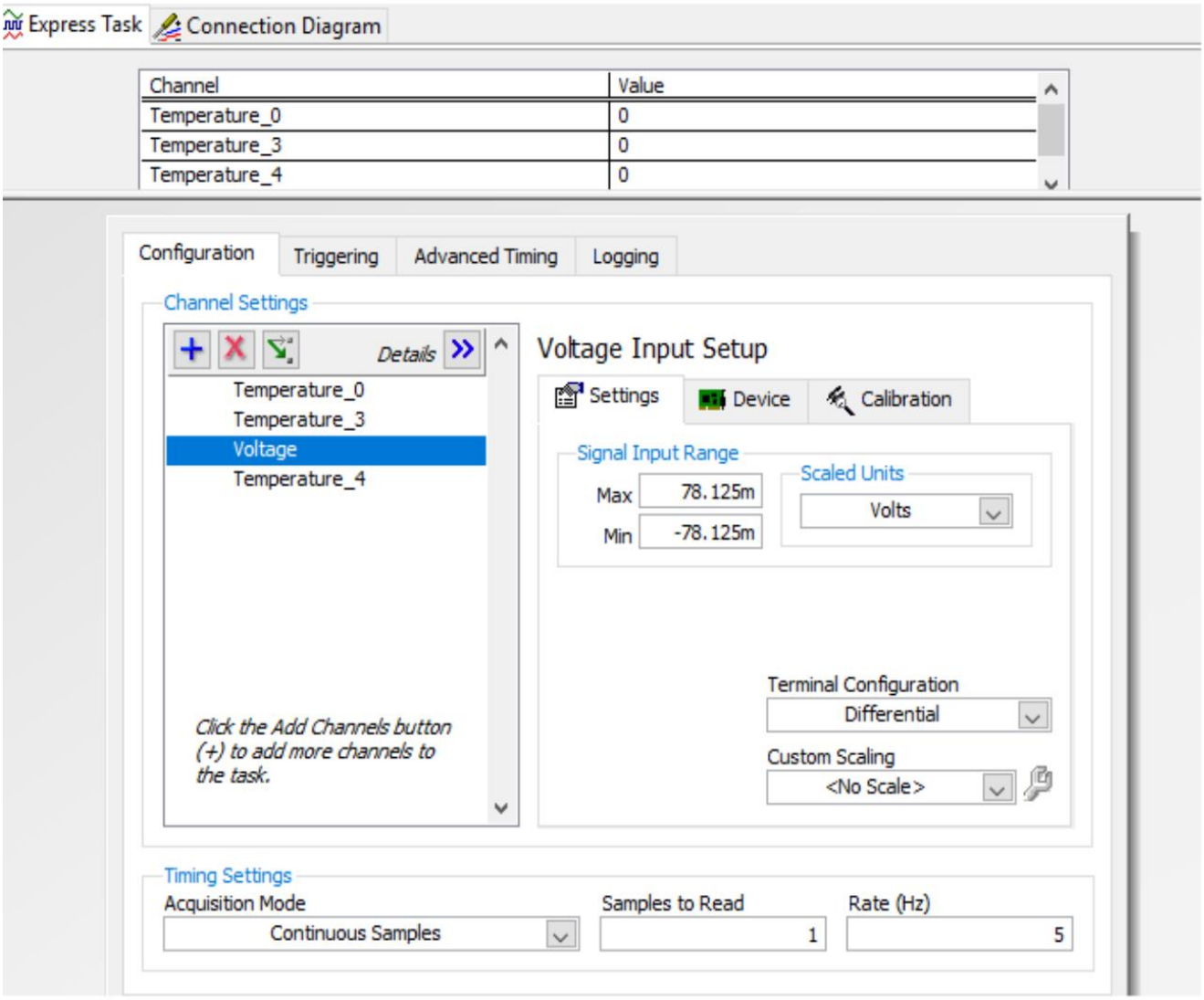

Fig.F4 Channels and sample properties.

Appendix G- The Data and temperature curves for the National Instrument Data Acquisition (NI) for the Parallel and Welded Thermocouples For three days

The data for parallel and welded thermocouples were taken and analyzed in this paper by using NI data acquisition for three days. They are in a **CD** and they are private.